

TAP Recommendations

No.	TAP Recommendation	SFPW and SFPUC Comment	Oct 31, 2019 Phase 1 Horizontal Geotechnical Report Reference	Required Actions	How Resolved	Response by Langan and Mission Rock Partners Langan responses in <b>black</b> , updates in <b>blue</b> MRP (S. Minden) responses in <b>red</b> , updates in <b>purple</b>	Referenced language from Langan Report dated 31 October 2019
1	Applicable Codes	SFPW: Applicable code to be determined based on time of permit submittal. Note that the 2019 model codes will reference ASCE 7-16 which requires site specific ground motion analysis that could change the design spectra required by ASCE 7-10.	Section 6.2	MRP to expand the response.	Reference Port Building Code for areas under its jurisdiction; Applicable Code determined upon application, not frozen to the 2016 Codes	11-6-19 Langan Response: 2016 California Building Code (ASCE 7-10)  12-10-19 Langan Response: Understood. We understand this project will be permitted now under the 2016 San Francisco Building Code.  <b>2-7-20 The applicable code for future phases will be updated with the current code at the time the phase is designed.</b>  <b>12-10-19 MRP Response: Note, the above Code is the basis of Seismic design. SF Public Works (SFPW), Public Utilities (SFPUC) and Transportation Authority (SFMTA) Codes and Standards are also being used as applicable for different features of the horizontal infrastructure.</b>	*Value obtained from United States Geological Survey (USGS) website for liquefaction analysis per ASCE 7-10 and 2016 California Building Code (CBC)  ** Site specific rotated maximum PGA = 0.46g. Analyses was performed using 0.47g consistent with the ASCE 7-10.
2	Long Term Settlement in Building Area	SFPW: The geotechnical report states typical over consolidation ratio (OCR) is about 1 to 1.6. Provide Pp (maximum past pressure) or OCR profile to demonstrate the site has OCR of 1.6 and at what depth the Young Bay Mud is normally consolidated. Provide the published coefficients (C $\alpha$ ) used for estimating secondary compression.	Section 7.2	TAP to review 10/31 Geotechnical Investigation (Horizontal Development) Section 7.2 for secondary	City considers recommendation from the TAP	See reference Section of Geotechnical Report	Section 7.2 "The results of consolidation testing in the Phase 1 Development site indicate the Bay Mud is generally slightly overconsolidated, but may be normally consolidated in some areas. Accordingly, we judge consolidation is complete under the existing fill loads that were placed in the late 1800s to early 1900s. These results are consistent with the thickness of the Bay Mud, the length of time the fill has been in place, and the history of site use. Based on consolidation theory, after primary consolidation is complete, soils that are subjected to a sustained load at their maximum past pressure (i.e. normally consolidated) will undergo strain-related movements associated with clay particle deformation (a phenomenon called secondary compression), leading to a small amount of future settlement over time. If secondary compression were ongoing at the site, we would calculate about ¼ to ½ inch of settlement in the last 8 years using published coefficients (C $\alpha$ ) for estimating secondary compression. However, thading & LCC , C 7 Series: plans, sections and profiles of utilities in streets, C8 Series: typical street cross sections and C9 Series: Detailss) or 500,000 light trucks per day (two axles with a combined weight of 8,500 pounds, examples include Box Vans, Utility Trucks, or a Pick-up with a Trailer). The TAP or SFDPW should assess if

TAP Recommendations

No.	TAP Recommendation	SFPW and SFPUC Comment	Oct 31, 2019 Phase 1 Horizontal Geotechnical Report Reference	Required Actions	How Resolved	Response by Langan and Mission Rock Partners Langan responses in <b>black</b> , updates in <b>blue</b> MRP (S. Minden) responses in <b>red</b> , updates in <b>purple</b>	Referenced language from Langan Report dated 31 October 2019
3	Construction Dewatering	SFPW: The Pilot program shows there are 15 inclined wellpoints at the crest of open cut on three sides of the pilot area. The 29-ft-wide pilot roadway section in the pilot represents about half of the future roadway section (total width of 60 ft.). The limit of open cut, if used as excavation technique for future roadway construction, will be much wider than the pilot (the pilot is dimensioned at 81.3 ft.). A dewatering program that is representative to future dewatering plan is needed to assess the groundwater profile during dewatering. In addition, Langan's Vertical Development geotechnical report stated that "Excavations for the below-grade structures will generally extend below the existing groundwater level; therefore, groundwater will need to be lowered to below excavation during construction. The rate of groundwater flow through the fill is anticipated to be high... In addition to dewatering wells, localized sumps and pumps could be used for dewatering and managing groundwater conditions during excavation." What are	Section 7.2	Specifications developed by MRP for "safe envelope"	Langan monitoring and assessing of the Pilot will provide guidance for them to develop controlling allowable limits for dewatering	11-6-19 Langan Response: That section discusses dewatering during construction and that the dewatering will be assessed during the LCC pilot test program. Monitoring is discussed in Section 8.4 of the 31 October 2019 report. 12-10-19 Langan Response: The LCC Pilot Section required the groundwater be drawn down to Elevation 88 feet at the test section. This was performed using dewatering wells as outlined in the LCC Pilot Program Submittal. As of 9 December 2019, groundwater at a distance of about 35 feet from the LCC Pilot only lowered about 6 to 9 inches following initiating dewatering as compared with the baseline elevation. Although dewatering continues, the groundwater levels are currently at or above the baseline elevations. 12-10-19 MRP Response: (See also Mission Rock Geotechnical Investigation for Phase 1 Horizontal Development, 31 October 2019, (the Geotech Report) Section 8.4 for Dewatering Recommendations)	Section 7.2 "During construction, localized dewatering will be required. Because of the likely relatively high permeability of the on-site fill, the dewatering required for the LCC excavations may lower the groundwater beyond the excavation areas. The depth of dewatering, permeability of the soil, and duration of the planned dewatering in any given portion of the site will influence the amount of groundwater is lowered. Stresses in the soil will increase as soil within the zone of lowered groundwater is no longer buoyant. Since placement of the historic fill, the compressible Bay Mud has been subjected to repeated cycles of groundwater fluctuation over more than 100 years, and is overconsolidated. However, care should be taken not to add excessive stress to the Bay Mud, in order to reduce the potential for initiating new primary consolidation or additional secondary compression. Therefore, where groundwater will be required to be lowered below the average typical low groundwater level (Elevation 90 feet), mitigation measures will be taken to offset the potential stress increase associated with the planned dewatering. We understand the contractor plans to limit dewatering to no more than 2 feet below the planned LCC excavation. As indicated on the onsite street improvement plans prepared for the project, the majority of the planned excavations for the placement of the LCC will bottom above Elevation 92 feet; therefore lowering the water 2 feet below the excavation depth will not lower the groundwater in the surrounding areas more than Elevation 90 feet. However, near the intersection of Shared Public Way and Channel Street, the excavation for the LCC will likely range from Elevation 90 to 92 feet, and the required dewatering will extend 0 to 2 feet below the average typical low groundwater level of 90 feet. In the southern portion of Bridgeview Street and in the

TAP Recommendations

No.	TAP Recommendation	SFPW and SFPUC Comment	Oct 31, 2019 Phase 1 Horizontal Geotechnical Report Reference	Required Actions	How Resolved	Response by Langan and Mission Rock Partners Langan responses in <b>black</b> , updates in <b>blue</b> MRP (S. Minden) responses in <b>red</b> , updates in <b>purple</b>	Referenced language from Langan Report dated 31 October 2019
4	Backfilling for Future Utilities and Emergency Repair	SFPW: Defer to result of pilot testing program. Appendix G of geotechnical report, Specification for Permeable/Open Cell Lightweight Cellular Concrete (P-LCC), Section 3.5 Placement, "Place P-LCC in lifts not to exceed 36 inches in thickness, unless otherwise recommended by the P-LCC manufacturer and approved by the GEOR." The 36" maximum lifts in the specification is acceptable as normal industry-practice. This is thinner than the Cellular Concrete Proposed Maintenance Policy and Procedures (dated 12/18/2018) that "for trenches with deeper backfill, LCC can be placed in single lifts of up to 6-7' with skilled crews" or "possible to place two lifts of 5' in a day with a 4 hour interval between the lifts." If thicker lift is used for emergency repair, the developer should demonstrate the recommended thickness is achievable.	Not addressed in Geotechnical Report	MRP to provide a detailed procedure; City to review	Defer Final Map condition until best practices developed during the construction phase	<p>MRP: A proposed Excavation and Backfill Procedure for LCC in Mission Rock Streets" is provided in Exhibit F.</p> <p>The procedure recommends 3' lifts for LCC backfill. <del>Higher lifts may be approved on a case-by-case basis.</del> When multiple backfill lifts are required, the trench would be covered with road plates between lifts as is the case for conventional soil backfill.</p> <p>MRP is still willing to accept responsibility for backfill of any public utility trenches in LCC in Mission Rock as an MOU condition.</p> <p>MRP: 2-10-20 Filter fabric to be provided between LCC and adjacent native soil, pipe bedding and cover, structural soil and other materials to prevent fines from migrating into the LCC</p> <p>List of Approved LCC Contractors has been added to Exhibit F</p>	
5	Stone Column Design and Installation	SFPW: SFPW defers to recommendations from the TAP on the disturbance of Young Bay Mud due to Stone Column/RIC. We understand that the TAP is also concerned that the installation of wick drain may disturb Young Bay Mud.	Sections 7.4 and	Specifications must be developed to mitigate potential impacts (disturbance and stress) to the Bay Mud layer:	Post ground improvement test panel project will gather data to determine the location of Bay Mud or lower limit of liquefiable soils	<p>11-6-19 Langan response: Section 7.4 provides a discussion on stone columns and that the disturbance of Bay Mud will be assessed during the test project.</p> <p>Section 8.1 provides detailed recommendations on ground improvement and the acceptance criteria.</p> <p>12-10-19 Langan Response: No response required at this time.</p> <p>2-10-20 MRP: In response to verbal comment form Port, we confirm that filter fabric (Mirafi fabric) will be placed between LCC and all adjacent soil, pipe bedding and cover, structural soil and any other material with fines to prevent migration of fines into LCC</p>	<p>Section 7.4: "Ground improvement in the fill may cause some disturbance of the underlying Bay Mud, which could result in some settlement. This condition will be evaluated during the ground improvement test program, and measures will be implemented to minimize the potential disturbance to the Bay Mud"</p> <p>Section 8.1: "To minimize the disturbance in the underlying Bay Mud, we recommend stone columns terminate at the bottom of the liquefiable fill, or one to two feet above the underlying Bay Mud, whichever is shallower. "</p>

TAP Recommendations

No.	TAP Recommendation	SFPW and SFPUC Comment	Oct 31, 2019 Phase 1 Horizontal Geotechnical Report Reference	Required Actions	How Resolved	Response by Langan and Mission Rock Partners Langan responses in <b>black</b> , updates in <b>blue</b> MRP (S. Minden) responses in <b>red</b> , updates in <b>purple</b>	Referenced language from Langan Report dated 31 October 2019
6a	Earthquake Considerations for LCC		Section 6.2	Include a discussion of the design basis earthquake and expected site/soil amplification effects, the design peak ground acceleration, and the expected level of ground motion within the LCC backfill. This information is needed by the TAP and others (e.g., utility and pipeline designers) to complete their engineering evaluations	Provide requested discussion and supporting documentation for the analysis and evaluations.	<p>11-6-19 Langan Response: Section 6.2 provides discussion of the ground motions.</p> <p>12-10-19 Lagan Response: The fundamental performance of the LCC under seismic loading is discussed in the Horizontal Geotechnical report dated 31 October 2019. However, as requested we have evaluated the seismic performance of the LCC compared to the demands expected during an MCEr Earthquake.</p> <p>To evaluate the potential for breakage of the LCC under the stresses of vertically propagating shear waves, we first evaluated the magnitude of the shear stress ratio (shear stress/effective stress) from our linear and non-linear evaluation of the site response analyses under MCEr loading at the site. The maximum shear stress ratio in the fill at the site is about 0.6 to 0.66. Therefore, the maximum anticipated shear stresses imposed on the LCC from an MCEr earthquake are on the order of 200 to 265 psf, which 10 percent of the target minimum LCC strength (2,880 psf), see Exhibit A. If there is an existing crack or cold-joint in the LCC and the residual strength at this interface is equivalent to a friction ratio of 35 degrees, the LCC still has sufficient strength to resist further degradation.</p> <p>In addition, considering these are linear elements, we evaluated the potential for LCC breakage from a horizontally propagation Rayleigh wave. Our analyses indicates the unit shear stress in the LCC is on the order of 1/4 to 1/2 of the minimum target</p>	<p>*Value obtained from United States Geological Survey (USGS) website for liquefaction analysis per ASCE 7-10 and 2016 California Building Code (CBC)</p> <p>** Site specific rotated maximum PGA = 0.46g. Analyses was performed using 0.47g consistent with the ASCE 7-10.</p>
6b	Earthquake Considerations for LCC	SFPW: Section 7.3 of the geotechnical report stated that "We have checked that during a seismic event, the shear strength of the LCC is greater than the anticipated peak cyclic shear stress generated by an earthquake. We therefore conclude the LCC should perform adequately under a seismic event. In addition, even if the LCC cracks it will still provide vertical support for the streets and improvements." Please elaborate on methodology and what earthquake ground motions were used to develop peak cyclic shear stress. Please provide dynamic properties of P-LCC.	Section 7.3	What is the magnitude of seismic demand placed on the LCC backfill in terms of the peak cyclic shear stress caused by the earthquake?	Same as above	<p>11-6-19 Langan Response: Section 7.3 provides discussion on peak cyclic shear stress vs LCC shear strength.</p> <p>12-10-19 Langan Response: see above.</p>	Section 7.3: "We have checked that during a seismic event, the shear strength of the LCC is greater than the anticipated peak cyclic shear stress generated by an earthquake. We therefore conclude the LCC should perform adequately under a seismic event. In addition, even if the LCC cracks it will still provide vertical support for the streets and improvements."



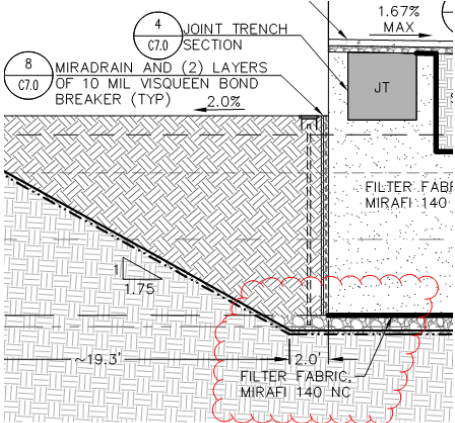
TAP Recommendations

No.	TAP Recommendation	SFPW and SFPUC Comment	Oct 31, 2019 Phase 1 Horizontal Geotechnical Report Reference	Required Actions	How Resolved	Response by Langan and Mission Rock Partners Langan responses in <b>black</b> , updates in <b>blue</b> MRP (S. Minden) responses in <b>red</b> , updates in <b>purple</b>	Referenced language from Langan Report dated 31 October 2019
6c	Earthquake Considerations for LCC			Evaluate whether or not the stiffness of the LCC would be sufficiently degraded so as to impact its long-term function and performance	Same as above	12-10-19 Langan Response: Based on our calculations the shear strength is greater than the anticipated peak shear stress. However, if the LCC does crack, it will still perform as intended.	
6d	Earthquake Considerations for LCC	SFPW: The vertical geotechnical report states, "At least six inches compressible material such as EPS14 geofoam should be placed between the LCC and below-grade elements; accordingly, passive resistance in the LCC should be ignored." Please confirm excavation method for LCC construction. Will formwork be constructed similar to LCC pilot and LCC will be poured within the roadway limits? How are the EPS14 geofoam and filter fabric installed against LCC roadway section without formwork?	Section 8.2	Consequences of cracking of the LCC apron should also be evaluated	Traffic signal poles, light poles, and full height trees should be evaluated with mitigating details provided no later than the next SIP	11-6-19 Langan Response: Agreed. 6 inches of compressible material is discussed in Section 8.2. <b>12-10-19 MRP Response: Next SIP will include structural calculations of light poles and any other structural elements embedded or found in LCC.</b>	Section 8.2: "To prevent application of high shear loads from adjacent buildings, 6 inches of compressible material should be provided between buildings and LCC."
6e	Earthquake Considerations for LCC			The planned bedding or wrapping materials placed around utilities placed in the LCC should be clearly identified in all project drawings and documents. Furthermore, their interface properties (i.e., material stiffness, coefficient of interface friction, adhesion, cohesion, etc.) are often required by utilities to complete their seismic and other pipeline evaluations.	PG&E gas and proposed telecom companies must provide a letter approving of the proposed trench backfill (currently proposed as LCC).	<b>12-10-19 MRP Response: We will provide standard sand bedding and shading in joint trench. This should not require any variances from current standards by PG&amp;E, ATT, Comcast or others.</b>	

TAP Recommendations

No.	TAP Recommendation	SFPW and SFPUC Comment	Oct 31, 2019 Phase 1 Horizontal Geotechnical Report Reference	Required Actions	How Resolved	Response by Langan and Mission Rock Partners Langan responses in <b>black</b> , updates in <b>blue</b> MRP (S. Minden) responses in <b>red</b> , updates in <b>purple</b>	Referenced language from Langan Report dated 31 October 2019
7	Buoyancy During Construction	SFPW: The intent of the TAP recommendation is during construction, not for the completed work. Note that there is still a potential issue with buoyancy for the completed work at the transition from the elevated supported streets to unsupported streets. See recommendation 13 below.	Section 7.3	The buoyancy calculations performed by the design team need revisions in light of the recent testing done by Castle Rock Consulting. In addition, these calculations need to evaluate the potential for buoyancy uplift for temporary/interim conditions where dewatering may have been discontinued or interrupted.	Langan has used 79 pcf as the basis of design. Saturated tests interpolates 27 pcf permeable LCC to be around 59 pcf and thus continue to have uplift. Langan must evaluate the data and provide justification for it's selected input.	<p>11-6-19 Langan Response: Section 7.3 discusses the hydrostatic uplift checks based on no saturation. However, based on tests the permeable LCC will become partially saturated, which reduces the hydrostatic uplift pressures on the LCC section. Therefore, our evaluation is conservative.</p> <p>12-10-19 Langan Response: We take no exception to the data showing the permeability may be on the order of 59 pcf, this value lies within the range of evaluated conditions. Langan's calculations that check for uplift are based on no infiltration (full hydrostatic pressures acting act the bottom of the LCC). Because the infiltration will increase density of the LCC, it will improve the factor of safety against uplift over time. If the project team wishes to value engineer the necessary section thickness based on site-specific data, this can be discussed with the team.</p>	Section 7.3: "To prevent significant hydrostatic uplift, open cell (porous) LCC will be used. The open cell LCC will allow water to flow through the material, preventing hydrostatic pressure from building up at the bottom of the LCC section. However, we have also checked the resistance to uplift of the LCC if the LCC is subjected to full hydrostatic pressures (i.e. acts impermeable) as an added check."
8	Long-Term Durability in Brackish Water	SFPW: SFPW defers to the response from	Not addressed in Geotechnical Report	Some testing should be performed to determine what the compressive strength losses will be when saturated with the brackish water on-site, at least through 28 days.	Developer transmitted 15 gallons of bay water to Colorado for testing. Initial tests show a 25% decrease in strength (same as regular water).	<p>11-6-19 MRP Response: MRP is working with General Contractor Granite and LCC subcontractor, Cell-Crete Aerix and Castle Rock Consultants to perform long term test on LCC samples cured in air, fresh water and groundwater from site. Samples of groundwater from the site were sent to Aerix's Lab in Colorado. Below is a description of the test, On October 18th, Aerix Industries molded forty (40) 3" x 6" cylinders from the same batch to test them for compressive strength under 3 different curing scenarios. The first scenario is a baseline where curing takes place as normal, with no exposure to saturation. In the second circumstance, a dozen cylinders are demolded at 7 days of age, placed in 4" x 8" PVC cylinder molds filled with fresh water and sealed. In the third scenario, a dozen cylinders are demolded at 7 days of age and placed in the 4" x 8" PVC molds but the molds are filled with brackish or salty groundwater and sealed. Samples cured the three different ways will tested for compressive strength at specific ages 28 days, 56 days, 3 months, 6 months, 9 months and 1 year.</p> <p>12-10-19 Langan Response: No response required at this time.</p>	

TAP Recommendations

No.	TAP Recommendation	SFPW and SFPUC Comment	Oct 31, 2019 Phase 1 Horizontal Geotechnical Report Reference	Required Actions	How Resolved	Response by Langan and Mission Rock Partners Langan responses in <b>black</b> , updates in <b>blue</b> MRP (S. Minden) responses in <b>red</b> , updates in <b>purple</b>	Referenced language from Langan Report dated 31 October 2019
8	Long-Term Durability in Brackish Water (Continued)					<p>1-24-20 MRP: Exhibit G shows test results through the 90 day breaks on 16 Jan 2020. From this data we note the following:</p> <p>1. Observations:</p> <p>a. The compressive strength of the fresh and brackish water-cured samples are 78% and 80% of the normal cured samples, (or a 22% and 20% reduction compared to normal curing), respectively.</p> <p>b. All sets showed steady increase of compressive strength over time. Between the 28 and 90 day breaks, the water cured samples increased roughly 10psi/month or 25% and the normal cured sample increased roughly 15%</p> <p>2. Preliminary Conclusions/Remarks</p> <p>a. Although the strength of the water cured samples are lower than the normal dry cured samples, they are well above the minimum compressive strength specified</p> <p>b. There is no significant difference in the effect of fresh water from brackish water curing. The brackish water cured samples are actually slightly stronger.</p> <p>c. There is a small increase in compressive strength over time after the initial 28 day cure time. This increase appears to be slightly more for the water cured samples. So far, the compressive strength is well below the 200 psi maximum specified for excavatability. We expect this increase to flatten out well below 200psi over the next nine months. This will be confirmed over the remaining test period.</p>	
9	Protection of the Pervious LCC from Fines Infiltration	SFPW: Developer to confirm if silt-barrier geotextile fabric will be installed during production for protection of the pervious LCC from fines infiltration. The response only shows a filter fabric in the pilot detail, but did not confirm it will be included in production LCC. Will formwork be constructed similar to LCC pilot and LCC will be poured within the roadway limits?	Not addressed in Geotechnical Report but this is shown in LCC Pilot Plans Sheet C6.0	A suitable silt-barrier geotextile filter fabric should be installed before placing pervious LCC in any excavation, to prevent migration of clay fines and clogging the pores.	Developer details tree planters with an internal filter fabric between soil and LCC in the 2nd SIP submittal.	<p>11-6-19 MRP Response:</p>  <p>12-10-19 Langan Response: No response required at this time.</p>	

TAP Recommendations

No.	TAP Recommendation	SFPW and SFPUC Comment	Oct 31, 2019 Phase 1 Horizontal Geotechnical Report Reference	Required Actions	How Resolved	Response by Langan and Mission Rock Partners Langan responses in <b>black</b> , updates in <b>blue</b> MRP (S. Minden) responses in <b>red</b> , updates in <b>purple</b>	Referenced language from Langan Report dated 31 October 2019
10	Waterline Leak Detection	<p>SFPW: SFPUC to respond.</p> <p>SFPUC response 12/17/19: By not objecting to Recommendation 10 of the LCC Pilot Project Program, the SFPUC is not necessarily approving of this leak detection methodology. Close coordination with SFPUC operators during the leak detection test along with internal coordination after the test will be required and the SFPUC reserves the right to employ a different technology or method to detect water line leaks in the LCC.</p>	Not addressed in Geotechnical Report, but is described in LCC Pilot Narrative (see excerpts in response)	The developer team should propose a method to identify and locate leaks in pipes that are embedded in LCC since the porosity of the LCC will prevent water from rising to the surface where it is visible.	A Developer method detailed in the LCC Pilot Project will be tested	<p>11-6-19 MRP Response: 2.10.19.2 Place 8 mil Polyethylene (PE) cover at bottom and sides of trench. Leave selvage to cover top and ends for trench. Note PE is proposed to be used in lieu of filter fabric in order to contain any leak in pipe. Water from leak will travel through pea gravel and through modified valve box and cover—see marked-up detail CDD-LP-250 as end of annotated plans.</p> <p>3.3Simulate pipe leak in LPW line</p> <p>3.3.33.3.1 Open gate valve in mock-up. Connect 4” fire hose to test rig end of pipe, close valve on test rig, connect other end of fire hose to hydrant or water truck pump.</p> <p>3.3.2Turn water supply on. Gradually open valve on test rig.</p> <p>3.3.4Observe water, verify water comes up through gate valve box and cover.</p> <p>3.3.53.3.4vClose gate valve in mock-up. Water leak should stop.</p> <p>3.3.6Turn off water supply, close valve on test rig.</p> <p>12-10-19 Langan Response: No response required at this time.</p> <p>01-24-20 <b>MRP Response: The Pilot demonstrated a leak detection method using a polyethylene wrap around pea gravel cover (shading) which conducted a simulated leak to the street through a valve riser. Subsequently, representatives from CCD requested that the polyethylene wrap would be replaced with permeable filter fabric and the sand cover be provided for the full depth of trench to the top of subgrade/bottom of pavement base. This will be reflected in the third SIP submission. Note that this only applies to LPW.</b></p>	

TAP Recommendations

No.	TAP Recommendation	SFPW and SFPUC Comment	Oct 31, 2019 Phase 1 Horizontal Geotechnical Report Reference	Required Actions	How Resolved	Response by Langan and Mission Rock Partners Langan responses in <b>black</b> , updates in <b>blue</b> MRP (S. Minden) responses in <b>red</b> , updates in <b>purple</b>	Referenced language from Langan Report dated 31 October 2019
11a	Pavement Design	SFPW: SFPW defers to the response from	Sections 8.2 and	CBR value, modulus of subgrade reaction, or resilient modulus for the LCC materials and subjected to low-strain repetitive loading	Developer has not addressed how long term performance (dependent upon LCC stiffness)	<p>11-6-19 Langan Response: Sections 8.2 and 8.8 discuss the use of LCC as subgrade below the pavement section. We agree with this comment, but the pavement is not being designed to any CBR value or modulus. Therefore, this has not been provided.</p> <p>12-10-19 Langan Response: See Exhibit B showing that the resilient modulus for subgrade in pavement design is an estimate of the elastic modulus of a material. See Exhibit C showing the elastic modulus for LCC from Cell-Crete. For the requested pavement design calculations, we have used a resilient modulus of 95 ksi. This is at the lower bound of the reported modulus for similar materials. See Exhibit B, C, and E.</p> <p>01-24-20 <b>MRP Response: See also Thesis on Use of LCC as a Subbase Material by S Averyanov, University of Waterloo, Ontario, Canada, 2018. Refer to Exhibit E attached.</b></p> <p>02-10-20 MRP: Response to verbal comment given by Port to MRP on thickness and type of base under pavement: The SIP Plans 3rd submittal show 4" of aggregate base material between the bottom of concrete pavement (sidewalks and PCC in streets) and the top of LCC. We believe that aggregate base, not sand is the most appropriate material for this application. Sand is generally not used as a bas or subbase material. We believe that 4" is adequate separation thickness to prevent damage to LCC during pavement removal for future repairs. From a pavement design standpoint, we have demonstrated the PCC alone on LCC subgrade is more than adequate, no base is needed.</p>	<p>Section 8.2: "We understand that the San Francisco standard pavement section will be used for the streets, consisting of 4 inches of asphalt concrete over 8 inches of concrete. The San Francisco standard pavement section does not take into account the subgrade below the concrete and many streets in Mission Bay are supported on heterogeneous fill with varying strengths and quality. The LCC is stronger than the pavement subgrade in Mission Bay and we judge the LCC is adequate for pavement subgrade."</p> <p>Section 8.8: "We understand that the San Francisco standard pavement section will be used for the streets within the Horizontal Development at Mission Rock, which consists of 4 inches of asphalt concrete over 8 inches of concrete. The San Francisco standard pavement section does not take into account the subgrade below the concrete and many streets in Mission Bay are supported on heterogeneous fill with varying strengths and quality. The LCC is stronger than the pavement subgrade in Mission Bay and we judge the LCC is adequate for pavement subgrade. We recommend the four-inch-thick subgrade material consist of some type of strong granular fill material."</p> <p>See Exhibit B, C, and E</p>

TAP Recommendations

No.	TAP Recommendation	SFPW and SFPUC Comment	Oct 31, 2019 Phase 1 Horizontal Geotechnical Report Reference	Required Actions	How Resolved	Response by Langan and Mission Rock Partners Langan responses in <b>black</b> , updates in <b>blue</b> MRP (S. Minden) responses in <b>red</b> , updates in <b>purple</b>	Referenced language from Langan Report dated 31 October 2019
11b	Pavement Design			Assumed properties of LCC, the pavement support, and design life calculations for the LCC should be provided for review	Provide the calculations	<p>12-10-19 Langan Response: as described in the geotechnical report for the project, the City and County of San Francisco have specified a pavement type for this project. This pavement section consists of 4 inches of Asphalt Concrete over 8 inches of Portland Cement Concrete (PCC) with an unconfined compressive strength of 4,500psi. In addition, a 4-inch layer of aggregate base is provided beneath the PCC layer. This composite section is not consistent with either rigid or flexible pavement design methodologies. However, the calculation in Exhibit D shows the assumed properties for a rigid pavement design consistent with AASHTO 1993 for the concrete section alone, ignoring the Asphalt Concrete and the underlying Aggregate Base cushion. This design calculation indicates the concrete section over the LCC is capable of supporting more than 11 million equivalent 18 kips axle loads (ESAL's). This ESAL value suggest that for a typical 20-year pavement design life the pavement could support either 395 trucks per day (three axles, max legal weight at rear, with a combined weight of 54,000 pounds, examples include dump, trash, fire, or full concrete trucks) or 500,000 light trucks per day (two axles with a combined weight of 8,500 pounds, examples include Box Vans, Utility Trucks, or a Pick-up with a Trailer). The TAP or SFDPW should assess if this loading and timeframe match their assumed design intent.</p> <p>See Exhibit D for example calculations.</p>	<a href="#">See Exhibit D</a>



TAP Recommendations

No.	TAP Recommendation	SFPW and SFPUC Comment	Oct 31, 2019 Phase 1 Horizontal Geotechnical Report Reference	Required Actions	How Resolved	Response by Langan and Mission Rock Partners Langan responses in <b>black</b> , updates in <b>blue</b> MRP (S. Minden) responses in <b>red</b> , updates in <b>purple</b>	Referenced language from Langan Report dated 31 October 2019
11c	Pavement Design			Recommend that the pavement designer evaluate this extreme loading case to see if potential cracking might occur from the truck loading. Also, it is recommended that plate load tests be conducted prior and after the vehicle loading to evaluate potential changes in vertical stiffness. Lastly, careful documentation should be made of any deflection or distress caused by the loading. It may be possible for the planned pilot LCC testing to incorporate these evaluations and	Provide the evaluations and tests and consider incorporating into the LCC Pilot Project.	11-6-19 Langan Response: Loading test being performed as part of the LCC pile testing.  12-10-19 Langan Response: This can be incorporated into the LCC Pilot if the modulus testing described in <b>Exhibit E</b> are not satisfactory to the TAP.	
12	Compressive Strength of Saturated LCC	SFPW: Not yet received to review.		The developer should perform testing of compressive strength of LCC cylinders when saturated with both brackish (saltwater) and on site ground water	Continue working with Aerix Industries and provide results to the City.	11-6-19 Langan Response: Currently being performed.  12-10-19 Langan Response: We understand there are ongoing tests regarding the compressive strength of the LCC in a saturated condition, and understand that there could be a 20 to 25 percent reduction of compressive strength. Based on this reduction, our analysis shows that the section still has a factor of safety against crushing greater than 2.  <b>12-10-19 MRP Response: See also response to issue 8 above.</b>	

TAP Recommendations

No.	TAP Recommendation	SFPW and SFPUC Comment	Oct 31, 2019 Phase 1 Horizontal Geotechnical Report Reference	Required Actions	How Resolved	Response by Langan and Mission Rock Partners Langan responses in <b>black</b> , updates in <b>blue</b> MRP (S. Minden) responses in <b>red</b> , updates in <b>purple</b>	Referenced language from Langan Report dated 31 October 2019
13	Tapered LCC Transitions	SFPW: MRP has indicated that they will design the tapered LCC transition zones from the elevated supported streets to unsupported streets to account for buoyancy effects. However, this has yet to be provided to us for review.		The developer team should evaluate the proposed tapered LCC transitions to confirm their effectiveness.	Transitions are not evident in SIP	<p>11-6-19 Langan Response: The LCC section will become thinner when approaching 3rd Street, but the LCC section will still be designed to unload the effective stress of the Bay Mud by 10 percent.</p> <p>12-10-19 The overall engineering design approach is to unload the Bay Mud by 10 percent at locations beneath the LCC. Therefore, once the weight of the pavement thickness, improvements are accounted for, in addition to unloading by 10%, the tapered section of LCC is still on the order of 5 to 7 feet thick. Therefore it may not look significantly tapered at locations where the LCC meets the adjacent roadways.</p> <p>2-6-20 Additionally, the LCC section includes unloading of the underlying Bay Mud. The stress decrease from the LCC decreases stress in the area beyond the footprint of the LCC. Therefore, if there is ongoing settlement in 3rd Street, the use of LCC will allow for a more gradual differential settlement from this unloading.</p>	
14	Placement of LCC Fill	SFPW: The specification in Appendix G is different from the specification in LCC Pilot submittal, Permeable/Open Cell lightweight Cellular Concrete (P-LCC) specification, dated 10/29/2019. Per Article 4.3.2 of the 10/29/19 specification, Field Falling Head Permeability test is part of the quality control testing. Field permeability testing should be demonstrated in the pilot testing. Core of the LCC used in the Pilot (in situ sample, cured in water after 28 days) shall be lab tested for permeability. This should be compared to the specified permeability (0.10 to 0.65 cm/s) to make sure water can freely move around within LCC.	See Appendix G for specification	QA/QC procedures	Consider suggestions from Castle Rock Consulting and develop QA/QC procedures	<p>11-6-19 Langan Response: See specification.</p> <p>12-10-19 Langan Response: No response required at this time.</p> <p>12-10-19 MRP Response: Stan Peter's of the TAP has developed recommendations for testing and inspection that will be incorporated in the final LCC Specification including field tests for cast density, sampling and testing frequency and procedures, lab tests for compressive strength, permeability and saturated density.</p> <p>01-24-20 Proposed Draft of the final Spec , including testing and inspection schedule is in Exhibit H</p>	
15	Future Sourcing of LCC		Not addressed in Geotechnical Report	A separate specification should be provided for small batch LCC for emergency repairs.	The specification is for the City to impress upon third party applicants of LCC post acceptance of the project.	<p>11-6-19 MRP Response: See response to recommendation 4 above</p> <p>12-10-19 Langan Response: No response required at this time.</p> <p>2-10-20 MRP Response: A list of approved LCC contractors was added in Appendix B of the Exhibit F Proposed Excavation and Backfill Procedures. Three local LCC contactor/vendors are listed: Cell-Crete, Throop and Confoam.</p>	

TAP Recommendations

No.	TAP Recommendation	SFPW and SFPUC Comment	Oct 31, 2019 Phase 1 Horizontal Geotechnical Report Reference	Required Actions	How Resolved	Response by Langan and Mission Rock Partners Langan responses in <b>black</b> , updates in <b>blue</b> MRP (S. Minden) responses in <b>red</b> , updates in <b>purple</b>	Referenced language from Langan Report dated 31 October 2019
16a	Pilot Test			The Developer should submit a written narrative description of the Pilot Test including objectives, construction sequence, and testing methodology.	This has been completed.	11-6-19 Langan Response: See Pilot Test plan and Narrative  12-10-19 Langan Response: No response required at this time.	
16b	Pilot Test			Demonstrate that the isolation joint can accommodate the anticipated differential settlements.	Consider testing as part of the LCC Pilot Project.	12-10-19 Langan Response: Comment is unclear. There will be six inches of compressible foam between the buildings and the LCC to accommodate differential settlement. If a different question is being asked, please let us know.  12-10-19 MRP Response: If desired separate mock-ups can be made for these joints as part of Vertical design and construction.  If the question is referring to differential settlement between the LCC and existing streets such as 3rd St. and Mission Rock St. This is not contemplated in the scope of the LCC Pilot, but has been addressed extensively in the BOD and SIP.  Note that the horizontal and vertical geotechnical recommendations have been coordinated so that no lateral resistance or forces at the below grade are transferred between the LCC and buildings.  2-10-20 MRP: We have added an new Exhibit I: Typical Sections at LCC Interfaces showing details of LCC, Pavement and utilities. Please also refer to the recent SIP 3rd Submittal Plan Sheet Series C6: plans and profiles of grading & LCC , C 7 Series: plans, sections and profiles of utilities in streets, C8 Series: typical street cross sections and C9 Series: Details	

TAP Recommendations

No.	TAP Recommendation	SFPW and SFPUC Comment	Oct 31, 2019 Phase 1 Horizontal Geotechnical Report Reference	Required Actions	How Resolved	Response by Langan and Mission Rock Partners Langan responses in <b>black</b> , updates in <b>blue</b> MRP (S. Minden) responses in <b>red</b> , updates in <b>purple</b>	Referenced language from Langan Report dated 31 October 2019
16c	Pilot Test			Test the LCC surface for damage prior to protecting it. Determine and note the depth of damage. This will inform any future repairs that must be made due to damage that may occur during construction.	Test the bare unprotected LCC by driving a typical maintenance vehicle over it and also while parked.	<p>12-10-19 Langan Response: Damaged LCC should be removed and replaced with new LCC as part of the routine repairs during the life of the roadway. This test therefore does not provide meaningful data and we do not recommend performing this test.</p> <p>12-10-19 MRP Response: Note that a temporary wearing surface such as AC grindings and or AC will be provided to protect the LCC during vertical construction. Any damage to the LCC from construction will be repaired with fresh LCC prior to permanent paving.</p>	

Project Title - Mission Rock Project Phase 1

Mission Rock LCC Pilot Construction and Testing Procedure Submittal

CDD Reviewed for water items only - forward to other agencies as appropriate

Mission Rock Partners (MRP) Responses in Blue Langan. Responses in Black

- Notes to Reviewers
1. Please complete your review and return comments to TBD.
  2. Please be as specific as possible and propose corrections or solutions to the problem identified.
  3. Please consolidate the comments for all reviewers in your division and make sure the reviewer is identified for each comment.
  4. Let us know if there is anything that we can do or any additional information that we can provide to assist in your review!

Please provide the following information for your agency:

Agency: SFPUC

Division/Unit: CDD

Primary Contact Name: Brandy Batelaan

Primary Contact Email: [bbatelaan@sfwater.org](mailto:bbatelaan@sfwater.org)

Primary Contact Phone:

Color key:

Red = consider incorporating ASAP for current pilot test

Yellow = MRP to provide written response. Possible action if response is not adequate.

Green = defer to maintenance/repair demonstration or training session at future date.

Comment #	Reviewer Name	Comment Date	Application Page #	Text, Figure or Other Document Reference	Comment / Issue	Proposed Revision or Solution (proposed by Fan Lau 12/18/19)	Response	Response Date
1				General	Forward to Fire Department for review	ASAP. Procedural action.	2-10-20 MRP: Fire Truck Test was coordinated with SFFD and performed on Thursday 1/16/20	
2				General	Add another test using the same conditions listed below, but with no valve or air valve riser.	ASAP. Change to design and installation of water main to include a control scenario for main break test.	2-10-20 MRP: Comment was received too late to make this change	
3				General	Part of the Testing Procedure shall include CDD Operations simulating a response to a main break. At a minimum, the CDD leak detection crew, CDD Operations, CDD Engineering, will need to detect and excavate for the main, and the pavement shall be subjected to H-20 loading after the main break has finished (to determine areas of undermining). The backfill material shall be fully cured at the time of this excavation. Excavation may include heavy machinery and hand-digging. the footprint of the excavation may be 6' wide x 5' deep, so that proper clearances can be provided to remove the main. Coordinate this simulation with CDD.	ASAP. Coordinate with CDD leading up to and during main break test.	2-10-20 MRP: Several on site meetings were held with Brian Barry, PE of CDD as well as other CDD representatives to coordinate the test and demonstration. Mr. Barry and other representatives also witnessed the leak repair demonstration on Friday, 1/17/20. As an outcome of this coordination and feedback after the test we have revised the trench details for Low Pressure Water (LPW) lines-- see response to TAP Recommendation #10.	
4				General, C5.0	The test shall occur at 72 psi for 1 hour. The size of the hole can be between 1/4" and 1" diameter.	ASAP. Change to installation of water main and operation of main break test.	2-10-20 MRP: Leak simulation was performed at residual pressure from nearest fire hydrant on 3rd St. which was about 60-70psi. Leak hole was approximately 3/4" round	
5				General	it appears the steel plates may be a bottleneck for the water to escape the trench. Describe how water is anticipated to exit the valve risers and what will happen to the valve covers.  Are the valve covers expected to become airborne?	Written response. If written response is inadequate, possible change to design and installation of water main.	2-10-20 MRP: The demonstrations showed that the water leak flowed past the plate and up the riser. Water gently bubbled up through the Valve Box riser and cover. The cover did not become airborne.	
6				General	The proposed test footprint appears to be too small. CDD requests that the test includes two sticks of pipe (40' length).	ASAP. This may not be possible.	2-10-20 MRP: Comment was received too late to make this change. The truck was accommodated by the addition of temporary ramps/berms on either end of the Pilot as shown in the Pilot Narrative Annotated Plans. The Pilot itself was subject to the full axel loads and outrigger loads of the truck tractor with latter fully extended and rotated.	

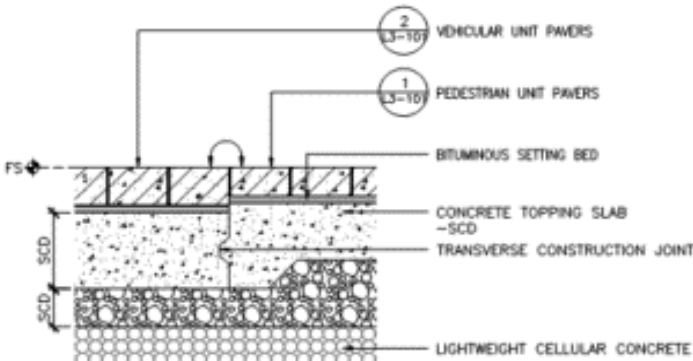
Comment #	Reviewer Name	Comment Date	Application Page #	Text, Figure or Other Document Reference	Comment / Issue	Proposed Revision or Solution (proposed by Fan Lau 12/18/19)	Response	Response Date
7				General	Confirm the pipe will not shift during the test. Provide pipe anchors and supports if appropriate.	Written response. If response is inadequate, possible change to design and installation of water main.	2-10-20 MRP: Confirmed, temporary thrust blocks and pipe restraints were provided and no pipe movement occurred	
8				C5.0	what is the intent of the callout that begins "3'x3'x1" spectacle flange..." ? This configuration needs further clarification. What is preventing these flanges from being be washed away?	Written response. If response is inadequate, possible change to design and installation of water main.	2-10-20 MRP: This was proved to contain the pea gravel surrounding the pipe. Flanges were held in position by positive connection to pipe at either end of the pipe at the face of the LCC mockup.	
9				C6.0	30PCF LCC is typically not allowed in SFWD trenches for trench backfill.  Trench backfill, bedding, and pipe zone immediate backfill should be sand. CDD will need to access the main in a main break in a timely manner. LCC may not allow for this. Additionally, after the main is repaired, CDD will likely restore with sand.  The City has a level-of-service goal to restore water within an 4-hour	ASAP. Comment regarding sand affects installation of water main.	2-10-20 MRP: Trench detail was modified to provide sand, not pea gravel for the full depth of the LPW trench to top of subgrade/bottom of pavement. See response to TAP Recommendation 10	
						Defer. Comment regarding repair to be deferred to maintenance/repair demonstration.	2-10-20 MRP: Repair demonstration took approximately 3 hours from start of pavement removal to backfill. Removal of LCC fill was done within approximately 30 minutes with a combination of excavator and hand digging.	
10				C5.0, modified CDD-LP-250	pipe shall be wrapped in v-bio for test. Add to plans and add callout	ASAP. Change to design and installation of water main.	2-10-20 MRP: Comment receive too late to implement.	
11				modified CDD-LP-250	bedding and pipe zone immediate backfill shall be sand, not pea gravel	ASAP. Change to design and installation of water main.	2-10-20 MRP: See above, sand will be used in SIP.	
12				modified CDD-LP-250	submit product for fiberglass screen. Why fiberglass? Why not steel mesh?	Written response. If response is inadequate, possible change to design and installation of water main.	2-10-20 MRP: This is a moot point since leak detection concept demonstrated in Pilot has been changed in favor of standard sand cover and backfill with filter fabric between trench sides and sand. Fiberglass screen was to prevent pea gravel from clogging riser box. Fiberglass was called out because it is non-corrosive. However this is irrelevant now	
13				C6.0, modified CDD-LP-250	2' clear (Horizontal) and 1' clear (vertical) is needed between outside edge of pipe and the edge of the trench for CDD to remove and replace the main in-kind. The above clearance dimensions assume shoring will be provided and that it can be provided in a way to meet these clearances.  The Engineer of Record shall demonstrate that the walls will not cave in without shoring. Also, the EOR shall demonstrate that shoring can be installed while maintaining these clearances.	ASAP. Change to design and installation of water main.	2-10-20 MRP: Stated clearances were maintained in Pilot and are followed in SIP. Repair demonstrated that walls did not cave without shoring.	
14				General	Upon completion of the water main break simulation, the pavement shall be subjected to vehicular loads to determine where road base has been undermined.	ASAP. Change to operation of main break test.	2-10-20 MRP: Pavement has not been restored in case further investigation is desired, however basecourse can be clearly seen at exposed edge of pavement cut. If desired pavement can be patched following CDD standard "T" patch detail. A vehicle can be driven on patch however it will be hard to actually run traffic because of small size of Pilot.	

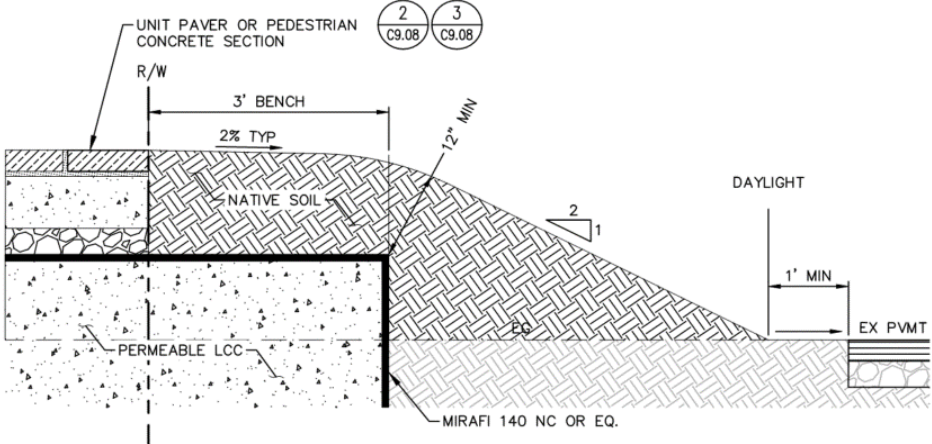


Comment #	Reviewer Name	Comment Date	Application Page #	Text, Figure or Other Document Reference	Comment / Issue	Proposed Revision or Solution (proposed by Fan Lau 12/18/19)	Response	Response Date
15				C7.0	Detail 1 / C7.0 indicates LCC is permeable. How will surrounding trenches and structural soil be protected from undermining? Is water expected wash away the structural soil? what is the trench backfill of the SD? Is water expected to wash away the SD backfill? How about Joint Trench?	Written response. If response is inadequate, possible change to design and installation of water main.	2-10-20 MRP: The LCC is permeable, but cohesive. Unlike soil, flowing water will not erode it at pressure < 2000psi. This is one of the advantages of LCC over conventions soil fill. The structural soil will be separated from LCC with filer fabric to prevent any fines in the structural soil from migrating into LCC-- see response to TAP Recommendations 5 and 16b	

TAP Panel Comments on Pilot Project

1				Narrative Section 1.3	In 1.3, are they just going to survey elevations of sidewalks and manhole rims, or will they also install TBMs (temporary bench marks) to monitor ground heave at various locations on and around the pilot surface?		2-10-20 MRP: Yes ground heave during hydrostatic uplift tests was measured at corners of the surrounding fill just beyond LCC during hydrostatic uplift tests	
2				Sheet C2.0	the “Referenced Documents” section appears to have older version of the GTECH report (the one we have is dated 31 October 2019 but the note says December 18, 2018 and Revised March 1, 2019). and older version of the POSF Building Code is referenced (Note says 2010 but it should be 2016).		1-2-2020 Langan Response: Understood, the project will be permitted under the 2016 SF Building Code.	
3					As requested, Field testing procedures for both Falling-Head Permeability and Natural Saturation Density have been developed, that can be performed on-site at three days. See Appendix L.		2-10-20 MRP: See Exhibit H: LCC Specification and TQA/QC Procedures, a the end of the Consolidated Comment Log	
4					A QC-QA Testing Schedule has been developed for the Pilot Project, and final construction. See Appendix L.		2-10-20 MRP: See comment above	
5					The Long-Term Durability Study is underway. The 28day results show approximately a 25% strength loss over the control dry samples, with no real difference whether submerged in fresh or on-site saltwater. The 56day results will be available on December 13 <sup>th</sup> . Verification by Langan that the loss of strength of the LCC when saturated, will still be acceptable.		2-10-20 MRP: The 90 day test results are included in Appendix G: Long Term Test of LCC Cured in Water at the end of this Log.	
6					• Discussion of the current permeability specs (0.65 to 0.1 cm/sec) will occur. A minimum of E-2 cm/sec has been proposed for the permeable LCC. Discussion with Langan should occur.		1-2-2020 Langan Response: A minimum permeability of E-2 cm/sec is acceptable from a geotechnical standpoint. This can be revised in the final version of the spec after the LCC Pilot Program is completed.	
7					A change to the LCC specifications should include placement when rain is anticipated; Cell Crete uses a criteria of postpone placement if rain of 0.25” within 10-12 hours is forecast.		1-2-2020 Langan Response: This can be added to the final version of the spec after the LCC Pilot Program is completed.	
8					• A field specification for Field Saturation Density of 50pcf or greater has been discussed. This is deemed acceptable for making decisions regarding de-watering terminations. This value has been achieved whenever the permeability is acceptable as well.		2-10-20 MRP: the 50pcf saturated density target has been incorporated in the LCC Specification-- see Exhibit H: LCC Specification and TQA/QC Procedures, a the end of the Consolidated Comment Log	

No.	Comment	Response
1	Construction details of interfaces of LCC, soils, buildings and how to connect utilities to the buildings:	<p>MRP: See Exhibit I: Typical Interface Sections and Details at the end of this Log</p> <p>Langan Response: From a geotechnical standpoint, there is no need for a special construction detail at the interfaces of LCC and neighboring streets. As currently envisioned, there is a layer of filter fabric (Mirafi 140 NC or similar) at what is presumably a near vertical interface. The LCC section on Mission Rock includes unloading of the underlying Bay Mud. This unloading decreases the stress in the Bay Mud beyond the footprint of the LCC. Therefore, if there is some small ongoing settlement in 3rd Street, the use of LCC will allow for a more gradual differential settlement near the interface from this unloading. As currently designed, the vertical development parcels are also designing for up to 1.5 inches of heave or settlement at the building interfaces, including utility connections. Utilities will be designed to accommodate this differential movement through flexible connections.</p>
2	Construction details for interface of raised streets to existing streets	MRP: See Exhibit I: Typical Interface Sections and Details at the end of this Log and Langan Response above
3	Construction details for pavers	<p>MRP: Generally the paver details will be the same as any normal City street. Pavers will be set on aon a bituminous setting bed on a 4" either a concrete slab for sidewalks or an 8" PCC slab in vehicle travel ways. See Exhibit I: Typical Interface Sections and Details at the end of this Log. Paver details can also also be found on the SIP drawings C10 Series: Details; and L3 Series Pavement Details. Below is an example Detail 1/L3-103</p>  <p>The diagram illustrates a cross-section of a pavement structure. At the base is a layer of 'LIGHTWEIGHT CELLULAR CONCRETE'. Above this is a 'CONCRETE TOPPING SLAB -SCD'. A 'TRANSVERSE CONSTRUCTION JOINT' is shown as a vertical line in the concrete slab. Above the concrete slab is a 'BITUMINOUS SETTING BED'. Two types of pavers are shown: 'VEHICULAR UNIT PAVERS' (labeled 2/L3-103) and 'PEDESTRIAN UNIT PAVERS' (labeled 1/L3-103). A 'FS' (Finish) line is indicated on the left side of the pavers. The diagram also shows a 'SCD' (Subgrade) layer below the concrete topping slab.</p>

4	How to construct and maintain LCC roads and sidewalks until and after buildings are built, including how maintain virtually vertical walls of LCC unloaded, loaded by construction or other vehicles, and under vibratory loads like pile driving	<p>MRP: horizontal LCC subgrade will be protected during constuction with 6-8" of AC grindings and/or temporary AC pavement. Vertical faces of LCC at Phase 1 parcels will be protected by the vertical contractors until gradebeams and kneewalls are poured. Construction loads will be kept back from the edges of LCC base on a 1:1 slope back from the base of the exposed LCC-- e.g. for a 4' face of exposed wall, no construction loads would be allowed &lt; 4' back from the edge. If loads were required to be placed closer than that distance, temporary shoring or embankment designed by a qualified shoring engineer would be placed against the face of the LCC to stabilize it. Vertical faces of LCC at future Phase development parcels (e.g. Parcel K and J) will be protected with a temporary earth and LCC berm-- see detail 5/C9.09 on SIP plasn and thumbnail below.</p> <p>Langan Response: Once cured, the LCC can maintain vertical edges, but if any damage occurs during construction, the damaged section of LCC will be replaced</p>  <p>The diagram is a technical cross-section of a road edge. From left to right, it shows: a 'UNIT PAVER OR PEDESTRIAN CONCRETE SECTION' on a 'R/W' (Right of Way) line; a '3' BENCH' with a '2% TYP' slope; 'NATIVE SOIL' above a 'PERMEABLE LCC' (Lightweight Cellular Concrete) subgrade. A vertical line separates the LCC from a '2:1' slope. A '1/2" MIN' dimension is shown for a vertical face. A 'DAYLIGHT' line is shown with a '1' MIN' dimension. An 'EX PVMT' (Existing Pavement) is shown on the right. A 'MIRAFI 140 NC OR EQ.' (MiraFi 140 NC or EQ.) is indicated for the slope. Two circular callouts with numbers 2 and 3 are present, with 'C9.08' below them.</p>
5	How to perform new installations and repairs, including procedures and specifications (routine and emergency work	MRP: This is covered in response to TAP Recommendation 4 and Exhibit F of the comment log
6	Stone columns final design and construction plans	Langan Response: After the ground improvement test program is complete, we will recommend a spacing of the stone columns to be used for the remainder of the site

# **MISSION ROCK LIGHTWEIGHT CELLULAR CONCRETE (LCC) TECHNICAL ADVISORY PANEL (TAP) COMMENT AND RESPONSE EXHIBITS**

Rev. 01  
10 February 2020

Exhibit A: LCC Shear Strength vs. Stress

Exhibit B: Resilient Modulus Definition

Exhibit C: LCC Modulus

Exhibit D: Pavement Design Calculations

Exhibit E: LCC as Subbase Material Thesis

Exhibit F: LCC Excavation and Backfill Procedure

Exhibit G: Long Term Testing of LCC Cured in Water

Exhibit H: LCC Specification (DRAFT)

Exhibit I: Typical Sections at LCC Interfaces

- Interface with Existing Street
- Interface with Vertical Parcel

EXHIBIT A  
LCC Shear Strength vs Stress  
Calculation



Goal: Estimate the Peak cyclic Shear in LCC due to Earthquake

Assum: Using DEEPSOIL profiles already developed for Site specific response spectrum, check what the Shear Stress Ratio ( $\frac{\tau}{\sigma'_v}$ ) is within the upper 10-12' of the soil column.

- $\tau$  = Shear Stress
- $\sigma'_v$  = Effective Stress
- DEEPSOIL can produce ( $\frac{\tau}{\sigma'_v}$ ) shear stress ratio
- Using DEEPSOIL, max  $\frac{\tau}{\sigma'_v}$  in the upper 12' is 0.63 to 0.66
  - $\tau = 0.66 \times \sigma'_v$

Based on Mechanical Properties of Lightweight Cellular Concrete for Geotechnical Applications by Tiwari et.al. (2017)  
the effective friction angle,  $\phi' = 35$  to  $40^\circ$ ,  $C = 36$  to  $78$  kPa  
 $35^\circ$  is considered conservative.

- $S_u = \sigma'_v \tan \phi' + C$
  - Assuming  $C = 0$ ,  $S_{u,LCC} = \sigma'_v \tan(35^\circ) = 0.7 \times \sigma'_v$
  - Peak Shear Stress is  $0.66 \times \sigma'_v$ 
    - $S_{u,LCC} > \text{Peak Shear Stress}$   
 $0.7 > 0.66$
  - Min Unconfined compressive Strength = 40 psi  
is  $S_u = \frac{40 \text{ psi}}{2} = 20 \text{ psi}$  or 2,880 psf
    - if  $\gamma = 30 \text{ psf}$ ,  $\sigma'_v$  for 12' LCC = 360 psf  
 $360 \text{ psf} \times 0.66 << 2,880 \text{ psf}$
- $\sigma'_v$  ranges from 300 to 400 psf  
 $\tau = \sigma'_v \times 0.66 = 200$  to  $265 \text{ psf}$

\* Conclusion: LCC Shear Strength > peak shear stress

EXHIBIT A

Mission Rock Horiz.

LCC Shear Strength vs. Stress

BY FDB

DATE 10/21/17

PROJ. NO. 750604203

CKD.

DATE

SHEET \_\_\_\_\_ OF \_\_\_\_\_

LANGAN



# Mechanical Properties of Lightweight Cellular Concrete for Geotechnical Applications

Binod Tiwari, M.ASCE<sup>1</sup>; Beena Ajmera, A.M.ASCE<sup>2</sup>; Ryan Maw, M.ASCE<sup>3</sup>; Ryan Cole, M.ASCE<sup>4</sup>; Diego Villegas<sup>5</sup>; and Peter Palmerson<sup>6</sup>

**Abstract:** Lightweight cellular concrete provides many advantages in geotechnical applications; however, its use has been limited because of a lack of understanding of its engineering properties. In this study, laboratory soil tests were conducted on lightweight cellular concrete having four different densities, and shear strength parameters, coefficients of permeability, and at-rest earth pressure coefficients were measured. Unconfined compressive strength and as undrained strength properties (total friction angle and cohesion intercept) of partially saturated materials were found to be dependent on the density of the lightweight cellular concrete specimen. However, the effective friction angle and cohesion intercept of the saturated materials were independent of the test unit weight over the range of stresses tested. The effective friction angle and cohesion values of the lightweight cellular concrete materials, determined from direct simple shear tests, were 35° and 36 kPa, respectively. Back-pressure saturated samples from isotropically consolidated drained and isotropically consolidated undrained triaxial tests yielded an effective friction angle of 34° and a cohesion intercept of 78 kPa, similar to the results obtained from the constant-volume direct simple shear tests. The at-rest earth pressure coefficient was found to range between 0.2 and 0.5, while Poisson's ratio for these materials was observed to range between 0.20 and 0.30. Recommendations are made for appropriate geotechnical engineering properties for the use of lightweight cellular concrete materials in earth-retaining structures. DOI: 10.1061/(ASCE)MT.1943-5533.0001885. This work is made available under the terms of the Creative Commons Attribution 4.0 International license, <http://creativecommons.org/licenses/by/4.0/>.

## Background

Lightweight concrete has been implemented in civil engineering construction for approximately 3,000 years, with the use of volcanic ash as a fine aggregate (Maruyama and Camarini 2015; Chandra and Bernisson 2003). Advances in technology and new materials have led to advancements in strength, durability, and production consistency. Today, lightweight cellular concrete (LCC) is gaining popularity in many construction applications such as to reduce earth pressures, minimize dynamic forces, mitigate settlement, and absorb earthquake forces in subsurface structures. As a result of these new applications, a better understanding is needed regarding the engineering properties of these materials.

The vesicular structure of LCC is obtained when air bubbles develop in a cement paste by stirring in water and proprietary admixtures (Maruyama and Camarini 2015). LCC poses a number of benefits, such as high durability, noncorrosivity, permanence,

lightweight density, high freeze-thaw resistivity, and low permeability, low water absorption capacity, and it provides high damping against dynamic loads. In addition, LCC provides a more economical alternative than traditional methods for reducing loads on different infrastructure (Maruyama and Camarini 2015; Tikalsky et al. 2004; LaVallee 1999; Aberdeen Group 1963).

Several researchers have examined different properties of LCC including thermal conductivity (Neville 2002; Loudon 1979; Aberdeen Group 1963), drying shrinkage (Aberdeen Group 1963; Narayanan and Ramamurthy 2000), and thermal expansion (Aberdeen Group 1963). Narayanan and Ramamurthy (2000) found that the unconfined compressive strength (UCS) of LCC increases linearly with an increase in density and inversely with an increase in moisture content. LaVallee (1999) and Zaidi et al. (2008) also reported values for the UCS. Compressive strength values can vary substantially based on the foaming agent used when preparing the LCC (Aberdeen Group 1963).

Many of the mechanical properties of LCC are currently unknown; an understanding of these properties is necessary in order to appropriately incorporate LCC into geotechnical applications. In this study, UCS, total and effective shear strength parameters, consolidation characteristics, at-rest earth pressure ( $K_0$ ) coefficients, hydraulic conductivity, and Poisson's ratio values were measured for LCC samples prepared at four different test densities. Using this information, recommendations for design of the backfill of mechanically stabilized earth (MSE) walls using LCC are provided.

## Materials and Methods

### LCC Casting and Curing

The LCC used in this study was prepared using two concurrent processes. In the first of these, one part Elastizell Foam Concentrate, a protein-based biodegradable surfactant by-product of the

<sup>1</sup>Professor, Dept. of Civil and Environmental Engineering, California State Univ., Fullerton, 800 N State College Blvd., E-419, Fullerton, CA 92834. E-mail: btiwari@fullerton.edu

<sup>2</sup>Assistant Professor, Dept. of Civil and Environmental Engineering, California State Univ., Fullerton, 800 N State College Blvd., E-318, Fullerton, CA 92834 (corresponding author). E-mail: bajmera@fullerton.edu

<sup>3</sup>Project Engineer, Gerhart Cole, Inc., 668 E 12225 S, Suite 203, Draper, UT 84020. E-mail: ryanm@gerhartcole.com

<sup>4</sup>Principal, Gerhart Cole, Inc., 668 E 12225 S, Suite 203, Draper, UT 84020. E-mail: ryan@gerhartcole.com

<sup>5</sup>Engineer, Cell Crete Corporation, 135 E Railroad Ave., Monrovia, CA 91016. E-mail: dvillegas@cell-crete.com

<sup>6</sup>Geotechnical Engineer, Cell Crete Corporation, 135 E Railroad Ave., Monrovia, CA 91016. E-mail: ppalmerson@cell-crete.com

Note. This manuscript was submitted on January 27, 2016; approved on November 4, 2016; published online on March 2, 2017. Discussion period open until August 2, 2017; separate discussions must be submitted for individual papers. This technical note is part of the *Journal of Materials in Civil Engineering*, © ASCE, ISSN 0899-1561.

food industry (EF 2015), was added to forty parts (1:40) water. The concentrate and water mixture were mechanically agitated through a small nozzle to produce a foam and subjected to compressed air action at a high pressure. Simultaneously, cement and water were mixed together using a specific mix design. The mixing occurred in a customized concrete mixer that was coupled with a progressing cavity pump. A volumetric blending system was used to merge the cement and water to produce the neat cement slurry, which was then pumped into a proprietary blending system where the pre-formed foam was introduced. This introduction produces an air-filled cellular concrete whose density is dependent on the ratio of foam and neat cement grout. Samples were cured in a moisture- and temperature-controlled environment, following the curing process outlined in ASTM C495/C495M-12 (ASTM 2012).

For each specimen tested, three different unit weight values were determined: (1) unit weight of the specimen prior to trimming, (2) test unit weight, and (3) dry unit weight of the specimen after it was oven-dried for at least 24 h. The unit weights prior to trimming ranged from 3.1 to 3.8 kN/m<sup>3</sup>, 3.4 to 4.7 kN/m<sup>3</sup>, 4.4 to 6.1 kN/m<sup>3</sup>, 3.8 to 6.6 kN/m<sup>3</sup>, and 4.9 to 7.5 kN/m<sup>3</sup> for Class II, Batch 1; Class II, Batch 2; Class IV; 7.1 kN/m<sup>3</sup> cast unit weight; and 8.6 kN/m<sup>3</sup> cast unit weight LCC samples. Similarly, the test unit weight ranged from 3.0 to 3.8 kN/m<sup>3</sup>, 3.3 to 5.0 kN/m<sup>3</sup>, 4.5 to 5.4 kN/m<sup>3</sup>, 5.0 to 6.8 kN/m<sup>3</sup>, and 5.1 to 7.5 kN/m<sup>3</sup>, respectively. The maximum cast unit weight was used to separate the four classes of LCC materials. The class definitions suggested in Caltrans (2013) were adopted in this study. The dry unit weight was not measured in the Class-II Batch-1 specimens, but ranged from 2.3 to 3.6 kN/m<sup>3</sup>, 3.3 to 4.3 kN/m<sup>3</sup>, 4.4 to 5.8 kN/m<sup>3</sup>, and 4.4 to 6.1 kN/m<sup>3</sup>, respectively, for the remaining LCC batches.

### Unconfined Compression Strength Test

Shear strength testing was performed on all of the LCC batches to characterize drained and undrained strength behavior. A strain rate of 0.5%/h, following the recommendations in ASTM D2166-00 (ASTM 2000), was selected. Shearing continued until the peak strength was measured. If the peak strength was not achieved by 15% axial strain, testing was terminated. The specimen was then removed from the apparatus and placed in an oven to dry for 24 h in order to measure its moisture content and determine its dry unit weight.

### Direct Shear Test

The DS test was conducted in accordance to ASTM D3080-11 (ASTM 2011c). The moist (partially saturated) specimens were first consolidated to the desired stress. Because the samples were partially saturated, the term *consolidation* is not appropriate for this type of DS testing. However, because a standard is not available for the DS test of partially saturated soils, and to follow the ASTM procedure for saturated soils, the term *consolidation* is used in this paper to refer to vertical deformation under a static vertical stress prior to application of shear stress. The shearing rates were set based on the results obtained through vertical deformation time data following the ASTM procedure. The strength measured with the DS testing was considered total stress in this study. In this study, a specimen was consolidated to a stress of 25 kPa, three each to stresses of 50, 75, and 100 kPa, one specimen to a stress of 200 kPa, and one specimen to a stress of 350 kPa. The primary consolidation was monitored with the use of a real-time computer-generated logarithm of time versus deformation curves. Once the primary consolidation was complete, the specimen was sheared at a rate of 0.1 mm/min, which was the fastest shearing rate determined from the consolidation data using ASTM D3080-11,

assuming that the peak shear stress would occur at 1 mm shear displacement, until the peak strength was measured. If the peak strength was not obtained within 7 mm of horizontal displacement, the test was terminated at that point. After the shearing phase, the specimen was removed from the DS box and placed in an oven for at least 24 h to measure the moisture content and determine the dry unit weight of the specimen.

### Direct Simple Shear Test

DSS tests were conducted using a Norwegian Geotechnical Institute (NGI) device (Bjerrum and Landva 1966; Øyvik et al. 1987). In this device, the sample was consolidated to the desired stress. For each batch, a total of 11 static DSS tests at four different consolidation stresses were performed. Specifically, three samples were each consolidated to a stress of 25, 50, and 100 kPa, and two samples were consolidated to a stress of 350 kPa. A real-time relationship between the logarithm of time and the vertical deformation was monitored to determine the completion of primary consolidation, at which point the specimens were subjected to undrained strain-controlled shearing at a rate of 5%/h, as recommended in ASTM D6528-07 (ASTM 2007). The shearing phase was continued until the peak shear strength was measured or a maximum of 25% shear strain was reached. The specimen was then removed from the apparatus and placed in an oven for at least 24 h to determine the moisture content and dry unit weight.

The majority of LCC specimens were back-pressure saturated using a permeameter connected to the sample, with cell pressure applied using a triaxial test assembly. The saturated sample was used to conduct a static DSS test using the process previously described. The sample was submerged in water as soon as it was removed from the permeameter and during sample preparation and testing. Several LCC samples were also tested without back-pressure saturation and tested in the moist condition. The effective shear strength parameters obtained from the saturated specimens were similar to those obtained from the partially saturated (i.e., moist) specimens. The advantage of the constant-volume DSS device used in this study is that the partially saturated specimens yielded results equivalent to those for the saturated specimens.

### Isotropically Consolidated Drained and Isotropically Consolidated Undrained Triaxial Tests

Triaxial shear strength testing was performed on cured, continuous (no visible cracks) LCC to characterize drained and undrained shear strengths. The range of the  $B$  values varied between samples tested and reached up to 0.94. The loading rate was calculated using both guidance provided by Bishop and Henkel (1967) from measured rates during consolidation and observations during testing. Isotropically consolidated drained (CID) triaxial testing was performed in general accordance with ASTM D7181-11 (ASTM 2011a) and Bureau of Reclamations Standard USBR 5755 (USBR 1990). Similarly, isotropically consolidated undrained (CIU) triaxial testing was performed in general accordance with ASTM D4767-11 (ASTM 2011b) and USBR 5750 (USBR 1990). Method A was selected to estimate the effective area of consolidated samples. Given the vesicular nature of the samples, no filter paper was used in sample preparation. Double membranes were used in testing, and appropriate corrections were applied to the testing results.

### $K_0$ Consolidation

The  $K_0$  consolidation triaxial testing was performed to measure Poisson's ratio and at-rest or  $K_0$  lateral stresses developed through consolidation by adjusting the lateral stresses to maintain no radial

volume change. Sample testing consisted of axial loading applied by the triaxial piston with an automated program, *TruePath* (Geotac 2005), adjusting the cell pressure to match the horizontal pressure transfer from sample consolidation. The automated balancing of cell pressure provided a direct measurement of the at-rest horizontal pressure of the tested sample under axial loading. The  $K_0$  consolidation testing was performed using USBR 5740-89 (USBR 1990).

### Hydraulic Conductivity

Hydraulic conductivity testing was performed using a flexible wall (i.e., membrane) and a triaxial cell in accordance with Method C of ASTM 5084-10 (ASTM 2010). The hydraulic conductivity testing included double membranes on the sample. An appreciable change in measured hydraulic conductivity values as a result of different confining stresses was not observed. The change in hydraulic conductivity did not appear to change with the amount of pore volumes of water tested through the samples.

### One-Dimensional Consolidation

One-dimensional (1D) consolidation testing was performed for a comparison with  $K_0$  loading and material behavior from one ID and triaxial loadings. Additionally, 1D consolidation testing was performed to measure the sensitivity of the sample to yielding and settlement versus axial loading following ASTM D2435/D2435M-11 (ASTM 2011d) and USBR 5700 (USBR 1990).

## Results and Discussion

### UC Test

Visual inspection of the LCC samples revealed that the vesicular sections of cellular concrete were crushed under unconfined compression (UC) loads. Failure initiated with the development of vertical cracks; with continued application of axial strain, pieces of LCC material would break away from the specimen along the radial directions. For concrete cylinders, this type of failure mode would be described as columnar, defined according to ASTM C39-15 (ASTM 2015). Pictures of failed specimens are available in Tiwari (2016).

For each group of specimens tested, the typical stress-strain curves obtained from the UC tests are shown in Fig. 1. Ductile behavior was observed in the Class-II and Class-IV specimens tested, whereas the specimens with cast unit weights of 7.1 and 8.6 kN/m<sup>3</sup> tended to exhibit more brittle behavior. Specifically, an increase in material unit weight resulted in an increase in peak strength. A decrease in the strain required to reach this peak strength as the test unit weight of the LCC specimens increased was also noted.

Fig. 1 shows that a typical curve of the UCS of LCC is dependent on the unit weight of the specimen tested. Fig. 2 shows the relationship between the test unit weight and the measured UCS. The results are presented separately for each batch tested. An increase in the air volumes present in lighter samples (samples with lower test unit weights) in comparison with the denser samples resulted in a decreased UCS. Thus, as shown in Fig. 2, as the test unit weight of the specimen decreases, the UCS also decreases. A best-fit polynomial regression line relating the UCS to the test unit weight is also shown in Fig. 2. The equation for the regression line is provided in Eq. (1), where  $UCS$  is the unconfined compressive strength in kPa and  $\gamma$  is the test unit weight in kN/m<sup>3</sup>. The coefficient of determination of this regression line is 0.94. Lines

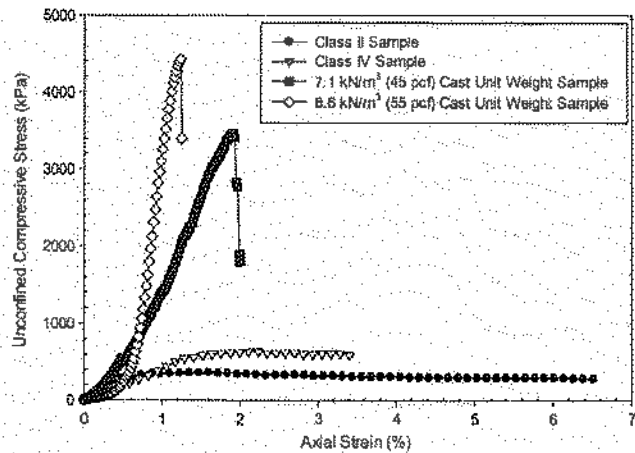


Fig. 1. Typical stress-strain curves from the UC test

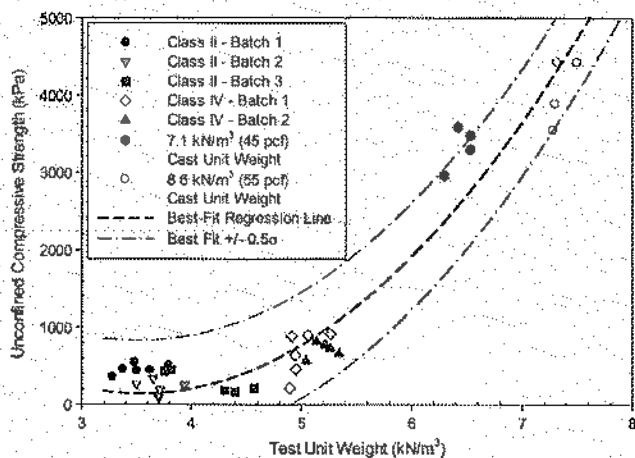


Fig. 2. Relationship between unconfined compressive strength of LCC specimens with their corresponding test unit weights

representing  $\pm 0.5$  standard deviations ( $\sigma$ ) from the best-fit regression are also shown in Fig. 2. All of the data, except one point, were observed to lie within the bounds established by these lines.

$$UCS = 291.98\gamma^2 - 2063.4\gamma + 3785 \quad (1)$$

### DS Test

Fig. 3 shows the shear stress versus horizontal displacement behavior of the LCC specimens at four normal stresses, as obtained from the DS tests. The results are for the LCC batch with a cast unit weight of 7.1 kN/m<sup>3</sup>. The shear stress versus horizontal displacement was similar in all LCC specimens tested and are available in Tiwari (2016). Presented in Fig. 4 are the Mohr-Coulomb failure envelopes obtained from the DS tests. As can be seen, an increase in the test unit weight of the specimens results in a significant increase in the cohesion intercept and a slight increase in the total friction angle of the LCC specimens. Notably, the term *total friction angle* used in this study corresponds to the friction angle of partially saturated LCC specimens obtained from the DS tests

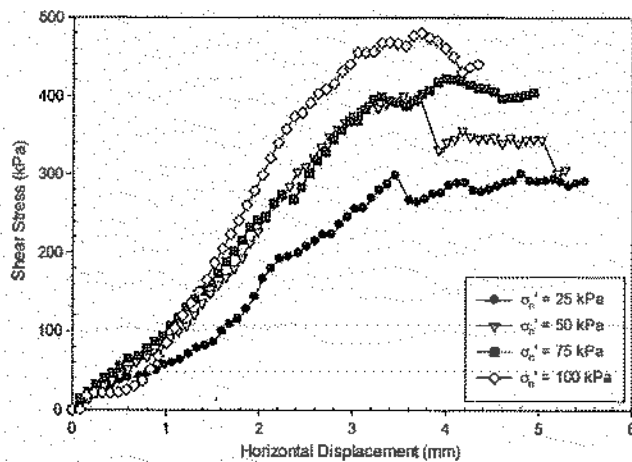


**Fig. 3.** Shear stress versus horizontal displacement from the DS tests on LCC specimens with a cast unit weight of  $7.1 \text{ kN/m}^3$  at four normal stresses

performed at the shearing rate specified earlier. Eq. (2) can be used to estimate the total friction angle ( $\varphi$ ), in degrees, of the specimen using the average test unit weight ( $\gamma$ ), given in  $\text{kN/m}^3$ . The coefficient of determination for Eq. (2) is 0.91. The relationship between the cohesion and average test unit weight is given by Eq. (3), which has a coefficient of determination of 0.60. The average test unit weight ( $\gamma$ ) is expressed in  $\text{kN/m}^3$  and the cohesion in kPa

$$\varphi = 1.187\gamma + 15.062 \quad (2)$$

$$c = 274.386\gamma - 654.958 \quad (3)$$

### DSS Test

Typical curves for shear stress versus shear strain and pore water pressure versus shear strain obtained from the constant-volume DSS test are shown in Fig. 5, which contains the results for a Class-II Batch-2 sample at a consolidation pressure of 100 kPa. The response observed in all LCC specimens was similar and can be found in Tiwari (2016). An increase in the normal stress corresponded to an increase in the shear stress and a decrease in the shear strain required to achieve the peak strength. Similarly, the peak shear stress increased as the test unit weight of the LCC specimens increased. The shear strain required to reach the peak strength decreased as the test unit weight increased.

The relationship between the undrained strength ratios, defined as shear strength normalized by consolidation pressure, and the consolidation pressure of the tested LCC materials is shown in Fig. 6, where the value of the undrained strength ratio does not decrease significantly when the consolidation pressure exceeds approximately 150 kPa. The LCC materials with lower test unit weights tend to have slightly lower undrained strength ratios at the same consolidation pressure compared with the materials with higher test unit weights. The effective stress failure envelope is shown in Fig. 7, where the effect of the test unit weight of the LCC is eliminated by examining the effective stress results obtained in the DSS device. The effective friction angle was computed to be  $35^\circ$  with the cohesion intercept equal to 36 kPa. Lines representing  $\pm 0.5$  standard deviation ( $\sigma$ ) from the failure envelope are also included in the figure. As can be observed, all of the data points obtained fell within these bounds.

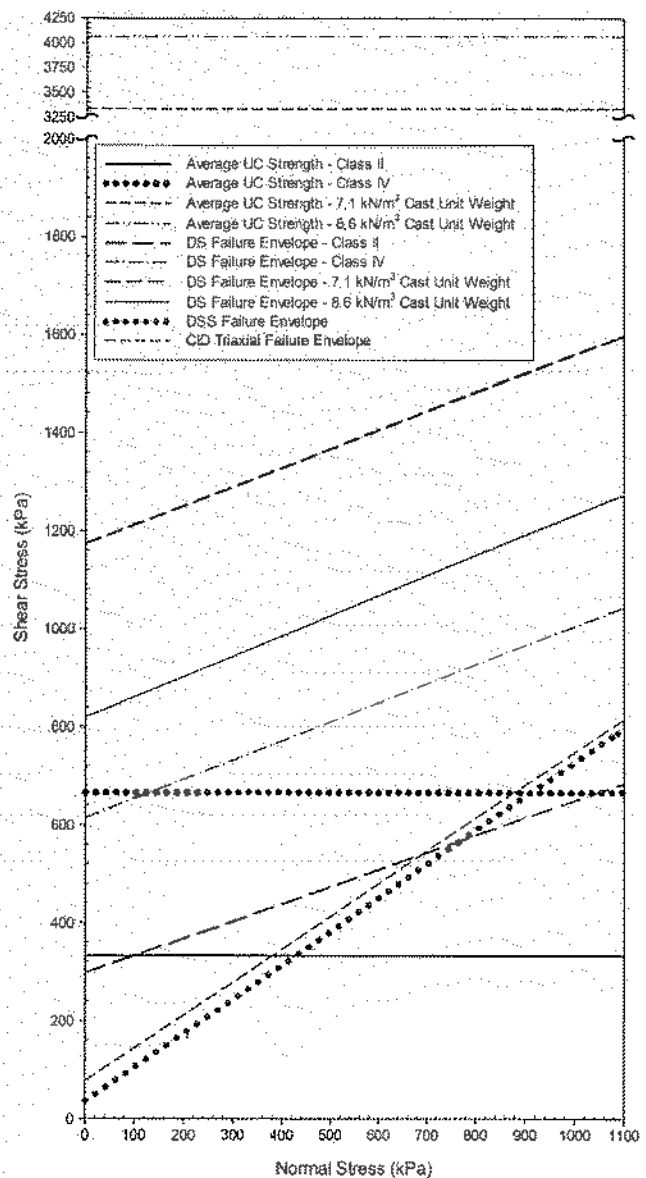


**Fig. 4.** Average shear envelopes of all sample types obtained from the DS, DSS, and CID triaxial tests

### CID and CIU Tests

Typical CID and CIU test results for the Class-II and Class-IV LCC samples are shown in Fig. 8. The were converted into a shear envelope and exhibited a cohesion intercept of 78 kPa and an effective friction angle of  $34^\circ$ , as shown in Fig. 4. This effective friction angle compares well with the results obtained from the DSS test, which is explained later.

### $K_o$ Consolidation

A summary of the measured  $K_o$  for two of the Class-II and Class-IV LCC samples are provided in Fig. 9. These plotted test results provide a comparison of the measured  $K_o$  pressures for the two LCC classes. As can be observed in Fig. 9, the  $K_o$  values ranged from approximately 0.4 to 0.5 for Class-II and from 0.2 to 0.3 for Class-IV. Also, as the test unit weight of the material increases  $K_o$  is found to decrease. Moreover,  $K_o$  decreases from 1.6 to the values

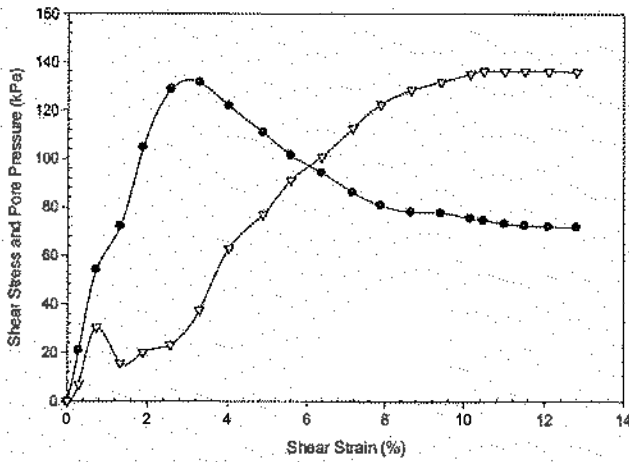


**Fig. 5.** Typical shear stress and pore pressure response with shear strain observed in the DSS device (presented here for the Class-II Batch-2 specimen at 100-kPa consolidation pressure)

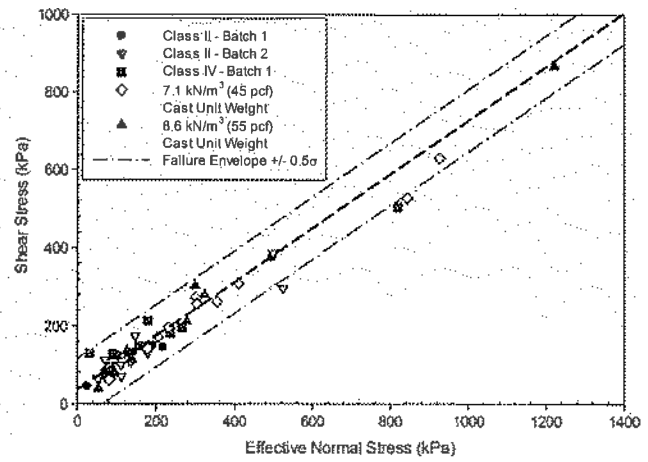


**Fig. 7.** Effective stress failure envelope obtained from the DSS tests for LCC specimens

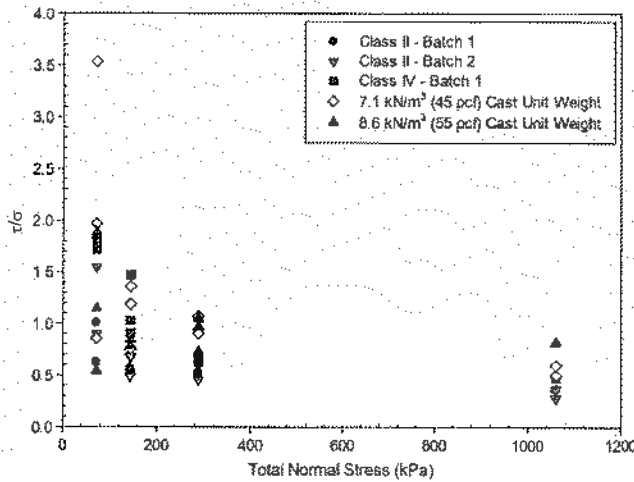


**Fig. 6.** Relationship between undrained strength ratio and consolidation pressure obtained from the DSS tests for LCC specimens

noted previously for an increase in major principal stress from approximately 10 to 150 kPa and remained more or less constant for higher major principal stresses. In Fig. 9, the lower value of  $K_o$  is observed after exceeding small axial strains.

Poisson's ratios relative to the major principal stress and axial strain are also shown in Fig. 9 for both Class-II and Class-IV LCC samples. The test results show a horizontal pressure exerted from the sample under axial loading and variation in the ratio of lateral transfer based on loading conditions. As can be observed, the Poisson's ratio generally ranges from 0.20 to 0.30.

### 1D Consolidation

A summary of the consolidation results for the Class-II and Class-IV LCC samples is shown in Fig. 10, where the test results indicate a notable difference in the elastic behavior of the two classes of cellular concrete. Class-IV specimens yield at a higher pressure with a lower deformation under higher vertical stresses. Also, Class-II and Class-IV LCC materials exhibit compressive

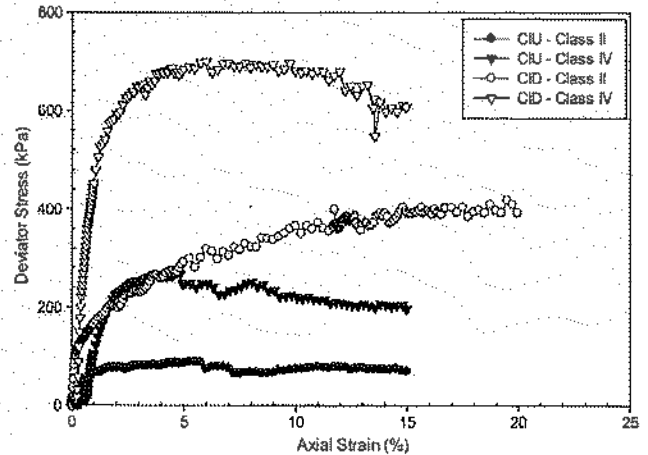


**Fig. 8.** Typical CID and CIU test results for Class-II and Class-IV LCC materials obtained at 86.2-kPa cell pressure

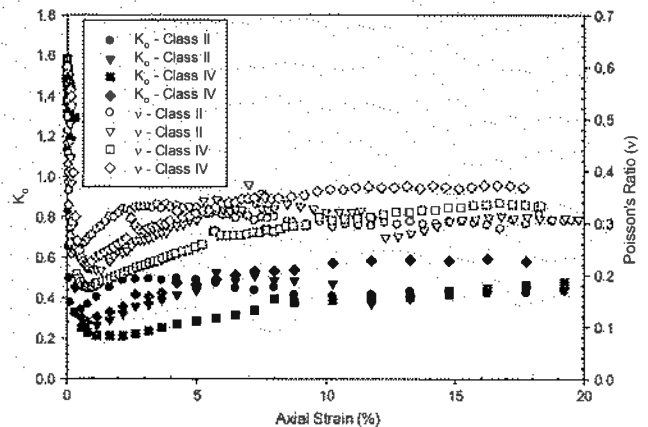


**Fig. 9.** Variation in  $K_o$  and Poisson's ratio with axial strain



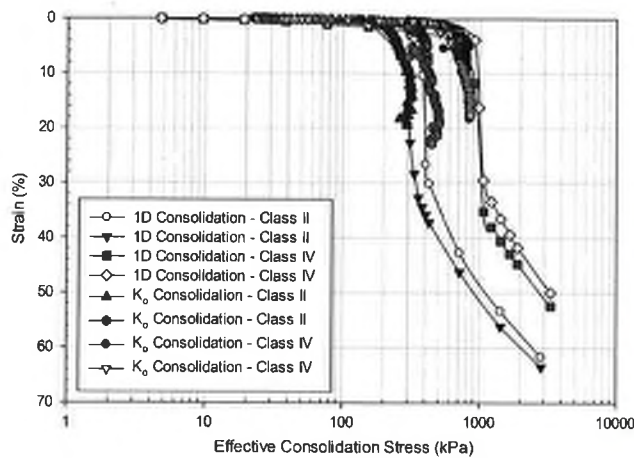


Fig. 10. Summary of consolidation test results for Class-II and Class-IV samples

behavior similar to that of soil specimens preconsolidated to equivalent pressures of 300 and 700 kPa, respectively.

The  $K_0$  consolidation test data are plotted in Fig. 10 to compare the consolidation curves developed from triaxial loading with that of one-dimensional loading. As can be seen, a reasonable agreement between  $K_0$  consolidation and 1D consolidation obtains under lower stresses, but the results diverge at higher stresses. The range over which the data appear to match between the two tests indicates that under lower loading pressures and strains/deformation,  $K_0$  pressures are more consistent but at higher strains/variability in those parameters may increase. As Fig. 10 shows, the samples exhibit significant strain for vertical stresses higher than 300 and 700 kPa for Class-II and Class-IV materials, respectively.

### Permeability

Reported values of hydraulic conductivity have ranged significantly with historic data on the order of  $10^{-6}$  cm/s (Soil Exploration Company 1981). Additional guidance provided by the U.S. Army Corps of Engineers (USACE 1996) cites typical values in the range of  $10^{-4}$  to  $10^{-5}$  cm/s. In this study, the measured hydraulic conductivity ranged from  $1.7 \times 10^{-4}$  to  $7.7 \times 10^{-4}$  cm/s in the Class-II specimens and from  $9.5 \times 10^{-4}$  to  $1.2 \times 10^{-3}$  cm/s in the Class-IV specimens. Given the variability in referenced hydraulic conductivity, the limited data, and the historic nature of the testing, additional hydraulic conductivity testing is recommended for future use.

## Application of LCC in Geotechnical Applications

### Recommended Mechanical Properties of LCC for Design

Presented in Fig. 4 are the combined results that show the average shear strength of LCC materials of different unit weights tested under different conditions. As can be observed, results obtained from the CID triaxial tests are plotted between the shear envelopes obtained with DSS and DS devices. Direct shear samples exhibit high cohesion values mainly due to the apparent cohesion resulting from suction in the partially saturated material. Unfortunately, the suction values could not be measured using the existing experimental setup. The shear envelope obtained with the DSS device represents the shear strength of saturated LCC samples, as a result

of the sample preparation sequence outlined previously. Moreover, DSS test results for samples with different unit weights and different degrees of saturation were plotted around a single shear envelope. Therefore, the effective friction angle obtained from the DSS test, which provided the conservative value (i.e., the value for the saturated condition) can be considered for design of engineering structures with or on the tested LCC materials. The at-rest earth pressure, obtained from the  $K_0$  consolidation tests, ranged from 0.2 to 0.5. Using the effective friction angle of  $35^\circ$ , obtained from the constant-volume DSS test, the calculated at-rest earth pressure coefficient, using Jaky (1944), was close to the upper limit of the measured  $K_0$  value range. Therefore, an effective LCC friction angle of  $35^\circ$  for design purposes should provide a reasonably conservative estimate of the drained strength for saturated samples. However, the drained shear strength should be limited by the strengths obtained from the UC tests. Because there is only a very small possibility that LCC materials will be fully saturated under normal conditions, use of total shear strength obtained with the DS tests may also provide reasonable estimates of shear strength. The shear strength obtained with the DS tests with no cohesion led to the friction angle of  $40^\circ$ , which was higher than the effective friction angles obtained for saturated LCC. However, the corresponding shear strength for partially saturated LCC was higher than that for fully saturated LCC up to certain effective vertical stress and lower for effective vertical stress higher than this limiting effective vertical stress. The design friction angle may be increased up to  $40^\circ$  with Class-II or Class-IV LCC subjected to normal stresses lower than 400 kPa, 7.1-kN/m<sup>3</sup> cast unit weight LCC subjected to normal stresses less than 500 kPa, and 8.6-kN/m<sup>3</sup> cast unit weight LCC subjected to normal stresses less than 1,000 kPa.

### Use of LCC for Backfill of Mechanically Stabilized Earth Walls

Current retaining/mechanically stabilized earth (MSE) wall design does not include cohesion because it is considered to be largely a transient property in granular materials. Therefore, it is recommended, at this stage of development, to use an effective friction angle of  $35^\circ$  and ignore cohesion when calculating external stability of retaining/MSE walls for long-term conditions. The effective friction angle may be increased up to  $40^\circ$  when Class-II or Class-IV 7.1 kN/m<sup>3</sup> cast unit weight and 8.6 kN/m<sup>3</sup> cast unit weight LCC is subjected to normal stresses less than 400, 500, and 1,000 kPa, respectively. It may be appropriate to include cohesion in temporary construction cases based on engineering judgment concerning duration and loading conditions. Although LCCs in typical wall conditions do not have a high likelihood of saturation, saturation is critical for accurate measurements of volume change for drained tests and generated pore pressures for undrained tests [ASTM STP977 (ASTM 1988)]. Given these considerations and assumptions, using the effective friction angle measured under near saturated laboratory conditions provides what is believed to be a reasonably conservative approach. The significantly higher cohesion obtained with the DS test for unsaturated LCCs indicates that LCC backfills may be temporarily freestanding and may not result in significant earth pressures under short-term conditions. However, given the potential for long-term material degradation and/or saturation under field conditions, which were outside the scope of this study, it is recommended that a traditional earth pressure approach using an effective friction angle from saturated testing (i.e.,  $35^\circ$ ) be used to evaluate the external stability of an MSE wall. This approach should also include consideration of capping or limiting strengths below ultimate values (i.e., UCS or



crushing) and sensitivity of the structure to settlement deformations. Additional research should be performed to evaluate reinforcement-LCC interface shear strength for MSE wall internal stability and for external stability when Coulomb's active earth pressure coefficients are used.

The application of the material characteristics outlined here should be used only after careful consideration by an experienced design professional. A laboratory testing program using an appropriate test method (i.e., DSS, CID, CIU) should be performed for the proposed LCC mix design under project-specific conditions.

## Summary and Conclusions

In order to characterize LCC materials for use in earth-retaining structures, LCC samples having of four unit weights were tested using various shear-testing devices and conditions to measure shear strength parameters, coefficients of permeability, and at-rest earth pressure coefficients. The results lead to the following conclusions:

- UCS, total friction angle and cohesion of the partially saturated LCC after 28 days of curing exhibited a strong correlation with the test unit weights;
- The effective stress failure envelopes for saturated LCC samples tested with the constant-volume DSS test exhibited an average effective friction angle of  $35^\circ$  and cohesion of 36 kPa;
- Results obtained from the CIU and CID triaxial tests on back-pressure saturated LCC samples exhibited an average effective friction angle of  $34^\circ$  and cohesion of 78 kPa, which were similar to the DSS test results; and
- The  $K_0$  values ranged from 0.2 to 0.5; the values of Poisson's ratio ranged from 0.20 to 0.30; The Class-II and Class-IV materials exhibited significant deformation at vertical stresses higher than 300 and 700 kPa, respectively.

It is recommended that cohesion be ignored and that the effective friction angle of saturated LCC ( $35^\circ$ ) be used for the materials characterized in this study. It is also suggested that external stability be evaluated using Rankine's active earth pressure because of the backfill of earth-retaining structures such as MSE walls. Interface friction between reinforcement and LCC materials along with wall-LCC materials should be measured separately for MSE wall internal stability and in case Coulomb's active earth pressure coefficients are used.

## Acknowledgments

This project involved the support of many individuals and organizations. The authors appreciate the help of graduate students at California State University, Fullerton, including Miss Sneha Upadhyaya, Mr. Duc Tran, Mr. Janak Koirala, Mr. Prakash Khanal, and Miss Smriti Dhital for conducting laboratory tests and analyzing the data. Mr. Hector Zazueta's help in the test setting is also highly appreciated. The authors also recognize the observations and insights provided by Gerhart Cole, Inc., team and particularly Mr. Zach Gibbs, who primarily performed the laboratory testing at Gerhart Cole.

## References

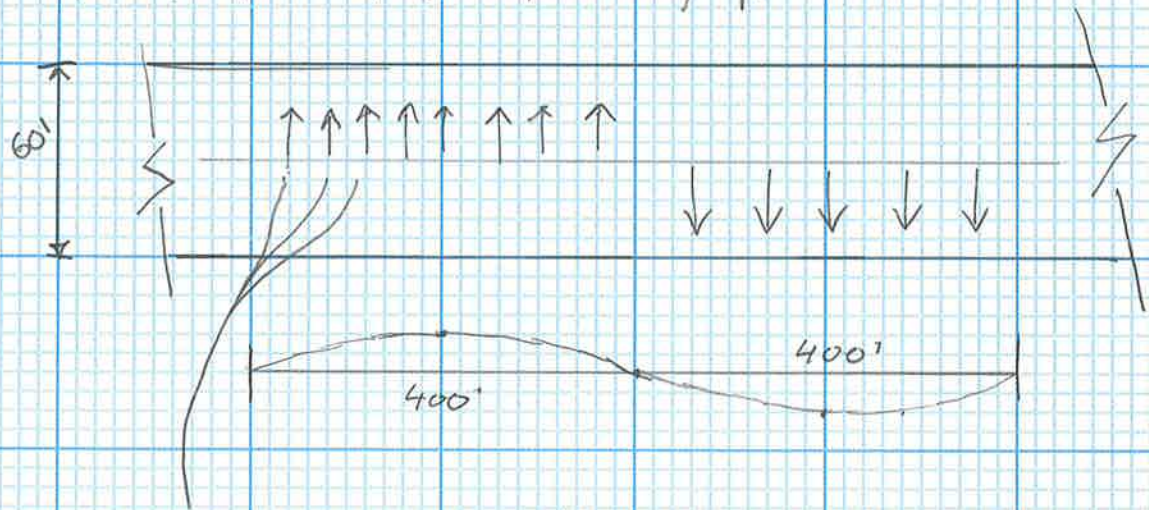
- Aberdeen Group. (1963). "Cellular concrete." *Publication No. C630005*, Aberdeen Group, Boston.
- ASTM. (1988). "Advanced triaxial testing of soil and rock." *ASTM STP977*, West Conshohocken, PA.
- ASTM. (2000). "Standard test method for unconfined compressive strength of cohesive soil." *ASTM D2166-00*, West Conshohocken, PA.
- ASTM. (2007). "Standard test method for the consolidated undrained direct simple shear testing of cohesive soils." *ASTM D6528-07*, West Conshohocken, PA.
- ASTM. (2010). "Standard test methods for measurement of hydraulic conductivity of saturated porous materials using a flexible wall permeameter." *ASTM D5084-10*, West Conshohocken, PA.
- ASTM. (2011a). "Method for consolidated drained triaxial compression test for soils." *ASTM D7181-11*, West Conshohocken, PA.
- ASTM. (2011b). "Standard test method for consolidated undrained triaxial compression test for cohesive soils." *ASTM D4767-11*, West Conshohocken, PA.
- ASTM. (2011c). "Standard test method for direct shear tests of soils under consolidated drained conditions." *ASTM D3080-11*, West Conshohocken, PA.
- ASTM. (2011d). "Standard test methods for one-dimensional consolidation properties of soils using incremental loading." *ASTM D2435/D2435M-11*, West Conshohocken, PA.
- ASTM. (2012). "Standard test method for compressive strength of lightweight insulating concrete." *ASTM C495/C495M*, West Conshohocken, PA.
- ASTM. (2015). "Standard test method for compressive strength of cylindrical concrete specimens." *ASTM C39-15*, West Conshohocken, PA.
- Bishop, A. W., and Henkel, D. J. (1967). *The measurement of soil properties in the triaxial test*, Edward Arnold Publishers, London.
- Bjerrum, L., and Landva, A. (1966). "Direct simple shear tests on a Norwegian quick clay." *Geotechnique*, 16(1), 1–20.
- Caltrans. (2013). "Notice to bidders and special provisions for construction on State Highway in Contra Costa County in and near Martinez from Arthur Road undercrossing to 0.5 mile north of Mococo overhead." *Project No. 0400000967*, Sacramento, CA.
- Chandra, S., and Brentsson, L. (2003). *Lightweight aggregate concrete science, technology and applications*, Standard Publisher Distributors, Göteborg, Sweden.
- Dyvik, R., Berre, T., Lacasse, S., and Raadim, B. (1987). "Comparison of truly undrained and constant volume direct simple shear tests." *Geotechnique*, 37(1), 3–10.
- EF (Engineered Fill). (2015). "Elastizell specification section 0223." (<http://elastizell.com/fillspec.html>) (Apr. 13, 2015).
- Geotac (Geotechnical Test Acquisition and Control). (2005). "TruePath version 5.4.4." Houston.
- Jaky, J. (1944). "The coefficient of earth pressure at rest." *J. Soc. Hungarian Arch. Eng.*, 7, 355–358.
- LaVallee, S. (1999). "Cellular concrete to the rescue." *Publication No. C99A039*, Aberdeen Group, Boston.
- Loudon, A. G. (1979). "The thermal properties of lightweight cellular concretes." *Int. J. Lightweight Concr.*, 1(2), 71–85.
- Manyama, R. C., and Camarini, G. (2015). "Properties of cellular concrete for filters." *IACSIT Int. J. Eng. Technol.*, 7(3), 223–228.
- Narayanan, N., and Ramamurthy, K. (2000). "Structure and properties of aerated concrete: A review." *Cem. Concr. Compos.*, 22(5), 321–329.
- Neville, A. M. (2002). *Properties of concrete*, Pearson Education, Essex, U.K.
- Soil Exploration Company. (1981). "Permeability tests low density Elastizell concrete cylinders." *Project No. 120-7690*, St Paul, MN.
- Tikalisky, P. J., Pospisil, J., and MacDonald, W. (2004). "A method for assessment of the freeze-thaw resistance of preformed foam cellular concrete." *Cem. Concr. Res.*, 34(5), 889–893.
- Tiwari, B. (2016). "Application of cell-crete in civil engineering—Phases I and II, static and dynamic properties." *Technical Rep. Project No. 50123514*.
- USACE (U.S. Army Corps of Engineers). (1996). "Controlled low strength material with coal combustion ash and other recycled materials." Washington, DC.
- USBR (U.S. Bureau of Reclamation). (1990). "Earth manual. Part 2." U.S. Dept. of Interior, Denver.
- Zaidi, A. A. M., Rahman, A. I., and Zaidi, N. H. A. (2008). "Behavior of fiber reinforced foamed concrete: Indentation test analysis." *Proc., Seminar on Geotechnical Engineering*, Johore, Malaysia, 92–101.



Goal: Estimate the Shear Stress in the LCC when the LCC is subjected to a surface wave.

Assumptions: Worst case is a surface wave (E.g. Rayleigh wave)

- $\lambda$  is 600 to 800' long. (use 800')
- Street is 60' wide
- $\phi = 35^\circ$  for both fill & LCC
- $\delta = \frac{2}{3}\phi$  = friction between LCC & underlying soil
- Assume Top of LCC at El. 105', bottom at 90', & W @ 94'
- Pavement + AB = 1' @ 150 pcf
- LCC = 8' = 27', Sat = 60 pcf (Net - 12 pcf due to buoyancy)



$$\text{Shear force/lf} = 60' \times \sigma_v' \tan(\delta)$$

$$\sigma_v' = 1 \times 150' + 10' \times 27 \text{ pcf} + (-12 \text{ pcf}) \times 4' = 372 \text{ psf} \Rightarrow \text{use } 400 \text{ psf}_{||}$$

$$\text{Shear force/lf} = 60' \times 400 \text{ psf} \times \tan\left(\frac{2}{3} \times 35^\circ\right) = 10,350 \text{ lb/ft}$$

• If section is 14' tall

$$\text{Unit Shear Stress}(\tau) = \frac{10,350 \text{ lb/ft}}{14'} = 740 \text{ psf or } 5.2 \text{ psi}_{||}$$

• if min UCS = 40 psi &  $\frac{1}{2} \text{ UCS} = S_u = 20 \text{ psi}$

• if section is only 8' thick &  $\tau = \frac{10,350 \text{ lb/ft}}{8'} = 1,295 \text{ psf or } 9 \text{ psi}_{||} < 20 \text{ psi}$

• Conclusion:  $S_{u, \text{LCC}} > \text{Shear Stress}$ , for a range of LCC thicknesses, & if LCC cracks, it should still perform well & support the street section

Mission Rock

LCC Shear Strength vs. Stress

BY

PDB

DATE

12/9/19

PROJ. NO.

750604203

CKD.

DATE

SHEET

1

OF 1

LANGAN

**EXHIBIT B**  
**Resilient Modulus Definition**

## Resilient Modulus

The Resilient Modulus ( $M_R$ ) is a measure of subgrade material stiffness. **A material's resilient modulus is actually an estimate of its modulus of elasticity ( $E$ ).** While the modulus of elasticity is stress divided by strain for a slowly applied load, resilient modulus is stress divided by strain for rapidly applied loads – like those experienced by pavements.

Resilient modulus is determined using the [triaxial test](#). The test applies a repeated axial cyclic stress of fixed magnitude, load duration and cycle duration to a cylindrical test specimen. While the specimen is subjected to this dynamic cyclic stress, it is also subjected to a static confining stress provided by a triaxial pressure chamber. It is essentially a cyclic version of a triaxial compression test; the cyclic load application is thought to more accurately simulate actual traffic loading.

<https://www.pavementinteractive.org/reference-desk/design/design-parameters/resilient-modulus/>

EXHIBIT C  
LCC Modulus



Min Modulus for LCC with similar densities as the LCC for Mission Rock project. 655 MPa = 95ksi

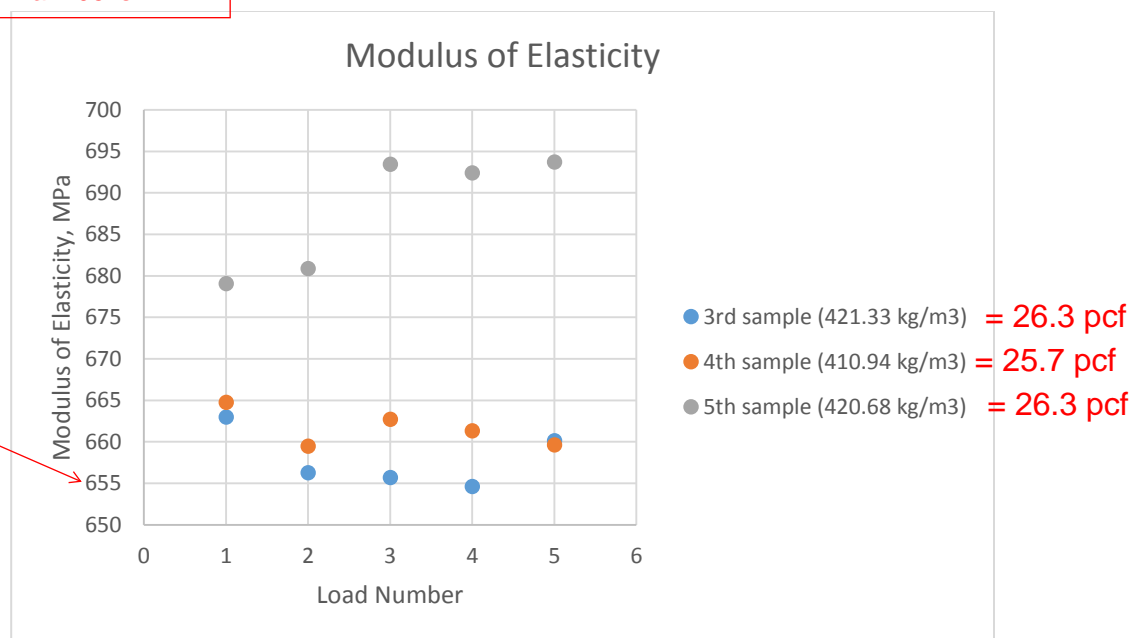


**Figure 5-9: Modulus of Elasticity Test Results for 28 Days Samples**

The average modulus of elasticity was determined as 657, 661 and 687 MPa for the 3<sup>rd</sup>, 4<sup>th</sup>, and 5<sup>th</sup> samples respectively. The result for modulus of elasticity for the 5<sup>th</sup> sample was obtained to be the highest, corresponding to the 420.68 kg/m<sup>3</sup> density, whereas for the 3<sup>rd</sup> sample modulus of elasticity was determined as the lowest with the sample density at 421.33 kg/m<sup>3</sup> (Figure 5-9). During the testing of the 5<sup>th</sup> sample, it was found that the reading increased from 680 to 693 MPa after the second cycle. This may be explained due to the fact that the test frame had some noise during testing and several adjustments were made to the longitudinal extensometer. According to Table 5-1, the lower limit for modulus of elasticity of the 400 kg/m<sup>3</sup> density is approximately 800 MPa, whereas laboratory results observed it to be in the range of 657 to 687 MPa.

The Poisson's ratio was observed in the range of 0.24 to 0.30 (Appendix III), which is consistent to the past literature (BCA, 1994).

#### 5.4.3 Relationship between Properties

Correlation between compressive strength and density is shown in Figure 5-10. The trend for 7 days samples was not typical because the lower density was observed, the higher compressive strength was, though 7 days samples had a good  $R^2$  value of 0.96. For the 14 and 21 days samples with hardened state density of 404 to 414 kg/m<sup>3</sup> the range of the compressive strength was relatively different, laying in the range of 1.2 to 1.69 MPa. For the 28 days samples, despite the expectations, compressive strength was observed to be at approximately same level as for other days samples (1.52 to 1.55MPa).



EXHIBIT D  
Rigid Pavement Design  
Calculation

Goal: Estimate the equivalent 18 kips axle loads (ESAL's) for the Mission Rock street section consisting of 4 inches of asphalt concrete (AC), over 8 inches portland cement concrete (PCC), over 4 inches of aggregate base (AB), and supported on lightweight cellular concrete (LCC).

Equation 5.2B-1 Rigid Pavement Design Equation  
from AASHTO Guide for Design of Pavement Structures (1993)

Parameters	
ZR (%)	0.9
So	0.34
D (in)	8
delta PSI	0.8
Po	4.5
k (pci)	1000
S'c (psi)	629
Ec (psi)	3400000
Jt	3.6
Cd	1
Pt	3.7

$$\log(W18) = 7.05$$

$$W18 \text{ (ESALs)} = 11,273,391.52$$

$$W18 = 10^{7.05}$$

$$\log_{10} W_{18} = Z_R \times S_o + 7.35 \times \log_{10}(D + 1) - 0.06 + \frac{\log_{10} \left[ \frac{\Delta PSI}{1.624 \times 10^6} \right]}{(D + 1)^{0.46}}$$

$$+ (4.22 - 0.32 \times p_t) \times \log_{10} \left[ \frac{S'_c \times \epsilon_{ef} [D^{0.75} - 1.132]}{215.63 \times f_c [D^{0.75} - \frac{18.42}{(\frac{E_c}{k})^{0.25}}]} \right]$$

Where:

- $W_{18}$  = 18-kip equivalent single axle loads (ESALs) over design life
- $Z_R$  = Standard normal deviate (function of the design reliability level)
- $S_o$  = Overall standard deviation (function of overall design uncertainty)
- $\Delta PSI$  = Serviceability loss at end of design life ( $p_o - p_t$ )
- $P_o$  = Initial serviceability;  $P_t$  = Terminal serviceability
- $k$  = Modulus of subgrade reaction (pci)
- $S'_c$  = PCC modulus of rupture (psi)
- $E_c$  = PCC modulus of elasticity (psi)
- $J_t$  = Joint load transfer coefficient
- $C_d$  = Drainage coefficient
- $D$  = PCC slab thickness (inches)

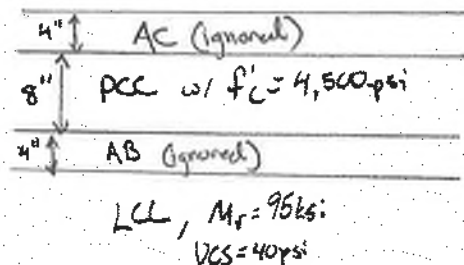


Table 6.2B-2  
Rigid Pavement Design Inputs

Parameter	Input Values
Design Life, Years	20 is normal. Other as Agency requires.
18k ESAL, ESAL <sub>20</sub> or other	See Section 4.1
Reliability Level (%), Refer to 1993 AASHTO for needed Z <sub>r</sub> value	<ul style="list-style-type: none"> <li>99% - Arterial, all Collector, Industrial Streets</li> <li>85% - Residential Street</li> </ul>
Overall Standard Deviation, S <sub>o</sub>	0.34
Initial Serviceability, P <sub>o</sub>	4.5
Terminal Serviceability, P <sub>t</sub>	<ul style="list-style-type: none"> <li>2.5 - Arterial, all Collector, Industrial Streets</li> <li>2.0 - Residential Streets</li> </ul>
Modulus of Subgrade Reaction, k	Use ACPA "k-value" Calculator: <a href="http://www.apps.acpa.org/apps/kValue.aspx">http://www.apps.acpa.org/apps/kValue.aspx</a> Moisture Treated Subgrade without any Intermediate Stiff Layers (ISL) shall be k = 60, for R-value of 1, or justify higher value.
Composite Modulus of Subgrade Reaction (k-value) using Intermediate Stiff Layer*. All materials to meet Section 4.2D requirements.	See below for Intermediate Stiff Layers use*: <ul style="list-style-type: none"> <li>Unbound Granular Base (UGB): M<sub>r</sub> = 20,000 psi.</li> <li>Chemically Treated Subgrade (CTS): use ACPA default minimum M<sub>r</sub> = 20,000 or by test.</li> <li>Mechanically Stabilized Base (MSB): M<sub>r</sub> = 37,000 psi.</li> </ul>
Modulus of Rupture, S'c	650 psi
Modulus of Elasticity, Ec	3,400,000 psi
Load Transfer Coefficient, Jt	See Table 5.2C-3: Doweels are recommended for all Arterial, Industrial & Collector roads
Drainage Coefficient, Cd	1.0 - Assumes subgrade has been considered as outlined in Section 4.2 and a drainage layer is provided

Note: \* Intermediate Stiff Layer (ISL) is required for all pavement designs where there is subgrade mitigation for swell or where the design subgrade resilient modulus is less than 5,000 psi. The Intermediate Stiff Layer provides long term stability for the pavement foundations in situations where the subgrade may experience elevated water content during the design life.

## Pavement Section

## CALCULATION PER MGPEC PAVEMENT DESIGN STANDARDS - 2019

Conclusion: This design calculation indicates the concrete section over the LCC is capable of supporting more than 11 million equivalent 18 kips axle loads (ESAL's). This ESAL value suggest that for a typical 20-year pavement design life the pavement could support either 395 trucks per day (three axles, max legal weight at rear, with a combined weight of 54,000 pounds, examples include dump, trash, fire, or full concrete trucks) or 500,000 light trucks per day (two axles with a combined weight of 8,500 pounds, examples include Box Vans, Utility Trucks, or a Pick-up with a Trailer)

## MISSION ROCK DEVELOPMENT LCC RIGID PAVEMENT CALCULATION

750604203  
LANGAN  
PDB/SAW  
9 DECEMBER 2019

EXHIBIT D

## F. Calculate Design ESALs

When designing for Arterial, Non-residential Collector and Industrial streets, this section presents the most involved generation of design ESALs. Residential streets and Residential collectors can be estimated with Default equations. Various inputs are needed and discussed below and used to determine the Design ESALs. ESALs calculated for 20 years (expressed as ESAL<sub>20</sub>) is the minimum recommended time for permanent pavements, and is shown in accordance with Equation 1:

**Equation 1 (=> ESAL calculation for 20 or 30 years)**

$$ESAL_{years} = \sum \left( LEF \text{ (flexible or rigid) class \#} \times VPD \times \frac{\text{days}}{\text{week}} \times \frac{\text{weeks}}{\text{year}} \times \text{Grown Years} \right) + \text{Defaults}$$

Where:

**LEF** = Load Equivalency Factor for each vehicle type (Class) on flexible or rigid pavement material type, Table 4.1G-1;

**VPD** = Vehicle per day in Design Lane, per each Vehicle Class Number (FHWA Classification system) in Table 4.1G-1. Lane distribution is assumed per Section 4.1D,

**Years** = Minimum 20 years for all permanent pavements. Less years may be used for temporary or short-term designs. More years such as 30 years for critical designs.

**Grown Years** = Use when yearly Growth Factors may apply. See Section 4.1E;

**Defaults** – See Section 4.1H. for default ESAL equations for special situations. The Designer may need to generate other add-on ESALs for specialized traffic loading sources for each project.

## G. LEFs (Load Equivalency Factors)

This section presents vehicle LEFs (load equivalency factors) taken from the 1993 AASHTO, Appendix MM for vehicles loaded near the maximum axle load limits, provided by Colorado regulated legal load limits or GVWR (Gross Vehicle Weight Rating) for un-regulated buses.

The LEF variables according to FHWA vehicle classification below and modified with descriptions, are based on the axle weights and configurations shown for flexible or rigid pavements as defined in Table 4.1G-1 below. Refer to Appendix A of this PDS for a description of the FHWA classification vehicles.

**TABLE 4.1G-1**

**LEF (Load Equivalency Factor) VARIABLES for EQUATION 1**

LEF from 1993 AASHTO Appendix MM, at equal traffic capacity for Flexible and Rigid pavement

Vehicle Class Number (FHWA), type	Vehicle Description	Axle Type and Loads pounds, front to rear, [average total = pounds] S = single, t = tandem	LEF - (Load Equivalency Factor)		LEF Ratio  Rigid / Flexible  (for information only)
			<u>Flexible</u> [ SN = 4, approx..9 inch]	<u>Rigid</u> [ D =8 inches]	
1	Motorcycles	1,000 single each end [2,000]	0.0002	0.0002	100%
2	Automobiles & Sport Utility	Average of 2,000 single, 3,000 single, with or not: 1,000 single trailer [5,500]	0.0018	0.0013	72%
3	Pickup with trailer -or- Utility & Box Vans (average)	2,000 single, 3,000 single, 6,000 2-axle trailer -or- 2,000 single, 4,000 single. [8,500]	0.0030	0.0028	92%
4 School Type A	<u>Bus</u> , 2 axles (10+ passenger)	5,000 single, 10,000 single. [15,000]	0.110	0.090	82%
4 School Type C or D [half loaded]	Bus, 2 axles (63-71 passenger)	10,000 single, 16,000 single. [26,000] Curb weight plus driver+ 40 passengers	0.747	0.694	93%
4 School Type C or D [GVWR]	Bus, 2 axles (63-71 passenger)	13,000 single, 23,000 single. [36,000] GVWR	2.791	3.014	108%
4 Bus, City, single unit	Bus, 2 axles, [RTD], 93% of GVWR	14,000 single, 25,000 single. (93% of 14.6k single, 27k single). [38,000]	3.701	4.084	110%
4 Bus, City Transit, articulated,	Bus, 3 axles, [RTD], Average: empty, GVWR	15,000 single, 24,000 single, 28,000 single full loaded. (10k,11k ,21k empty). [54,500]	5.328	5.875	110%
5 _SUT	<u>Single Unit Truck</u> , Two axles	8,000 single, 17,000 single. [25,000]	0.864	0.838	97%
6 _SUT	Three axles, max legal at front & total	20,000 single, 34,000 tandem. [54,000] (ex: full concrete)	2.580	3.420	133%
6 _SUT	Three axles, max legal at rear & total	14,000 single, 40,000 tandem. [54,000] (ex: dump, trash, small fire)	2.418	3.897	161%
<b>6 _SUT</b> <i>*unweighted average</i>	See above	See above	2.499	3.659	146%
7 _SUT	Four axles, max legal at rear & total maximum legal.	10,000 single, 34,000 tandem, 10,000 single pusher or tag. [54,000] (ex: concrete truck).	1.314	2.038	155%

7 _SUT	Four axles, maximum legal.	12,000 single, 3 x 14,000 single. [54,000]	1.377	1.222	89%
<b>7 _SUT</b> <i>unweighted average</i>	<i>See above</i>	<i>See above</i>	<b>1.346</b>	<b>1.630</b>	<b>121%</b>
<b>5+6+7 _SUT</b> <i>*unweighted average</i>	<b>See 5, 6, 7</b>	<b>See 5, 6, 7</b>	<b>1.036</b>	<b>1.523</b>	<b>147%</b>
8 _MUT-1	<b>Multi-Unit Truck, One Trailer</b> , Three or Four axles,	12,000 single, 20,000 single, 34,000 tandem. [66,000] ** less than max legal.	2.793	3.601	129%
9 _MUT-1	Five axles, one trailer, less than max. legal.	10,000 single, 2 x 34,000 tandem [78,000]	2.322	3.824	165%
9 _MUT-1 [Curb weight only]	Five axles, one trailer, less than max. legal.	8,000 single, 16,000 & 8,000 & tandem [36,000] curb weight = fueled, no cargo	0.102	0.123	129%
10 _MUT-1	Six or more axles, one trailer with tridem. Max. legal	9,000 single, 26,000 tandem, 45,000 tridem [80,000]	1.313	2.551	194%
<b>8+9+10 _MUT</b> <i>One Trailer *unweighted average</i>	<b>See 8, 9, 10</b>	<b>See 8, 9, 10</b>	<b>2.143</b>	<b>3.325</b>	<b>155%</b>
11 _MUT-2	<b>Multi-Unit Truck, Multi-Trailers</b> Five or less axles.	10,000 single, 3x 18,000 single, 1x 16,000 single [80,000]	3.747	3.694	99%
12 MUT-2	Six axles, multi-trailers.	12,000 single, 34,000 tandem, 1 x 10,000 + 2 x 12,000 single. [80,000]	1.851	2.497	135%
13 _MUT-2	Seven or more axles, multi-trailers	12,000 single, 22,000 & 24,000 tandem, 10,000 & 12,000 single . [80,000]	1.027	1.209	118%
<b>11+12+13 _MUT</b> <i>Multi Trailer *unweighted average</i>	<b>See 11,12,13</b>	<b>See 11,12,13</b>	<b>2.208</b>	<b>2.467</b>	<b>112%</b>

Notes: \*SUT = Single Unit Truck, \*MUT-# = Multi Unit Truck (Combination of tractor and # of trailers), \*Any axle may have single or dual wheels. GVWR =gross vehicle weight rating



EXHIBIT E  
LCC as a Subbase Material  
Thesis

**Analysis of construction experience of using lightweight  
cellular concrete as a subbase material**

by

Sergey Averyanov

A thesis

presented to the University Of Waterloo

in fulfilment of the

thesis requirement for the degree of

Master of Applied Science

in

Civil Engineering

Waterloo, Ontario, Canada

© Sergey Averyanov 2018

## **AUTHOR'S DECLARATION**

I hereby declare that I am the sole author of this thesis. This is a true copy of the thesis, including any required final revisions, as accepted by my examiners.

I understand that my thesis may be made electronically available to the public.

## ABSTRACT

Canada has the second largest territory in the world and its pavement network has over 1,000,000 km of roads spread over regions with various existing soil types. One of the challenges for engineers is to determine the soil type for a particular road project and to develop a pavement design accordingly. It is very important to identify weak or frost-susceptible soils, as they are influenced greatly by weather conditions which may lead to settlement issues and may affect the overall pavement performance. One viable option to overcome the consequences of settlement problems is the usage of lightweight materials, such as Lightweight Cellular Concrete (LCC), which reduces the effective stress on the underlying soil. This material has a number of advantages including: it is lightweight; exhibits superior thermal properties; is freeze-thaw resistant; has good flowability; is cost-effective; and sustainable.

This study aims to assess LCC in terms of performance in past projects, mechanical properties of LCC from the ongoing project as well as prediction of its field performance in the future. Already existing road sections with the installed LCC as a subbase were studied. The available information from those road sections was compiled and analyzed to establish similarities and differences in the cases as well as challenges and recommendations for LCC installation. All projects were aiming to solve the settlement problem. It is observed that settlement usually occurs on localized parts of the road and not on its whole length. After visual inspection, some of the studied sections, such as Winston Churchill Boulevard and Highway 9 were found to have no severe rutting or fatigue cracking, however, longitudinal and transverse cracking were observed at Dixie Road, particularly at the adjacent section to the Granular base pavement.

The samples from the ongoing site were collected for laboratory testing. Results from the laboratory determined the density of the LCC in the hardened stage as approximately  $40 \text{ kg/m}^3$  lower than its plastic density. The similar information was found in the literature. However, compressive strength of the in-situ cast material was determined to be higher than for the similar densities in the previous findings. Modulus of elasticity also differs from the typical values, whereas it was found to be lower. Poisson's ratio values were found to be in the typical range.

To predict the ability of the road sections to bear the designed traffic loads and to predict in-service performance, the case studies with settlement issues were considered. Failure criteria analysis has been conducted. The results of the failure criteria analysis indicated that the usage of LCC as a subbase material is more durable than the conventional granular material with similar thickness. This also shows that using LCC as a subbase layer material could be potentially effective.

## ACKNOWLEDGEMENTS

I would first like to thank my supervisor Dr. S.L. Tighe from the Civil and Environmental Engineering Department at the University of Waterloo, for her support and guidance over the course of this research.

I would also like to express my gratitude to my thesis readers Dr. W.C. Xie, from the Department of Civil and Environmental Engineering at The University of Waterloo and Dr. V. Henderson – an adjunct professor from the Department of Civil and Environmental Engineering at the University of Waterloo. Thanks also to the Civil Engineering Department lab technicians, Richard Morrison, Douglas Hirst, Peter Volcic, Ya Ting Yang, and Azka Aqib.

Appreciation is also extended to CEMATRIX and National Sciences and Engineering Research Council (NSERC) for the supply of research materials and funding this project. Special thanks to Dan Hanley, Brad Dolton, Dr. J. Li, Steve Bent, and Cameron Nerland from CEMATRIX for sharing their knowledge during my research.

In addition, I would like to thank my colleagues at the University of Waterloo who contributed their time and effort during my project. Namely, Dr. H. Baaj, Frank Mi-Way Ni, Abimbola Grace Oyeyi, Eskedil Melese, Daniel Pickel, Dahlia Malek, Drew Dutton, Seyedata Nahidi, Frank Liu, Qingfan Liu, Taha Younes, Yashar Azimi Alamdary, Zaid Alyami, Luke Zhao, Taher Baghaee Moghaddam, Jessica Rossi, Beverly Seibel. This work would not have been possible without your help.



## DEDICATION

*This thesis is dedicated to my family, whose support and love  
have made this a possibility.*

## TABLE OF CONTENTS

AUTHOR'S DECLARATION.....	ii
ABSTRACT.....	iii
ACKNOWLEDGEMENTS.....	iv
DEDICATION.....	v
Table of Contents .....	vi
List of Figures .....	ix
List of Tables.....	xi
List of Abbreviations.....	xiii
1 Introduction.....	1
1.1 Background .....	2
1.2 Research Hypotheses.....	3
1.3 Research Scope and Objectives.....	3
1.4 Thesis Organization.....	3
2 Literature Review .....	5
2.1 Lightweight Cellular Concrete (LCC).....	5
2.2 Composition of LCC .....	7
2.3 Properties of LCC.....	8
2.3.1 Fresh State.....	8
2.3.2 Hardened State .....	10
2.4 Challenges .....	15
2.5 Sustainability .....	16
2.6 Applications.....	17
2.7 Applications in Pavement Engineering .....	18
2.8 Summary of Literature Review and Research Gaps.....	19
3 Field Performance Review.....	20
3.1 Methodology .....	20
3.2 Case Studies .....	21

3.2.1	Dixie Road. Region of Peel, Caledon, Ontario, Canada .....	22
3.2.2	Brentwood Light Rail Transit (LRT) Bus-Lane. Calgary, Alberta, Canada .....	31
3.2.3	Winston Churchill Boulevard. Brampton, Ontario, Canada .....	34
3.2.4	Highway 9. Holland Marsh, Ontario, Canada .....	36
3.2.5	View and Vancouver Streets, City of Victoria, British Columbia, Canada .....	40
3.3	Summary of Case Studies .....	44
3.4	Discussions and Recommendations .....	45
4	Pavement Design and Analysis .....	48
4.1	Introduction into Pavement Design .....	48
4.2	Pavement Design with Lightweight Cellular Concrete (LCC) .....	48
4.3	Analysis Method .....	49
4.4	Failure Criteria Analysis .....	50
4.4.1	First Approach .....	51
4.4.2	Second Approach .....	55
4.4.3	Third Approach .....	59
4.5	Summary .....	65
5	Toronto Project .....	66
5.1	Site Description .....	66
5.2	Approach .....	67
5.3	Production and Placement .....	67
5.4	Laboratory Tests .....	69
5.4.1	Unconfined Compressive Strength .....	70
5.4.2	Modulus of Elasticity and Poisson's Ratio .....	74
5.4.3	Relationship between Properties .....	76
5.5	Summary .....	77
6	Conclusions and Future Recommendations .....	78
6.1	Conclusions .....	78
6.2	Future Recommendations .....	79
	References .....	81

Appendix I.....	86
Appendix II.....	89
Appendix III.....	91

## LIST OF FIGURES

Figure 1-1: Typical Cross Section of a Rural Conventional Asphalt Concrete Pavement (TAC, 2013) .....	1
Figure 2-1: Texture of Wet LCC (Maher and Hagan, 2016) .....	6
Figure 2-2: "Wet" Mix Equipment (Dolton et al., 2016) .....	6
Figure 2-3: "Dry" Mix Equipment (Dolton et al., 2016) .....	7
Figure 2-4: Instability Issues with Ultra-Low Density LCC (Field Performance) .....	9
Figure 2-5: Lightweight Cellular Concrete being Placed with a Flexible Hose (Taylor et al., 2016) .....	10
Figure 2-6: Splitting Tensile Strength Test Setup.....	12
Figure 2-7: Global Use of Cellular Concrete (Oginni, 2015) .....	17
Figure 3-1: Overview of Research Methodology.....	21
Figure 3-2: Road Section Location (Google maps, 2018) .....	22
Figure 3-3: Typical Cellular Cross Section (Griffiths and Popik, 2013) .....	23
Figure 3-4: Construction Process of Dixie Road, Region of Peel, Caledon, Ontario, Canada (CEMATRIX) .....	24
Figure 3-5: Condition of Dixie Road, Region of Peel, Caledon, Ontario, Canada.....	25
Figure 3-6: Ground Penetrating Radar Equipment .....	26
Figure 3-7: GPR Longitudinal Image of Southbound Lane, L10 (Griffiths and Popik, 2013) .....	27
Figure 3-8: GPR Transverse Images at Longitudinal Crack Locations, L4, and L5 (Griffiths and Popik, 2013) .....	28
Figure 3-9: FWD Truck and Trailer (Griffiths and Popik, 2013) .....	28
Figure 3-10: Structural Number Comparison Plot (Griffiths and Popik, 2013) .....	29
Figure 3-11: Site Location (Google Maps, 2018) .....	31
Figure 3-12: Bus Lane. (a) Reconstruction Process. Placing the LCC (CEMATRIX) (b) After Installing the LCC Layer (CEMATRIX) .....	32
Figure 3-13: Pavement Distresses on the non-LCC section - 1(CEMATRIX, 2018).....	33
Figure 3-14: Pavement Distresses on the non-LCC section - 2(CEMATRIX, 2018).....	33
Figure 3-15: Location of the Road Section (Google Maps, 2018).....	34



Figure 3-16: Pavement Structure. Winston Churchill Boulevard (CEMATRIX).....	35
Figure 3-17: Condition of Winston Churchill Boulevard, August 2017 .....	35
Figure 3-18: Highway 9 Site Location (Google Maps, 2018) .....	36
Figure 3-19: Highway 9 Site Location with the Local Landscape (Google Maps, 2018) .....	36
Figure 3-20: Highway 9 Construction Process (CEMATRIX).....	38
Figure 3-21: Condition of Highway 9, Three Years after Construction .....	39
Figure 3-22: Condition of Highway 9, Three Years after Construction .....	39
Figure 3-23: Site location. (Google maps, 2018).....	40
Figure 3-24: View Street and Vancouver Street Construction Process. Wet Mix Equipment (CEMATRIX) .....	41
Figure 3-25: Benkelman Beam Deflection Testing .....	42
Figure 4-1: Pavement Structure with LCC.....	49
Figure 4-2: Vertical and Tensile Stresses. Comparison for Dixie Road, Highway 9 and Winston Churchill Blvd (WESLEA software, 2018) .....	54
Figure 4-3: Allowable Number of Load Repetition. Fatigue Cracking and Rutting for Dixie Road, Highway 9 and Winston Churchill Blvd (WESLEA software, 2018).....	58
Figure 4-4: Predicted Damage. Fatigue Cracking and Rutting for Dixie Road, Highway 9 and Winston Churchill Blvd (WESLEA Software, 2018).....	64
Figure 5-1: Site Location (Google Maps, 2018) .....	67
Figure 5-2: Construction Process. Toronto, May 2018.....	68
Figure 5-3: Samples, Collected on Site.....	69
Figure 5-4: Weather Forecast during Construction and Casting the Samples .....	70
Figure 5-5: Unconfined Compressive Strength.....	71
Figure 5-6: UCS Test Results .....	72
Figure 5-7: Average UCS Test Results.....	73
Figure 5-8: Modulus of Elasticity and Poisson's Ratio Test Setup .....	75
Figure 5-9: Modulus of Elasticity Test Results for 28 Days Samples .....	76
Figure 5-10: Correlation of Compressive Strength and Density.....	77

## LIST OF TABLES

Table 2-1: Typical Properties of LCC Based on British Concrete Association (BCA, 1994).	11
Table 2-2: Empirical Model for Cellular Concrete Modulus of Elasticity Determination (Amran, Farzadnia and Ali, 2015) .....	13
Table 2-3: Summary of Cellular Concrete Applications Based on Density (Sari and Sani, 2017) .....	18
Table 3-1: Comparison of Pavement Structures .....	27
Table 3-2: Project Specifications and QC Results (Maher and Hagan, 2016).....	38
Table 3-3: Benkelman Beam Results (Golder Associates Ltd. Report, 2008).....	42
Table 3-4: FWD Test Data.....	43
Table 3-5: Summary of the Available Cases of Using LCC as a Subbase Material in Pavement Construction in Canada.....	44
Table 4-1: WESLEA Settings for Dixie Road, Highway 9 and Winston Churchill Boulevard (Material Properties of the Pavement) .....	50
Table 4-2: ESALs for Three Road Sections in Ontario .....	51
Table 4-3: Vertical and Tensile Stresses. Dixie Road.....	51
Table 4-4: Vertical and Tensile Stresses. Highway 9 .....	52
Table 4-5: Vertical and Tensile Stresses. Winston Churchill Blvd .....	52
Table 4-6: Allowable Number of Load Repetition. Fatigue Cracking and Rutting for Dixie Road .....	55
Table 4-7: Allowable Number of Load Repetition. Fatigue Cracking and Rutting for Highway 9.....	56
Table 4-8: Allowable Number of Load Repetition. Fatigue Cracking and Rutting for Winston Churchill Boulevard.....	56
Table 4-9: Predicted Damage (Fatigue Cracking and Rutting) of Pavement with Granular B Subbase. Dixie Road (WESLEA, 2018) .....	60
Table 4-10: Predicted Damage (Fatigue Cracking and Rutting) of Pavement with LCC Subbase. Dixie Road (WESLEA, 2018).....	60
Table 4-11: Predicted Damage (Fatigue Cracking and Rutting) of Pavement with Granular Subbase. Highway 9 (WESLEA, 2018).....	61

Table 4-12: Predicted Damage (Fatigue Cracking and Rutting) of Pavement with LCC Subbase. Highway 9 (WESLEA, 2018) .....	61
Table 4-13: Predicted Damage (Fatigue Cracking and Rutting) of Pavement with Granular Subbase. Winston Churchill Boulevard (WESLEA, 2018) .....	62
Table 4-14: Predicted Damage (Fatigue Cracking and Rutting) of Pavement with LCC Subbase. Winston Churchill Boulevard (WESLEA, 2018) .....	62
Table 5-1: Typical Properties of Cellular Concrete Based on British Concrete Association (BCA 1994) .....	73

## **LIST OF ABBREVIATIONS**

AADT	Average Annual Daily Traffic
AASHTO	American Association of State Highway and Transportation Officials
ACD	Activity Cycle Diagram
ARA	Applied Research Associates
ASTM	American Standards Tests and Methods
BCA	British Concrete Association
CBR	California Bearing Ratio
CPATT	Centre for Pavement and Transportation Technology
ESAL	Equivalent Axle Single Load
FWD	Falling Weight Deflectometer
GPR	Ground Penetrating Radar
HMA	Hot Mix Asphalt
PC	Portland Cement
LCC	Lightweight Cellular Concrete
LCCA	Life-Cycle Cost Analysis
LVDT	Linear Variable Displacement Transducers
LRT	Light Rail Transit
MEPDG	Mechanistic-Empirical Pavement Design Guide
MTO	Ministry of Transportation Ontario
RAP	Recycled Asphalt Pavement
RCA	Recycled Concrete Aggregate
SCC	Self Consolidating Concrete
TAC	Transportation Association of Canada
QA	Quality Assurance
QC	Quality Control
UCS	Unconfined Compressive Strength

# CHAPTER 1

## 1 INTRODUCTION

Canada has the second largest territory in the world and its pavement network has over 1,000,000 km of roads (TAC, 2013). The typical pavement structure in Canada consists of a surface layer, which can be made up of bituminous layers or rigid concrete layers, a granular base and a subbase overlying the subgrade (Figure 1-1). The main purpose of the layers is to support the wheel loads from traffic and distribute it to the underlying subgrade. When designing pavement, it is very important to take into consideration: thickness of each layer; volume and composition of traffic; climate; range of construction materials available; desired serviceable life; and subgrade type and strength (TAC, 2013).

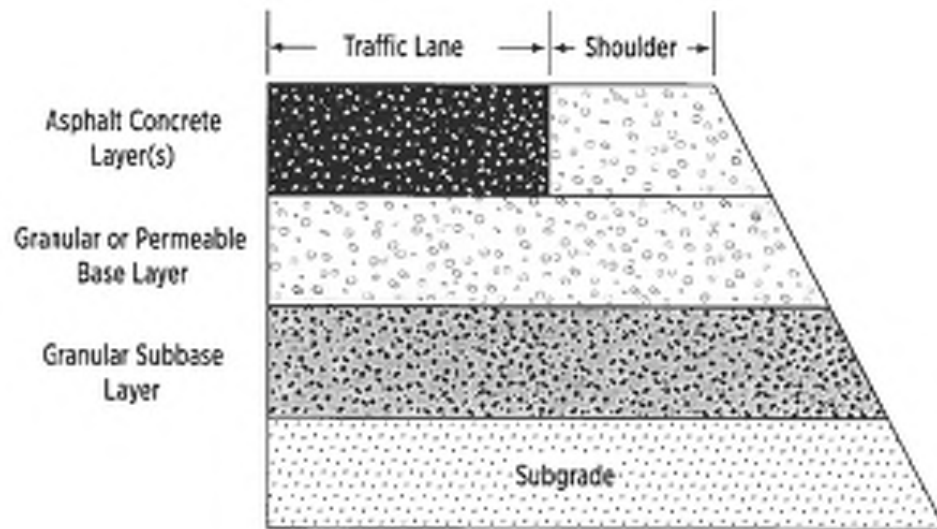


**Figure 1-1: Typical Cross Section of a Rural Conventional Asphalt Concrete Pavement (TAC, 2013)**

The subgrade type is a very significant factor because Canada's road network is spread over regions with various existing soil types. Some of these soil types, such as weak or frost-susceptible soils are referred to as difficult geotechnical conditions. In addition to the type of soil, serious temperature fluctuations in winter months, as well as thawing during spring months, play a significant role in pavement performance with respect to the subgrade. Frost heave in winter months as well as thawing during spring months influences the settlement of pavements and reduces bearing capacity of the pavement layers. Materials that are commonly used in the subbase layer include unbound granular materials, which have low insulation

properties and may lead to penetration of frost through the pavement structure straight to the subgrade (Hoff et al., 2002).

As a result of having unbound granular materials in a subbase, water can easily penetrate through the pavement structure into the subgrade and saturate the underlying soils. Thus, during the freeze-thaw cycles, those soils may become unstable, leading to settlement and causing distresses to the whole pavement structure (Hoff et al., 2002). To address this problem, it is recommended to remove weak organic soils from exposed subgrade areas prior to placement of embankment materials. In some cases, it is time-consuming and not economically beneficial, to replace these weak soils with stiff and stable materials or pavement structure. Another feasible solution may be using geosynthetics, including geotextiles, geofabrics, and geogrids, to provide “bridge” embankments over thick deposits of these organic-rich soils (TAC, 2013).

In order to overcome settlement issues due to excessive weight of pavement, the following materials may be utilized: (TAC, 2013)

- Expanded polystyrene
- Expanded lightweight clay
- Air cooled blast furnace slag
- Recycled Concrete Aggregates (RCA)
- Reclaimed Asphalt Pavement (RAP)
- Waste glass and ceramic

To address the problem of weak soils, and to mitigate settlement and fast deterioration of the pavements, Lightweight Cellular Concrete (LCC) is considered as another potential solution. For a better understanding of the benefits and drawbacks of using LCC, as well as performance evaluation of the pavement structure, analysis of construction experience of using LCC as a subbase material has been performed in this research.

## **1.1 Background**

LCC, sometimes referred to as "foamed concrete" or "aerated concrete", is a useful construction material with many applications. It differs from conventional concrete in that it does not contain any coarse aggregate. Instead, it is made from a mixture of cement and water that is mixed with a foaming compound to generate a matrix of small air bubbles, which makes the concrete extremely lightweight. Apart from being lightweight, LCC is a cost-effective and sustainable material and has superior thermal properties, freeze-thaw resistance, and good flowability. LCC technology was originally developed in Sweden in the early 1900s, but was not put into commercial use until after World War 2. More recently, technological advances in LCC have led to its use for various applications. Today, LCC is used in areas that require strong, yet lightweight and inexpensive materials. Commonly, LCC is used as a lightweight fill material

in embankments and beneath roads, or as an energy-absorbing material. Though many of its properties are still not thoroughly studied, the usage of LCC is becoming more popular in construction projects in North America and abroad.

For the most part, lightweight fill materials are progressively utilized in civil engineering purposes such as backfilling, slope stabilization, embankment fills, and pipe bedding (Horpibulsuk et al., 2014). The main intent of lightweight fill materials is to be used as an alternative construction material that significantly reduce the weight of fills, thereby mitigating excessive settlements and bearing failures. This can subsequently result in more economic designs for structures such as retaining walls and base layers of roadways.

## **1.2 Research Hypotheses**

The primary hypotheses of this research are as follows:

- Pavement structures with already installed LCC as a subbase can exhibit result in good pavement performance
- Pavement performance of LCC pavement can be predicted using WESLEA analysis
- Mechanical properties of LCC samples cast in-situ are different from the typical values in the literature

## **1.3 Research Scope and Objectives**

The scope of this project is to review the condition and performance of existing road sections that were constructed using LCC as well as to evaluate the mechanical properties of this material during the construction. This methodology will enable the prediction of future performance. To achieve this goal, the specific objectives are as follows:

1. Assess the condition of existing pavement sections with LCC as a subbase material
2. Conduct an analysis of the LCC performance of the existing roads
3. Determine structural properties of in-situ LCC

## **1.4 Thesis Organization**

The components of the thesis include outline of scope and objectives, literature review, review of case studies, performance evaluation of LCC in past and current projects and prediction of the future performance (failure criteria analysis). At the end of the thesis, conclusions and recommendations will be provided.



This thesis is organized into six Chapters.

Chapter 1 explains the scope and objectives of the research project and provides the thesis organization.

Chapter 2 provides an extensive review of the literature related to Lightweight Cellular Concrete, its composition and properties. Fresh and hardened states of LCC are presented by various mechanical properties of the material. This Chapter covers methods of producing LCC and presents benefits and drawbacks of this material. In addition, potential sustainable benefits from using LCC are presented in this Chapter. Number of applications of LCC are presented in Chapter 1, as well as applications in pavement engineering. Research gaps are also described in this Chapter.

Chapter 3 presents case studies of using LCC as a subbase material in pavement engineering across Canada. This Chapter describes each of the cases separately by discussing the location of the site, problem, possible solutions to the issue, construction process, results and tests that were done after construction. At the end of the Chapter, a table summarizing all of the case studies is presented. The most crucial issues that future contractors could potentially face, as well as recommendations, are discussed in Chapter 3.

Chapter 4 describes performance prediction analysis by introducing failure criteria. Three case studies from the previous Chapter were taken as the examples of pavement structure and were analyzed on bearing capacity of the layer, ability of the pavement to resist fatigue cracking and rutting issues, and potential number of ESALs that the pavement could potentially preserve without any maintenance.

Chapter 5 provides the results of the laboratory testing of the samples collected from the ongoing Toronto project. Site and project details are described in this Chapter. The tests were conducted at the Centre for Pavement and Transportation Technology (CPATT). The laboratory results were analyzed and correlation between the properties was made. Values, obtained from the laboratory work were compared to the typical values for LCC in the literature.

Chapter 6 contains the conclusions and recommendations based on the research conducted for the thesis.

## CHAPTER 2

### 2 LITERATURE REVIEW

This Chapter provides a summary of the relevant literature related to this thesis. It describes composition, methods of production, mechanical properties and applications of Lightweight Cellular Concrete (LCC).

#### 2.1 Lightweight Cellular Concrete (LCC)

ASTM C796 (2012) defines LCC as:

“A lightweight product consisting of Portland Cement, cement-silica, cement-pozzolan, lime-pozzolan, or lime-silica pastes, or pastes containing blends of these ingredients and having a homogeneous void or cell structure, attained with gas-forming chemicals or foaming agents (for cellular concretes containing binder ingredients other than, or in addition to Portland Cement, autoclave curing is usually employed)”.

Cellular concrete is relatively homogeneous compared to conventional concrete, as it does not contain coarse aggregate, so there is limited variation in its properties. The properties of Lightweight Cellular Concrete (LCC) depend on its microstructure and composition, methods of pore-formation and curing. LCC is lightweight, easy to construct, and economical in terms of transportation. LCC is comprised of cement or lime mortar matrix, in which air-voids are entrapped by a suitable aerating agent (Ramamurthy, Nambiar and Ranjani, 2009). Traditional concrete mix components densities may vary between  $1000 \text{ kg/m}^3$  (water) and  $3200 \text{ kg/m}^3$  (cement) (Darshan, 2016). By appropriate method of production, LCC densities are considerably lower, ranging from  $250 \text{ kg/m}^3$  to  $1800 \text{ kg/m}^3$ , but typically between  $400 \text{ kg/m}^3$  and  $600 \text{ kg/m}^3$  (Dolton et al., 2016). This makes LCC desirable as a very low-density material. The cellular pore network of LCC also provides a high degree of thermal insulation, as well as considerable savings in material. Figure 2-1 shows the texture of wet LCC as it is being placed from a pipe.



**Figure 2-1: Texture of Wet LCC (Maher and Hagan, 2016)**

LCC can be produced in two different ways: “dry” mix or “wet” mix. Figure 2-2 shows “wet” mix process, where cement, water, and admixtures are pre-batched into a slurry and sent to site in trucks. Once on site, the temperature, density, and viscosity of the slurry is measured to confirm compliance with the requirements to make LCC. After quality is verified, the slurry is delivered into the LCC equipment, which then injects foam into the slurry and pumps the LCC into place (CEMATRIX, 2018). The “dry” mix process is better for high-volume projects (Figure 2-3). All the components are blended on site to form the slurry, then foam is injected and the concrete is pumped into place (Dolton et al., 2016). With a skilled and experienced construction team, installation is usually quick and inexpensive. Those two factors usually come as a significant part of the overall project cost (Loewen, Baril, and Eric, 2012).



**Figure 2-2: "Wet" Mix Equipment (Dolton et al., 2016)**



Figure 2-3: “Dry” Mix Equipment (Dolton et al., 2016)

## 2.2 Composition of LCC

LCC is typically composed of Portland Cement, water, pre-formed foaming agent, with no coarse aggregate. Sometimes pozzolan materials such as fly ash, silica fume, slag, or various chemical admixtures are also included (Ozlutas, 2015).

### Portland Cement

The main cementitious component of LCC is Portland Cement. The content is approximately  $300\text{--}400\text{ kg/m}^3$  in the lightweight cellular concrete mix and it can vary depending on the desired density and strength of the final product (Jones, 2001).

### Pozzolan Materials

Pozzolans are a broad class of siliceous or siliceous and aluminous materials, which, in themselves, possess little or no cementitious value. In order to improve compressive and flexural strength, reduce cost, heat of hydration, drying shrinkage, thermal conductivity and sustainability, fly ash, blast furnace slag or silica fume may be added to PC (Dolton et al., 2016; Kearsley and Wainwright 2001; 2002). Jones et al. (2017) stated that replacing Portland Cement with fly ash up to 40% could significantly reduce the embodied carbon dioxide by 65% compared to the 100% Portland Cement mix while has a similar 28-day compressive strength (0.25 MPa compared to 0.31 MPa). However, the drawbacks of using fly ash are the slow rate of strength gain, and it might cause foam instability as the water demand may increase (Ozlutas, 2015).

## **Fine Aggregates**

Fine sand typically is composed of 2mm maximum size aggregates for use in LCC with dry densities equal to or greater than  $600\text{kg/m}^3$ . In lower density LCC, fillers like fly ash can be used instead (BCA, 1994; Dransfield, 2000). Carbon nanotubes (CNTs) have also been incorporated to LCC mix as fillers for support. They are found to develop more homogenous cell structure with closed cell bubbles (Yakovlev et al., 2006). However, CNTs can form clumps and ultimately cause foam instability, this will require dispersion in water which might not prove effective (Ozlutas, 2015).

## **Water**

The cement to water ratio used for LCC ranges from 0.4 to 1.25 (Kearsley, 1996). It must be noted that the quantity of water required is dependent on the composition and use of the material which relies on consistency and stability (Ramamurthy, Nambiar and Ranjani, 2009). Excess water in the mix leads to segregation while insufficient water content may collapse the mix (Nambiar and Ramamurthy, 2006).

## **Foam**

A foaming agent is usually added to the base mix (cement slurry) to produce the bubble structure in the LCC material. Foaming agents can either be blended with the base mix after they have been produced separately or mixed along with the ingredients for the base mix (Byun, Song and Park, 1998). The former is being used more often. The main requirement is that the foaming agent be stable and firm in order to resist mortar pressure (Koudriashoff, 1949). Foam can either be wet or dry. Studies have reported stability issues with the wet foam producing bubble sizes of between 2 mm to 5 mm. However, dry foam is reported to have more reliability in terms of stability with bubble sizes of 1mm (Aldridge, 2005). Examples of foaming agents include detergents, resin soap, hydrolized protein, saponin, and neopar (Ramamurthy, Nambiar and Ranjani, 2009; Valore, 1954a).

## **2.3 Properties of LCC**

### **2.3.1 Fresh State**

Fresh state of cellular concrete is described as free-flowing, self-leveling and self-compacting. The higher the air volume in the LCC is, the easier it is to place it. In addition, it does not need further consolidation during placement (Ozlutas, 2015). However, in some mixes with the increased volume of the air, cohesion of the mix increases and self-weight of the mix reduces, thus, resulting in reducing of the self-leveling properties of the cellular concrete (Nambiar and Ramamurthy, 2006). There are two main properties that describe fresh state of the LCC: stability and consistency.

### 2.3.1.1 Stability

Khayat and Assaad (2002) defined stability as a state that is required to ensure the presence of an adequate air void system and maintain it in a stable state until the time of hardening in Self-Consolidating Concrete (SCC).

Factors affecting mix stability are the following: (Brady, Jones, and Watts, 2001; Jones, Ozlutas and Zheng, 2016)

- Environmental conditions (wind, evaporation, temperature, vibration)
- Materials used (quality and volume of foam)
- Quality of production (mixing and placing processes)

It was stated by a number of researchers (McGovern, 2000; Aldridge, 2005; Jones and McCarthy, 2005b, 2006; Mohammad, 2011) that instability of LCC was a result of poor foam quality as well as the type of constituents used. However, in the case of instability at ultra-low densities ( $600 \text{ kg/m}^3$  and less), the stability of the mix has been observed to occur even in the absence of the above-mentioned factors (Ozlutas, 2015). The nature of stability or instability depends on the size of the bubbles in the bubble structure. The draining properties of LCC allow water to penetrate inside the material and if stays there, causing the increase in the bubbles inside the structure; thus, collapsing the foam. Meanwhile, the strength of bubbles decreases and cannot support the pressures. Figure 2-4 demonstrates typical instability issue.



**Figure 2-4: Instability Issues with Ultra-Low Density LCC (Field Performance)**



### **2.3.1.2 Consistency and Workability**

Consistency and workability of cellular concrete are usually characterized by its flowability. The presence of air-voids in the fresh mix due to the addition of stable foam agents allows LCC to be placed easily. The lightweight concrete can be pumped through flexible hoses over a distance of 200 m. Furthermore, its flowability allows it to easily spread into complex forms. It settles into place without the use of compaction equipment as it is self-consolidating material. This makes it an excellent candidate for pipe bedding, and for fill around utilities or not easily accessible areas. Since it flows so easily, forms usually have to be lined with plastic to prevent seepage. Also, the surface of LCC pours cannot be sloped greater than 1 degree due to its low viscosity (Taylor et al., 2016). Figure 2-5 shows a typical placement of LCC by flexible hose.



**Figure 2-5: Lightweight Cellular Concrete being Placed with a Flexible Hose (Taylor et al., 2016)**

### **2.3.1.3 Compatibility**

According to Amran, Farzadnia, and Ali (2015), the compatibility of LCC is referred to as a condition of strong interaction between the mix design and its constituent parts, in particular between chemical admixtures and the foam agent. Thus, at the areas where the mixture constituents fail to interact, the compatibility of foam mortar decreases. In addition, segregation challenges may occur when there is no interaction between the surfactant and plasticizers (Brady, Jones and Watts, 2001).

### **2.3.2 Hardened State**

Hardened state is characterized by mechanical, physical, durability and functional properties of the cellular concrete. These properties include compressive, flexural and tensile strength,

modulus of elasticity, porosity and permeability, drying shrinkage, freeze-thaw resistance, and Poisson's ratio.

### **2.3.2.1 Compressive Strength**

The compressive strength represents the capacity of a material to resist loads due to compression. LCC has considerably lower range of densities (from 250 kg/m<sup>3</sup> to 1800 kg/m<sup>3</sup>) than conventional concrete, thus lower compressive strength (Table 2-1). In general, compressive strength depends not only on density, but also on number of parameters such as rate of foam agent, w/c ratio, sand particle type, the curing method, cement/sand ratio, and characteristics of additional ingredients and their distribution (Valore, 1954b; Deijk, 1919; Valore, 1954a).

**Table 2-1: Typical Properties of LCC Based on British Concrete Association (BCA, 1994)**

Dry Density (kg/m <sup>3</sup> )	Compressive Strength (MPa)	Modulus of Elasticity (MPa)	Thermal Conductivity (3% moisture) (W/mK)	Drying Shrinkage (%)
400	0.5-1.0	800-1000	0.10	0.30-0.35
600	1.0-1.5	1000-1500	0.11	0.22-0.25
800	2.0-2.5	2000-2500	0.17-0.23	0.2-0.22
1000	2.5-3.0	2500-3000	0.23-0.30	0.15-0.18
1200	4.5-5.5	3500-4000	0.38-0.42	0.09-0.11
1400	6.0-8.0	5000-6000	0.5-0.55	0.07-0.09
1600	7.5-10	10 000-12	0.62-0.66	0.06-0.07

### **2.3.2.2 Split Tensile Strength**

Tensile strength is typically used as a concrete performance measure for pavements because it best simulates tensile stresses at the bottom of the concrete surface course as it is subjected to loading. These stresses are typically important in controlling structural design stresses (Pavement Interactive, 2018). A diametric compressive load is applied along the length of the cylinder until it fails. The test setup is shown in Figure 2-6. Because concrete is much weaker in tension than compression, the cylinder will typically fail due to horizontal tension and not vertical compression. The splitting tension test on regular concrete shows the value of 10% of its compressive strength (Raphael, 1984). For cellular concrete, it is still to be determined, but according to Amran, Farzadnia, and Ali (2015), the tensile strength is in the range between 20% and 40% of its compressive strength.

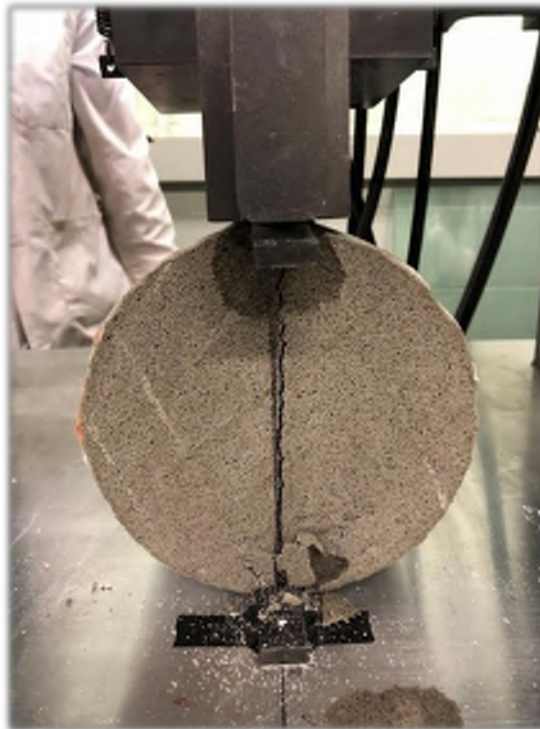


**Figure 2-6: Splitting Tensile Strength Test Setup**

### **2.3.2.3 Modulus of Elasticity**

The modulus of elasticity in pavement design represents how much the concrete will compress under load (TAC, 2013). The modulus of elasticity generally correlates with compressive strength of LCC. Conventional concrete has a modulus of elasticity of 14,000 to 41,000 MPa, depending on compressive strength and aggregate type. It is reported that E-value of LCC is four times lower than conventional concrete (Jones and McCarthy, 2005b). In cellular concrete, the modulus of elasticity is more related to its density. According to the studies, for range of dry density from 500 to 1600 kg/m<sup>3</sup>, the modulus of elasticity typically falls between 1.0 and

12 kN/m<sup>2</sup> respectively (Brad, Jones and Watts, 2001). In addition, it was stated by Jones and McCarthy (2005b) that E-value is dependent on the composition of the mix, and may be altered by fly ash or sand addition. Table 2-2 presents the relationship between compressive strength, modulus of elasticity and density.

**Table 2-2: Empirical Model for Cellular Concrete Modulus of Elasticity Determination (Amran, Farzadnia and Ali, 2015)**

<b>Equations</b>	<b>Annotations</b>
$E = 33W^{1.5}(fc)^{0.5}$	Pauw's equation
$E = 0.99 (fc)^{0.67}$	Fly ash utilized as fine aggregate
$E = 0.42 (fc)^{1.18}$	Sand is utilized as fine aggregate
$E = 5.31 \times W - 853$	Density ranges from 200 to 800 kg/m <sup>3</sup>
$E = 6326(\gamma_{con})^{1.5} (fc)^{0.5}$	$\gamma_{con}$ = unit weight of concrete  $fc$ = compressive strength of concrete where average Poisson's ratio=0.2, and using polymer foam agent
$E = 57,000 (fc)^{0.5}$	Density of conventional concrete limited between 2200 and 2400 kg/m <sup>3</sup> substituting with 80 kg/m <sup>3</sup> for steel
$E = 9.10 (fc)^{0.33}$	$fc$ = compressive strength of concrete
$E = 1.70 \times 10^{-6} p^2 (fc)^{0.33}$	p = plastic density (kg/m <sup>3</sup> )

#### **2.3.2.4 Drying Shrinkage**

Drying shrinkage is a damaging process to concrete that is caused by the loss of absorbed water from the material. Due to high total porosity (40-80%) drying shrinkage is of high significance in lightweight cellular concrete. The main reasons that intensify shrinkage include pore size decrease as well as a growing number of small-sized pores. Drying shrinkage of LCC where cement is the only binder is notably higher than the one manufactured with lime or lime and cement. Air-cured specimens have very high drying shrinkage potential. On the contrary, moist-cured cement and sand mixes demonstrate drying shrinkage values ranging from 0.06% to over 3.0% when dried at normal temperature, the lowest numbers are correlated with higher densities and higher percentage of sand. The time dependence of shrinkage is inclined by the properties of material, size of specimen and shrinkage climate. In addition to these factors, shrinkage value varies according to the initial moisture content. In the range of higher moisture content (>20% by volume), comparatively insignificant shrinkage takes place accompanied by loss of

moisture, which, in its turn, can be explained by the presence of a large amount of big pores which do not facilitate shrinkage (Darshan, 2016).

#### **2.3.2.5 Poisson's Ratio**

Poisson's ratio shows the lateral to axial strain relationship for a material under the load. Its value is obtained using the strains resulting from uniaxial stress only. Poisson's ratio is one of the input parameters for MEPDG (TAC, 2013). The typical range of Poisson's ratio for cellular concrete with densities of 1000 kg/m<sup>3</sup> to 1400 kg/m<sup>3</sup> is 0.13 to 0.16 and 0.18 to 0.19 respectively (Lee et al., 2009). Neville (2011) reported that the Poisson ratio for normal weight concrete is 0.15 to 0.22. Study by Tiwari et al., (2017) found Poisson ratio for LCC to range between 0.2 to 0.3 for LCC densities between 230 kg/m<sup>3</sup> to 800 kg/m<sup>3</sup>.

#### **2.3.2.6 Porosity and Permeability**

Porosity is a measure of the voids in cellular concrete in comparison to the total volume. Porosity can affect the other material properties such as compressive strength, flexural strength, and durability (Amran, Farzadnia and Ali, 2015). However, Amran, Farzadnia, and Ali (2015) are reporting that the permeability and the degree of fluid flow through the concrete matrix were not significantly related to the total porosity, but to larger capillary pores. The porosity of LCC concrete allows the aggressive fluids to penetrate inside the matrix of the concrete in the hardened stage. Porosity of the hardened concrete may be affected by mix design compositions, foam agents, w/c ratio and the curing type. The porosity depends on degree of infusion characteristics such as water absorption, sorption, and permeability.

According to Sabir, Wild and O'Farrell (1997), permeability is defined as a measure of the water flow under pressure in a saturated porous medium. Permeability of the cellular concrete has a significant correlation with the water absorption of the material. Water absorption of the cellular concrete is twice conventional concrete at similar water to binder ratio. Moreover, permeability may be affected by the inclusion of aggregates or mineral admixtures and entrained air in the cement paste (Amran, Farzadnia and Ali, 2015).

#### **2.3.2.7 Freeze-Thaw Resistance**

Lower density LCC has been observed to have good freeze-thaw resistance due to the voids restraining the expansion forces from frozen water (Brady, Jones and Watts, 2001). Freeze-thaw characteristic of LCC is dependent on its initial depth of penetration, absorption and absorption rate (Jones, 2001).

#### **2.3.2.8 Thermal Insulation and Conductivity**

Another benefit of LCC which stands out against the other materials is its thermal properties. The air entrapped within the concrete acts as an insulator, so heat does not easily transfer

through. This makes LCC desirable as an insulation in buildings, or in tank bases to prevent heat damage to liners (Taylor et al., 2016). Moisture content, density and components of the material account for its thermal conductivity. Density is the key factor in thermal conductivity, as the way of curing the product (moist-curing or autoclaving) is of no importance here. The number of pores and their arrangement are essential for thermal insulation as well. Smaller pores have been found to facilitate better insulation (Darshan, 2016). Concrete is inert and fireproof and does not easily conduct sound, which further suggests it would be a good material for insulation.

A drawback for LCC of being a good insulator is frost heave. Because of that, there can be differential heating and cooling between the cellular concrete and the surrounding materials. If the LCC is used in pavement subgrade, water can seep through the highly porous matrix and pool in areas. Differential cooling in the wintertime can cause ice to form, which expands and causes upheaval that can damage overlying pavements and structures. To mitigate this risk, LCC forms should be sloped downward to the sides and extended out past the overlying road or structure so water cannot pool at the base of the concrete (Maher and Hagan, 2016).

#### **2.3.2.9 Buoyancy Forces**

Density of LCC can be less than half the density of water, so if the concrete is submerged there will be buoyancy forces. For an application such as a river embankment fill material, this could be a major problem: if river banks rise, buoyancy forces can push the concrete upwards causing upheaval and failure of the overlying pavements and structures (Friesen et al., 2012).

## **2.4 Challenges**

Number of advantages and disadvantages were discussed in this Chapter. Challenges, associated with LCC are summarized as follows:

- LCC has high potential of drying shrinkage because of the significant amount of cement in its composition (up to 80 % of cement). According to Ramamurthy (2009), LCC can be 10 times more susceptible to drying shrinkage than conventional concrete.
- Instability issues could be a significant problem, especially at the ultra-low densities of LCC during construction process.
- Initial cost might be higher than for similar lightweight materials or for Granular materials, if measuring them  $m^3$  to  $m^3$ . However, in most projects less  $m^3$  of LCC is needed to obtain the same performance.
- Since LCC has good flowability, it may be challenging to place it on the slope surfaces. The technique of “lifts” may be used, when LCC is being placed by levels in steps. Although, this method requires additional framework.

- Another issue with LCC material can be its seepage through the underlying layers when it is placed over the open graded layers. Additional protective layers such as polyethylene sheets may be used to prevent this problem.
- Groundwater seepage control of the excavations, where LCC will be placed, is required. This needs to be done to prevent floating of the material, as LCC density for the case studies was  $475 \text{ kg/m}^3$ , which is less than water density ( $1000 \text{ kg/m}^3$ ).

## 2.5 Sustainability

Sustainable development according to the World Commission on Environment and Development (WCED, 1987) is defined as: “Development that meets the needs of the present without compromising the ability of future generations to meet their own needs”.

The potential sustainability benefits of using LCC are outlined below:

- At low densities, it can contain 80 -90% voids which means less virgin material usage and waste produced (Ozlutas, 2015).
- Reduction in the use of non – renewable natural resource by eliminating coarse aggregates, and fine aggregates at densities below  $600 \text{ kg/m}^3$  (BCA, 1994).
- It makes use of industry by-product such as slag and fly ash thereby reducing the amount of waste disposed (Dolton et al., 2016; Jones et al., 2012; Awang et al., 2014). Fly ash can also be used to replace Portland Cement up to 75% in lower density LCC, this has the advantage of reducing embodied CO<sub>2</sub> (eCO<sub>2</sub>).
- No need for compaction as it flows freely, therefore noise pollution reduction during construction and less energy consumed as compaction is eliminated (Jones and McCarthy, 2005a).
- Not only has it great constructability as the material can be installed very quickly, but also can be placed during winter time with some protective measures and during the light rain (Maher and Hagan, 2016).
- LCC can be easily excavated and removed as it has low strength.
- It can be recycled and used for producing more cellular concrete (Jones et al., 2012).
- LCC has been shown to have good freeze-thaw resistance (Ramamurthy, Nambiar and Ranjani, 2009), fire resistance, sound absorption, and superior thermal insulating properties which improve with lower plastic densities (Wei et al., 2013; Jones and McCarthy, 2005a).
- Due to its high strength-to-weight ratio, there is typically less material required for fill operations, which means less machinery is required during manufacturing and construction, leading to less energy use, less greenhouse gas emissions, and less noise pollution (Dolton et al., 2016).



## 2.6 Applications

Lightweight fill materials are increasingly being used in civil engineering applications such as roadway base layers, embankment fill material, grout for tunnels and pipes, soil stabilization, fill for abandoned mines or other types of void fill, landslide repair, arrestor material at the end of airport runways, sound-dampening walls, fireproof insulation, and retaining wall backfill (Maher and Hagan, 2016; Horpibulsuk et al., 2014). The air bubble structure of LCC is exceptional at absorbing energy, so there have been successful uses of this material in military ranges, as rockfall protection, and in airports as the safety barrier in order to safely slow down planes and jets if they were to overshoot their runways (Taylor et al., 2016). Amran, Farzadnai, and Ali (2015) report a significant interest in LCC in North America, and in Canada in particular, not only because this material has a wide range of applications but also because of the increased prices for the other lightweight building materials. The annual market size of cellular concrete is estimated to be about 250,000 – 300,000 m<sup>3</sup> in United Kingdom including massive mine stabilization project. In Western Canada, the market size of LCC is about 50,000 m<sup>3</sup> and it is actively growing. North Koreans mostly use cellular concrete in floor heating systems with the total market for this country as 250,000 m<sup>3</sup>. In order to reduce the effect of earthquakes and to mitigate the effect from temperature changes, cellular concrete is being used in the Middle East. It can be used as a great thermal insulator for those cases (Amran, Farzadnia and Ali, 2015).

LCC has been used in more than 50 countries. Oginni (2015) presented Figure 2-7, indicating use of cellular concrete technology globally. Asia and Europe alone accounted for 83% of the use of cellular concrete technology economy worldwide.

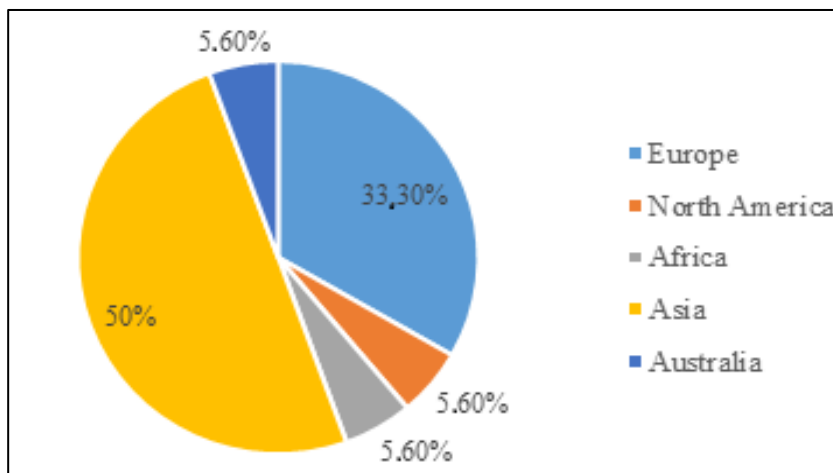


Figure 2-7: Global Use of Cellular Concrete (Oginni, 2015)

The main intent of lightweight fill materials is an alternative construction material to significantly reduce the weight of fills, thereby mitigating excessive settlements and bearing failures. This can subsequently result in more economic designs for structures such as retaining walls and base layer of roadways. The summary of the typical usage of the cellular concrete based on its density is studied and presented in Table 2-3. Moreover, density is potentially easier to control than compressive strength while placing the LCC.

**Table 2-3: Summary of Cellular Concrete Applications Based on Density (Sari and Sani, 2017)**

<b>Density (kg/m<sup>3</sup>)</b>	<b>Application</b>
300-600	Replacement of existing soil, soil stabilization, raft foundation.
500-600	Currently being used to stabilize a redundant, geotechnical rehabilitation and soil settlement. Road construction.
600-800	Widely used in void filling, as an alternative to granular fill. Some such applications include filling of old sewer pipes, wells, basement, and subways.
800-900	Primarily used in production of blocks and other non-load bearing building element such as balcony railing, partitions, parapets, etc.
1100-1400	Used in prefabrication and cast-in-place wall, either load bearing or non-load bearing and floor screeds.
1100-1500	Housing applications.
1600-1800	Recommended for slabs and other load-bearing building element where higher strength required.

## **2.7 Applications in Pavement Engineering**

Various lightweight fill materials including LCC have been developed in recent years for usage in various civil engineering applications (Arulrajah et al., 2015). It has potential success in being used as a material for structural purposes, stabilization of weak soils, base layer of sandwich solutions for foundation slabs, industrial floor and highway as well as subway engineering applications (Kadela, Kozlowski and Kukielka, 2017).

Maher and Hagan (2016) state that the biggest issue in constructing the highways and roads over peat, organics or soft soil deposits is continual and long-term settlements that are hard to address. Full depth reconstruction requires long-term closures of the damaged pavement section. Moreover, it is usually expensive and not an efficient way of solving the problem. According to Kadela, Kozlowski, and Kukielka (2017), areas with difficult geotechnical conditions are characterized as weak soils, including grounds containing layers of organic layers. Factors, influencing decision-making processes of choosing the proper method for

dealing with those issues include geological substrate system, size of loads acting on subsoil, excessive moisture of soil, technological capabilities and costs of using the technology. Kadela, Kozlowski, and Kukielka (2017) introduced several methods of dealing with those weak soils and LCC as a potential solution to this issue was studied.

Maher and Hagan (2016) stated that using cellular concrete in the areas with weak soils allows pavement to be “floated” over the subgrade as the density of this material is a quarter of that of conventional granular fill and it is a less expensive solution than traditional lightweight materials such as polystyrene. In terms of ability of the lightweight cellular concrete to bear the loads, Kadela, Kozlowski, and Kukielka have presented the results of numerical simulations that proves that using cellular concrete as a subbase layer is potentially possible in terms of bearing the loads. The same study has shown that the tensile stress in the lower zone of the subbase layer is lower than the flexural strength of LCC that was tested.

## **2.8 Summary of Literature Review and Research Gaps**

Lightweight Cellular Concrete offers potential construction, performance, sustainable and cost benefits when used in a pavement structure. As an alternative roadbed support over weak soils, LCC has been installed as pavement subbase material to provide more stable and stronger foundations. It has been placed in a few pavement sections across Canada and preliminary information shows that it can improve pavement performance. However, there is a lack of integrated field and laboratory evaluation, adequate information, and practices of using LCC as pavement subbase layer. There is a need to investigate the in-situ performance as a material incorporated into the pavement structure.

The overall purpose of this project is to summarize the information about the performance of the pavement sections with LCC in its structure. The laboratory tests are concentrated on mechanical properties and the possible correlation between parameters, characterizing cellular concrete in terms of density, UCS, and modulus of elasticity.

Another aim of this research is to predict the LCC performance for a given sections and compare it to the typical pavement structures in terms of failure criteria.

## **CHAPTER 3**

### **3 FIELD PERFORMANCE REVIEW**

This Chapter describes five road sections with installed Lightweight Cellular Concrete (LCC) layer as a subbase. All the available information was compiled in a table and analyzed at the end of the Chapter. Similar features of the road sections, as well as challenges during construction and recommendations for the future construction of similar pavement, are discussed in this Chapter. In addition, methodology for the thesis is described in this Chapter (Figure 3-1).

#### **3.1 Methodology**

For analyzing the construction experience of using LCC as a subbase material, past projects (case studies) were studied. As a first step of collecting the data, published papers on the past projects where LCC was installed as a subbase layer were studied. After that, technical reports were analyzed and visual inspections on the road sections were completed. All of the available information from the road sections was compiled and analyzed concluding in similarities and/or differences in the performance.

After analyzing the data from the past projects, the next step was to predict performance of the installed LCC sections in the future. Chapter 4 aimed to predict the performance of the road sections located in Ontario in terms of fatigue cracking and rutting resistance. In addition, bearing capacity of the road sections was determined. These parameters were discussed under the failure criteria analysis. Furthermore, the comparison between LCC and Granular B subbase materials that were installed on the same road sections was completed and discussed.

Knowing the current condition of the LCC road sections that were reconstructed in the past as well as having an idea of the predicted performance of the sections in the future, it is crucial to understand the mechanical properties of LCC that are currently being used in construction. In Chapter 5, mechanical properties of the in-situ cast samples will be determined and compared to the typical values in literature. In addition, the relationship between the mechanical properties of LCC will be discussed.

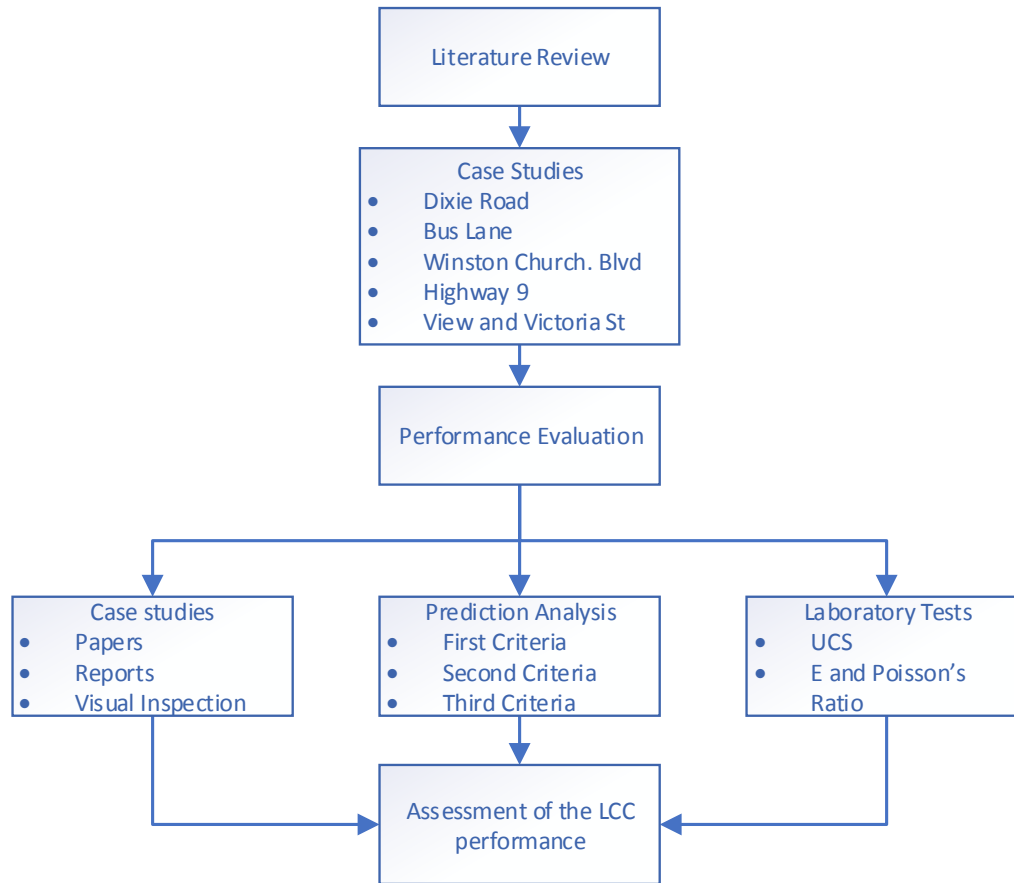


**Figure 3-1: Overview of Research Methodology**

### 3.2 Case Studies

LCC may be used in many applications in infrastructure projects. Currently, there are not many companies who produce and provide cellular concrete solutions. There are several cases when LCC was installed into roadway sections and infrastructure applications in Canada. The scope of this project is to study the LCC as a subbase layer.

Five road sections that were constructed using LCC as a subbase layer were investigated, including Dixie Road, Winston Churchill Boulevard, Highway 9, Brentwood Light Rail Transit (LRT) Bus-Lane and View and Vancouver Streets. All five sections have similar pavement structures, including an asphalt concrete surface layer, an unbound granular base layer, a lightweight cellular concrete subbase layer, and subgrade soil. The pavement surface distresses were determined by following ASTM D6433, which classifies nineteen types of pavement distresses. These distresses such as alligator cracking, bleeding, corrugation, longitudinal and transverse cracking, and rutting were inspected. The inspections were conducted manually

instead of using automated data collection vehicles. The results of the field inspections are described in the following sections.

### 3.2.1 Dixie Road. Region of Peel, Caledon, Ontario, Canada

#### 3.2.1.1 Background

The Region of Peel reconstructed a 120-metre section of rural highway in 2009. The main issue, within the section, was ongoing settlement for a number of years. The proposed solution was required to be environmentally friendly and to minimize the impact on the adjoining wetlands. Instead of removing and replacing the existing embankment with granular material, the Region chose to use lightweight cellular concrete as an alternative. Traditional reconstruction would have required considerable dewatering, extensive peat removal, the erection of sheet piling and then replacing peat with granular materials. Figure 3-2 demonstrates the location of the road.



Figure 3-2: Road Section Location (Google maps, 2018)

A geotechnical investigation was completed before reconstruction of the road in 2009. This investigation included pavement cores and boreholes throughout the settlement area, resulting in the following conclusions:

- Thickness of the asphalt layer ranged from 150 mm to 280 mm
- Granular base/subbase was at the depth from 1.4 to 1.8 m
- Peat/marl deposits were located from the depth of 2.1 m up to 5.4 m. with  $M_r = 17$  MPa

After the geotechnical investigation was done by a contractor. Full excavation of the weak soils, followed by backfilling with granular material was suggested. The pavement structure to support 500,000 cumulative ESALs was recommended as follows:

- Removal of existing material - 5.2 m
- Hot Mix Asphalt - 140 mm
- Granular A Base Course - 150 mm
- Granular B Type I Subbase - 400 mm

Instead of removing and replacing the embankment to a depth of 5.2 m, the Region chose the following pavement structure:

- Hot Mix Asphalt - 140 mm
- Granular A Base Course - 150 mm
- LCC CEMATRIX CMEF-475 (CEMATRIX Manufactured Engineering Fill) - 650 mm

The typical cross section for the cellular concrete section is presented in Figure 3-3.

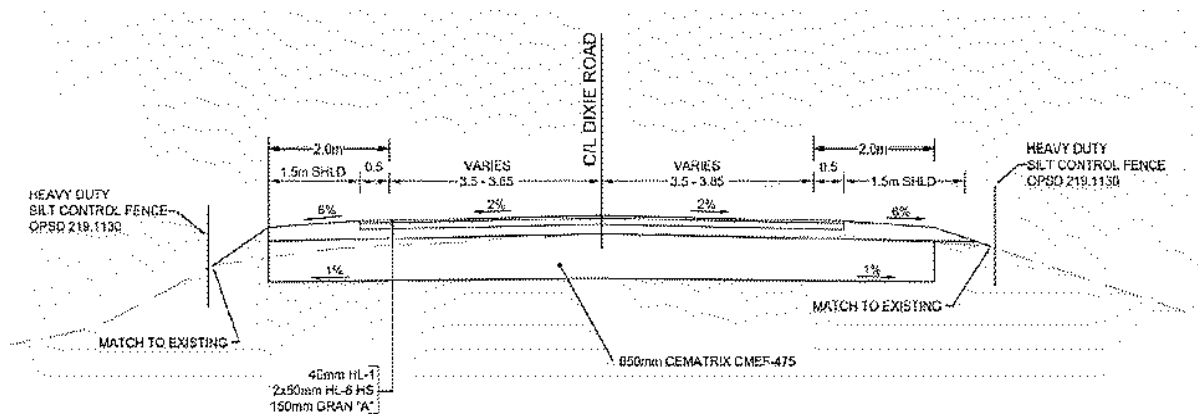


**Figure 3-3: Typical Cellular Cross Section (Griffiths and Popik, 2013)**

Cellular concrete was produced and placed on site by CEMATRIX Company with the dry-mix production units. The construction process is shown in Figure 3-4.





**Figure 3-4: Construction Process of Dixie Road, Region of Peel, Caledon, Ontario, Canada (CEMATRIX)**

#### **3.2.1.2 Field Investigation**

Griffiths and Popik (2013) investigated the in-place performance in 2013. The evaluation of the section included the following:

- Visual condition survey of the existing pavement surface
- Ground Penetrating Radar (GPR) survey with various transverse scans to provide layer thicknesses and subsurface images of the pavement utilizing the CEMATRIX LCC
- Falling Weight Deflectometer (FWD) testing to determine the structural capacity of the lightweight cellular concrete section in comparison with the adjacent pavement

#### **Visual Condition Survey**

The visual pavement condition survey of the site was completed on June 4, 2013, and concluded that pavement section was in good condition. In total, three slight longitudinal cracks and one moderate pavement distortion/heave were observed in the area. Figure 3-5 shows the cracks. The longitudinal cracks were located in the northbound lane, approximately at the midpoint of the site.



Longitudinal Cracking (centreline)



Transverse Cracking



Minor crack



Transverse Cracking

**Figure 3-5: Condition of Dixie Road, Region of Peel, Caledon, Ontario, Canada**

All three cracks were found to be close to the centreline, with a slight meander into the outer wheel-path. The pavement distortion/heave at the north transition extended for approximately 25 m and appeared to be worse in the southbound lane, than in the northbound direction. The distress appeared to be caused by a heave in the area marked at the end of the LCC material. The adjacent pavement sections were also investigated, and it appears to be in excellent condition without any distresses. In general, the condition of the section is performing adequately after three years of construction.

It was also observed that LCC material was exposed at the SB shoulder rounding. It was observed that part of the gravel, which was intended to cover and protect the LCC from weather, was eroded into the ditch. Thus, the LCC layer was easily broken from the exposed edge.

### **A. Ground Penetrating Radar**

As part of this evaluation, a Ground Penetrating Radar (GPR) survey was completed. GPR is a non-destructive device that uses a radar pulse to produce subsurface images. Ground Penetrating Radar equipment is shown in Figure 3-6.

The GPR survey was completed in order to identify the thicknesses of the pavement layers and the border with the adjacent road sections. More comprehensive GPR surveying was completed at the areas containing longitudinal cracking. The GPR data was collected by summarizing results obtained from 3 cycles of measurement for each line:

1. Using SmartCart, equipped with a NOGGIN 250 MHz GPR sensor
2. Using SmartCart, equipped with a NOGGIN 500 MHz GPR sensor
3. Using SmartCart, equipped with a NOGGIN 1000 MHz GPR sensor



**Figure 3-6: Ground Penetrating Radar Equipment**

Griffiths and Popik (2013) reported that thicknesses of the pavement layers varied (some of which were within the normal range and some were not). For example, Table 3-1 shows a part of the report for lane №10 (L10):

**Table 3-1: Comparison of Pavement Structures**

<b>Layers</b>	<b>Designed, mm</b>	<b>GPR reading (range), mm</b>
<b>Asphalt</b>	140	126-178
<b>Granular Base</b>	150	68-235
<b>LCC</b>	650	Vary because of the not flat underlying subgrade

Longitudinal and transverse images of the lanes were also obtained (Figures 3-7, 3-8).

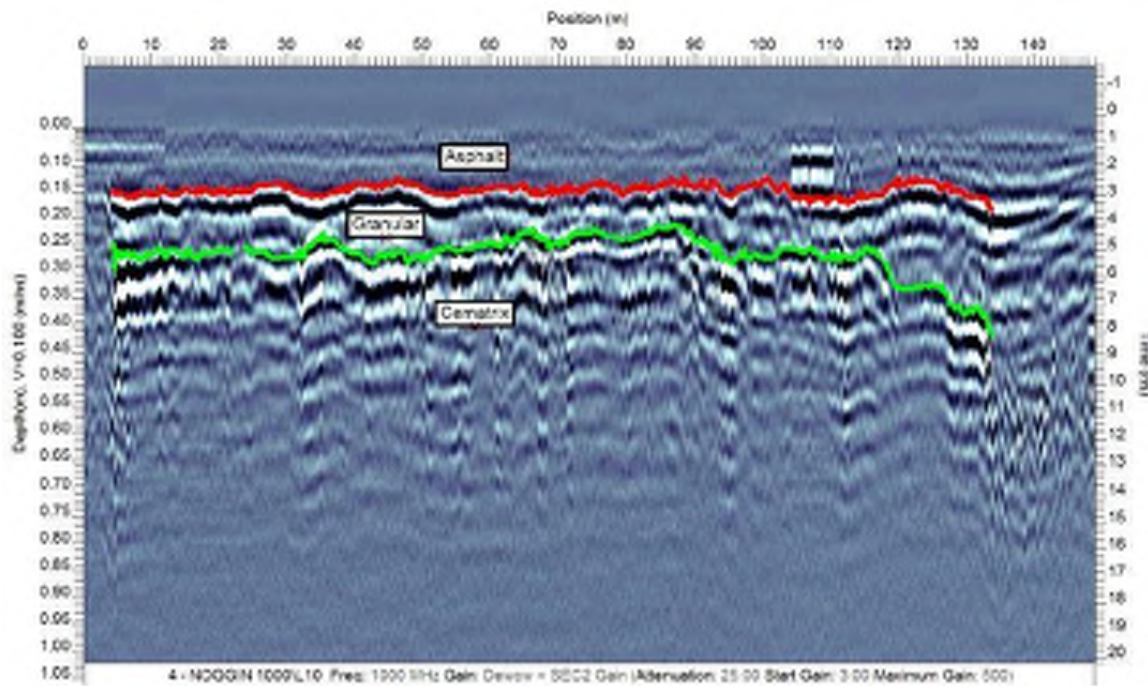


**Figure 3-7: GPR Longitudinal Image of Southbound Lane, L10 (Griffiths and Popik, 2013)**



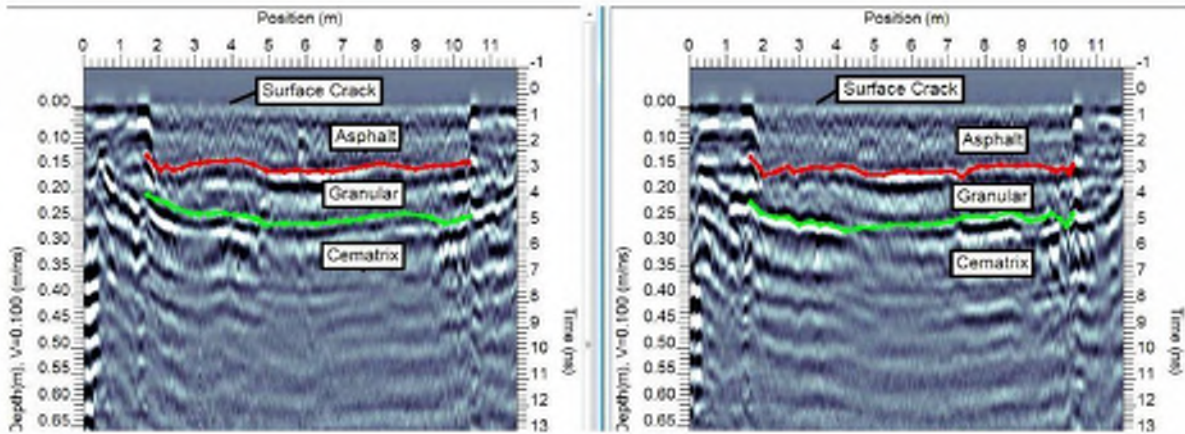


**Figure 3-8: GPR Transverse Images at Longitudinal Crack Locations, L4, and L5 (Griffiths and Popik, 2013)**

### **B. Falling Weight Deflectometer**

Pavement load/deflection testing was completed on July 30, 2013, and included 54 tests. The Dynatest Falling Weight Deflectometer (FWD) was used for the structural evaluation of this pavement section. On the traditional road section, from the both sides of the LCC section, FWD testing was completed every 5 m in southbound and northbound directions. For the transition areas, between LCC and traditional section, FWD testing was completed on 2 m intervals for a length of 10 m. Each test included 4 drops, with the first drop being a seating load, and the following three loads at roughly 30, 40 and 75 kN. The testing equipment is shown in Figure 3-9. Full FWD report is presented in Appendix I.



**Figure 3-9: FWD Truck and Trailer (Griffiths and Popik, 2013)**

The collected FWD data was analyzed based on the pavement thickness measured by the GPR survey. For the purposes of the FWD analysis within the Lightweight Cellular Concrete section, the LCC layer was assumed to be part of the pavement structure. Two parameters were determined: the composite elastic pavement modulus and the structural coefficient. The composite elastic pavement modulus of LCC section ranged from 714 to 737 MPa, which is higher than the adjacent section (514 to 670 MPa). This resulted in increasing of the composite pavement structural number of LCC section, which ranges from 175 to 224 mm while the adjacent section range from 128 to 154 mm.

The structural coefficient of the LCC material was determined by the analysis of FWD data. The structural coefficients of the asphalt and Granular base layers used in the analysis were 0.38 and 0.12 respectively (Griffiths and Popik, 2013). In comparing the overall strength of the LCC section, the composite elastic pavement modulus of the pavement structure incorporating the LCC material was found to be stronger, than the adjacent conventional pavement structures (Figure 3-10).

The calculated structural number (SN) for each layer was added together and subtracted from the SNEff at each FWD test location. The resulting SN for the LCC layer was divided by the layer thickness of 650 mm to obtain the equivalent AASHTO structural coefficient for the LCC material. The averaged back-calculated structural coefficient for the LCC material used on this site is approximately 0.2, after removing outliers that were more than one standard deviation of the average. In conclusion, following the AASHTO flexible pavement design methodology for designing a flexible pavement utilizing the CEMATRIX LCC-475 (with a density of 475 kg/m<sup>3</sup>), a structural coefficient of 0.2 should be used. Structural coefficient was obtained after the road had been in use for four years, thus, some adjustments may be applied to the structural coefficient. Similar tests may be conducted in the future on the newly constructed pavements in order to determine structural coefficient soon after construction.

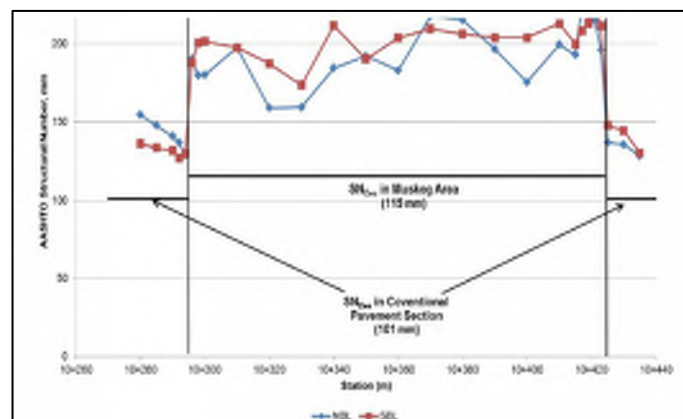


**Figure 3-10: Structural Number Comparison Plot (Griffiths and Popik, 2013)**

### **3.2.1.3 Findings and Discussion**

1. In general, the pavement structure on Dixie Road appeared to be in good condition, with few distresses. With the LCC section in service for roughly three years, it is encouraging to see that the condition of the roadway in this section continued to perform similarly to the pavements adjacent on either side of the LCC section.
2. The overall average asphalt thickness along the whole road section is close to the designed number – 148 mm vs 140 mm. The thickness of the Granular base is not consistent and in some places, it is thinner than the design requirement of 150 mm. The lowest thickness of the Granular base is 68 mm which was found in the place where longitudinal cracks were observed by visual survey.
3. It was also observed that the top of the LCC layer was not flat at the border with the adjacent road section. It was observed on the longitudinal image of the GPR survey. Because of that, the granular layer was detected as thick as 235 mm instead of designed 150 mm. Griffiths and Popik (2013) linked this information with the fact that some distortions on the pavement surface in this area were observed as consequences of some ground movement continued after construction.
4. In order to access those distresses and its cause, a detailed forensic investigation was recommended.
5. It can be noticed that on the GPR transverse images that pavement layers were shown as a bowl shape, with the sides of the layers going up. Griffiths and Popik (2013) reported that this is a result of the top surface, which was constructed with a crossfall but was shown on the image as a flat line. If these images were adjusted to include the surface crossfall of the pavement and shoulders, then the top of LCC layer would have shown a relative flat surface.
6. The construction of the LCC embankment should be completed in lifts, with suitable layer thicknesses to optimize strength of the material, with the practical construction of the embankment. It is recommended that the individual lift thickness do not exceed 300 mm. Furthermore, the design of each lift should be such that the edges of the upper lift are offset by a minimum of 500 mm inward from the edge of the lower lift. The LCC layer should be constructed with a pyramid shape, with the top lift constructed 0.5 m beyond the edge of the travel lane. The staggering of the various lifts of the LCC embankment will allow for easier grading of the embankment slopes while maintaining adequate coverage of the LCC material at all times.
7. The top lift should also be constructed with a minimum 1 percent cross-fall, so that subsurface drainage is maintained at the top of the LCC material toward the outside ditches. Any imperfections in the transverse profile of this layer could create a ‘bath-tub’ situation, which would trap water at this layer interface. This could affect the performance in the Granular base material placed on top of the LCC layer. The embankment slopes should be covered using Granular base type material, with the



embankment slope designed to minimize erosion of the material that could potentially expose the LCC. Transitions at each end of the LCC embankment should also be carefully designed to provide a smooth transition and minimize any abrupt heaves with the adjacent earth embankments. It is critical that frost susceptible material is not used to construct the transition areas. Furthermore, the design of these transitions will need to ensure that they are constructible while meeting the foundation requirements for embankment stability.

### 3.2.2 Brentwood Light Rail Transit (LRT) Bus-Lane. Calgary, Alberta, Canada

The Brentwood bus-lane in Calgary was experiencing heavy loading due to the single rear axles of city buses. The bus lane had traffic volumes of up to 100 buses per hour and had frost-heaved substantially and became virtually impossible to drive on. The subbase of the road was composed of saturated silty deposits, over 30 m in depth. The subgrade soil had a California Bearing Ratio (CBR) of 0.8%. In 2000, the road was completely reconstructed with the following structure:

- 125 mm of asphalt
- 150 mm of Granular base course
- 200 mm of CEMATRIX CMRI-475 Insulating Road Base
- 50 mm of drainage rock (with subdrains beneath the curb & gutter)
- Geotextile fabric

The location of the road section is presented in Figure 3-11.

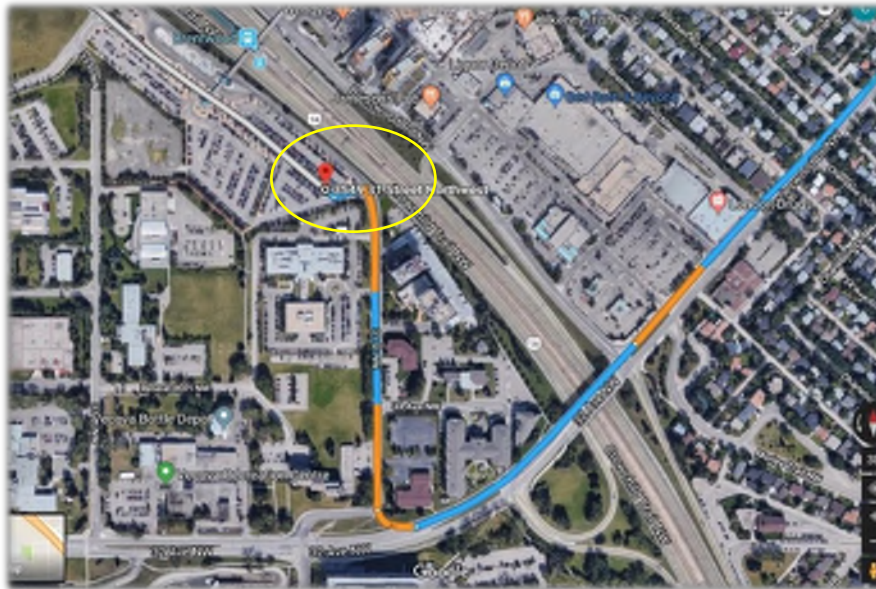


**Figure 3-11: Site Location (Google Maps, 2018)**

Figure 3-12 presents the reconstruction process of the bus-lane before and after pouring the LCC material.



**Figure 3-12: Bus Lane. (a) Reconstruction Process. Placing the LCC (CEMATRIX) (b) After Installing the LCC Layer (CEMATRIX)**

Since construction, the road has experienced no frost heaving and required no additional remediation between 2000 and April 2018. A Benkelman Beam Deflection Test resulted in 0.012 inches (0.30 mm) of deflection, much less than the 0.035 inches (0.89 mm) allowed for such a road.

The performance of the LCC section in comparison to the adjacent conventional pavement structure is shown in Figures 3-13 and 3-14. The transition area between the LCC and non-LCC section is obvious and distresses at the conventional section were observed after the visual inspection in April 2018. The Lightweight Cellular Concrete section performed for a significant period of time (18 years) without any potholes and severe cracks. No maintenance was conducted to this section of the road during its service life.



Figure 3-13: Pavement Distresses on the non-LCC section - 1(CEMATRIX, 2018)

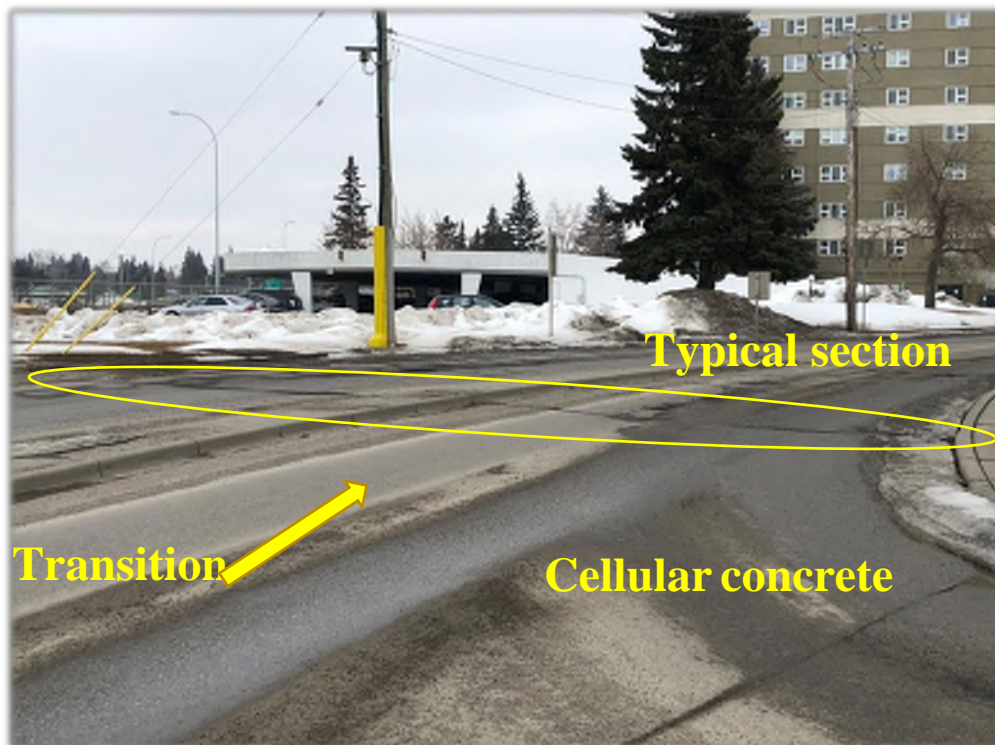


Figure 3-14: Pavement Distresses on the non-LCC section – 2 (CEMATRIX, 2018)



### 3.2.3 Winston Churchill Boulevard. Brampton, Ontario, Canada

The reconstruction of Winston Churchill Boulevard is similar to the Dixie Road project. It is a two-lane rural road. The project was completed in 2016. The location of the road section is presented in Figure 3-15.



**Figure 3-15: Location of the Road Section (Google Maps, 2018)**

The pavement structure consists of the following layers:

- Asphalt concrete layer - 120 mm
- Granular A base layer - 240 mm
- Lightweight Cellular Concrete at the density of  $475 \text{ kg/m}^3$  – 550 mm
- Existing subgrade – peat

The pavement structure that was installed on Winston Churchill Boulevard is shown in Figure 3-16.

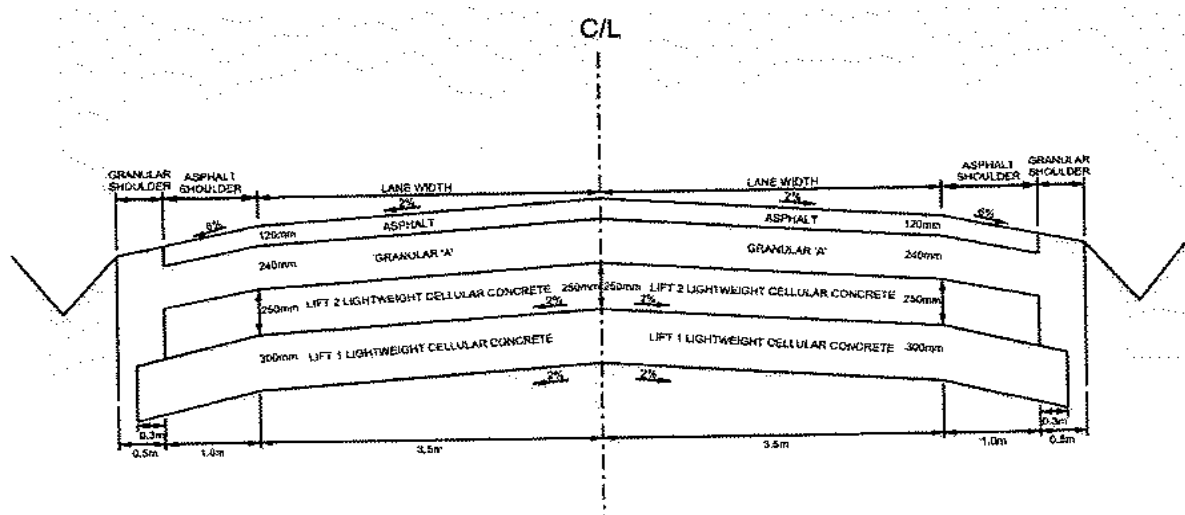


**Figure 3-16: Pavement Structure. Winston Churchill Boulevard (CEMATRIX)**

The field inspection found that the pavement remains in good condition after one year of construction. No severe cracks or rutting were found during the inspection (Figures 3-17 a, 3-17 b).



*(a)*



*(b)*

**Figure 3-17: Condition of Winston Churchill Boulevard, August 2017 (one year after construction).  
(a), (b) – Overall Condition of the Road**

### 3.2.4 Highway 9. Holland Marsh, Ontario, Canada

The Highway 9 site is located north of Toronto. It is 1.5 km meters west from Highway 400. The location of the problematic area on Highway 9 is presented in Figure 3-18.



**Figure 3-18: Highway 9 Site Location (Google Maps, 2018)**

The construction project on Highway 9 aimed to overcome a weak soil problem. The soil in this area included thick organic deposits, which are challenging for pavement design. According to the geotechnical investigation, completed by Stantec in 2014, pavement structure was underlain by organic material ranging from 3.7 to 7.0 m. The site is located directly adjacent to the Pottageville Swamp Conservation Area wherein organic soil materials such as peat can be found at the surface (Figure 3-19). Inorganic soil was also observed, consisting of soft to firm clayey silt to silty clay and compact silt and sand. The groundwater level ranged from 1.5 m to 2.3 m below the surface of the existing pavement.



**Figure 3-19: Highway 9 Site Location with the Local Landscape (Google Maps, 2018)**

Settlement was observed on a portion of Highway 9 in 2014. Asphalt padding and other temporary repairs were considered as possible solutions to this issue, but it would only add additional weight to the current pavement structure, thus leading to potential further settlement. The potential for future repairs was a deterrent. LCC was chosen as an economical and sustainable remediation treatment to address the continued settlement, reduce safety concerns and minimize future maintenance costs. The use of LCC reduced the need of deep excavation, thus, reducing a considerable amount of excess material requiring disposal, construction time, amount of backfill material, and reducing the impact on the environment (Maher and Hagan, 2016).

The section was reconstructed in 2014. The settlement problem was observed only at the eastbound lanes, so traffic was temporarily moved to the westbound lanes. The settlement remediation treatment included excavation of a length of 100 m to a depth of 1.5 m to provide the pavement structure of:

- Asphalt concrete layer – 200 mm
- Granular “O” base layer – 200 mm
- Lightweight Cellular Concrete at the density of  $475 \text{ kg/m}^3$  – 1100 mm
- Existing subbase

The permeability of the subgrade fill material was relatively low, so no polyethylene sheet was used to mitigate the loss of LCC material. A biaxial geogrid with a minimum tensile strength of 0.8 kN/m was installed in a LCC layer at a depth of 0.3 m below the top of the LCC.

The placement of the LCC was completed in three days. In total,  $905 \text{ m}^3$  of LCC material was placed. Figure 3-20 demonstrates the construction process of installing the LCC layer. During the placement of cellular concrete, Quality Control (QC) testing including casting unconfined compressive strength cylinders, wet cast density, and air temperature. A list of the QC specifications is presented in Table 3-2.





**Figure 3-20: Highway 9 Construction Process (CEMATRIX)**

In order to mitigate the presence of water below the LCC layer, a drainage system was developed, including 1% slope of the bottom of LCC layer to the existing subgrade, a transversely installed subdrain at the end of LCC, and a longitudinally installed subdrain on the highway centerline. All these measures were done to capture water that could pond below the LCC. In addition, transition sections were arranged from both ends of the LCC section. Those transitions were critical in mitigating differential performance of LCC and adjacent sections.

**Table 3-2: Project Specifications and QC Results (Maher and Hagan, 2016)**

<b>Item</b>	<b>Project Specification Requirements</b>	<b>QC Results</b>	<b>Average of QC Results</b>
<b>Minimum Unconfined Compressive Strength</b>	1.0 MPa @ 28 days	0.9 to 1.7 MPa	1.3 MPa
<b>Wet Cast Density</b>	523 to 578 kg/m <sup>3</sup>	525 to 580 kg/m <sup>3</sup>	550 kg/m <sup>3</sup>
<b>Air Temperature</b>	Protection required for sub-zero temperatures	10 to 17 <sup>0</sup> C	14 <sup>0</sup> C
<b>Cellular Concrete Temperature</b>	-	22 to 26 <sup>0</sup> C	24 <sup>0</sup> C
<b>Max. Lift Thickness</b>	500 to 600 mm	300 to 500 mm	N/A

Field visual inspection was completed in 2015, one year after construction. It was observed that the pavement was performing well. Figures 3-21 and 3-22 show that no severe distresses were found on the pavement surface. One negligible imperfection was noted in the transition area.

Another field visual inspection was completed in 2017, three years after construction. The field inspection stated that the pavement remained in good condition after three years of service. No severe cracks or rutting were observed during the inspection.



**Figure 3-21: Condition of Highway 9, Three Years after Construction**



**Figure 3-22: Condition of Highway 9, Three Years after Construction**

### 3.2.5 View and Vancouver Streets, City of Victoria, British Columbia, Canada

The City of Victoria was experiencing several settlements in the area around the intersection of Vancouver Street and View Street (Figure 3-23). The intersection had been reconstructed several times previously, but the major settlement issue continued to occur. Settlement was a major issue in this area because of the excessive decay and consolidation of the underlying peat. The option of removing and replacing the weak soils was proposed, but because it was an expensive and impractical procedure, finding a different solution was a priority. Moreover, since this intersection is located in the downtown area, the time of the closures played a big role in selecting a construction approach.



**Figure 3-23: Site location. (Google maps, 2018)**

Dolton et al. (2016) reported that due to excessive total differential settlement in the area, the roadways and sidewalk experienced surface distresses and damage had occurred to underlying utilities. These roadways were originally built over a peat layer that extends up to 5.3 m below the existing ground surface. Below the peat is a thick layer of soft silty clay overlying bedrock at a depth of 30 – 40 m. Use of Lightweight Cellular Concrete was chosen for this project with the following pavement structure design:

- Asphalt concrete – 75 mm
- Crush Granular base course - 150 mm of 20 mm



- LCC with wet density of  $475 \text{ kg/m}^3$  – 500 mm
- Existing subgrade

The construction at View Street and Vancouver Street in the City of Victoria, British Columbia was completed from September 2007 to April 2008 in several stages. The LCC was produced on site, and as it is shown in Figure 3-24, using the “wet” process of production (Dolton et al., 2016). LCC with wet density of  $475 \text{ kg/m}^3$  was used as subbase in this project. Quality Assurance/Quality Control (QA/QC) testing was carried out during construction and found that cast density ranged between  $435 \text{ kg/m}^3$  to  $486 \text{ kg/m}^3$  with an average of  $462 \text{ kg/m}^3$ . Cylinders were also cast according to ASTM C495 for Compressive strength of LCC and results revealed an average of 1.0 MPa (range 0.8 to 1.1 MPa) at 28 days.



**Figure 3-24: View Street and Vancouver Street Construction Process. Wet Mix Equipment (CEMATRIX)**

Total length of the sections that were reconstructed was 430 m on View Street and 137 m on Vancouver Street with a total of  $2,246 \text{ m}^3$  of LCC. It was placed over fourteen pour days of construction. Gravel backfill compacted with no vibration was placed on the cellular concrete before traffic was allowed on the roadway.

Golder Associates Ltd. carried out Benkelman Beam and Falling Weight Deflectometer (FWD) testing at about 20 m intervals in February 2008. The intention of the test was to carry out the test within the outer wheel paths, however, due to different obstacles, some inner wheel paths were tested as well. The weather conditions during the testing were cloudy, with an air temperature of  $13^{\circ} \text{ C}$  and pavement temperature of  $10^{\circ} \text{ C}$ .

The Benkelman Beam test is a method for measuring pavement deflections under static wheel loads. As presented in Figure 3-25, a 3.65 m beam is placed between the dual tires of a truck (80 kN axle load) and height measurement gauge on the end of the beam measure the vertical

rebound of the pavement after the truck is driven away (TAC, 2016). The testing was following the ASTM D 4695 “Standard Guide for General Pavement Deflection Measurements” procedure. The Benkelman Beam deflection data analysis was carried out in accordance with the Asphalt Institute MS-17 method: “Asphalt Overlays for Highway and Street Rehabilitation, Manual Series № 17”. No seasonal correction factor was applied for Maximum Pavement Spring Rebound (MPSR) due to winter conditions. The average rebound was 0.63 mm on View Street and 0.65 mm on Vancouver Street (Table 3-3).

**Table 3-3: Benkelman Beam Results (Golder Associates Ltd. Report, 2008)**

<b>Section</b>	<b>Average Rebound Reading (mm)</b>	<b>Temperature Corrected Rebound (mm)</b>	<b>Standard Deviation</b>	<b>Mean plus 2 STDV</b>	<b>MRSR (mm)</b>
<b>View St. New Pavement</b>	0.63	0.73	0.15	1.03	1.03
<b>Vancouver St. New Pavement</b>	0.65	0.75	0.23	1.21	1.21
<b>View St. Old Pavement</b>	0.53	0.57	0.41	1.40	1.40



**Figure 3-25: Benkelman Beam Deflection Testing**

Falling Weight Deflectometer (FWD) testing was also conducted. This involves evaluating the dynamic response to the fall of the weight from a recorded height. Seven sensors were installed and spaced out at known distances from the load plate to measure deflection. FWD testing was following ASTM D 4694 “Standard Test Method for Deflections with a Falling-Weight-Type Impulse Load Device”. Three load levels were used to determine the deflection response (40, 50, and 75 kN approximately) at each test point.

The measured FWD dynamic deflections were normalized to represent the equivalent deflection for a standard wheel load of 40 kN at an asphalt pavement temperature of 21<sup>0</sup> C. The pavement surface modulus, which indicates the overall strength of the pavement, was also determined. A summary of the FWD testing data is shown in Table 3-4. Spring correction factor was not applied. Results reflected consistent static deflection for the LCC sections, and that the deflection of the non-LCC section was 111% times higher than that of the LCC section. The elastic moduli of the LCC was also reported to be 445 MPa (Standard deviation 146 MPa) and 341 MPa (Standard deviation 99 MPa) which are higher than the typical values for gravel (University of Waterloo, 2011). The elastic moduli of various layers were estimated using ELMOD software (Dynatest 2006). The mean elastic modulus derived from LCC layer was inferred to be 341 MPa on View Street and 445 MPa on Vancouver Street.

**Table 3-4: FWD Test Data**

<b>Street Name</b>	<b>Normalized Deflection (mm)</b>				<b>Pavement Surface Modulus (MPa)</b>	
	Mean	Standard Deviation	Mean+ 2 STDV	Static Deflection	Mean	Standard Deviation
<b>View St. New Pavement</b>	0.49	0.08	0.64	1.0	361	60
<b>Vancouver St. New</b>	0.43	0.05	0.55	0.85	402	53
<b>View St. Old Pavement</b>	0.51	0.41	1.36	2.11	488	238

### 3.3 Summary of Case Studies

**Table 3-5: Summary of the Available Cases of Using LCC as a Subbase Material in Pavement Construction in Canada**

	<b>Dixie Road, Region of Peel, Ontario</b>	<b>Highway 9, Holland Marsh, Ontario</b>	<b>View and Vancouver Streets, City of Victoria, British Columbia</b>	<b>Brentwood Light Rail Transit (LRT) Bus-Lane. Calgary, Alberta</b>	<b>Winston Churchill Boulevard, Brampton. Ontario</b>
<b>Location</b>	Ontario 43°80'49.24" N 79°84'98.97" W	Ontario 44°02'52.65"N 79°61'25.19"W	British Columbia 48°42'45.48"N 123°35'67.65" W	Alberta 51°08'51.72"N 114°12'95.76" W	Ontario 43°69'87. 0"N 79°92'11. 0"W
<b>Cause of Reconstruction</b>	Settlement. Length-120m Peat/marl deposits were located from the depth of 2.1 m to 5.4 m below the existing pavement surface	Settlement. Length-100m Underlain with organic materials (peat) and inorganic (soft to firm clayey silt to silty clay or compact silt and sand)	Settlement. Length- 430m on View Street and 137m on Vancouver Street. Excessive decay and consolidation of the underlying peat	Length-60m. Severe frost heave and subsequent spring thaw weakening of the frost susceptible soils.	Settlement. Length- 300m. Underlain with peat.
<b>Date of Construction</b>	August- November 2009	October 2014	November- February 2007	Summer (July- August) 2000	Summer 2016
<b>Road Type</b>	Rural highway	Highway	Urban	Urban	Rural
<b>Structure</b>	AC-140mm; Granular 'A'- 150mm; LCC-650mm	AC-200mm; Granular "O" base layer-200mm; LCC-1100mm; Biaxial geogrid (300m from the top of LCC layer)	AC-75mm; Crushed Granular base course- 150mm; LCC-500mm; (Tensar BX1100 geogrid was placed between the LCC layers)	AC-125mm; Granular base course-150mm; LCC-200mm; drainage rock- 50mm; Geotextile fabric (at the bottom of LCC layer)	AC-120mm; Granular base course- 240mm; LCC- 550mm; geogrid reinforce fiber glass



<b>Material Composition</b>	CEMATRIX CMEF-475. "Dry" mix	CEMATRIX-475. "Wet" mix	CEMATRIX-475. "Wet" mix	CEMATRIX CMRI-475.	CEMATRI X-475. "Dry" mix
<b>Performance Evaluation</b>	Visual inspection, FWD, Benkelman Beam test	Visual inspection	FWD, Benkelman Beam test	Visual inspection, Benkelman Beam test	Visual inspection
<b>Construction Challenges</b>	Water, stability issues, transition areas	Transition areas, drainage, stability issues	Underlying utilities, Stability issues	Heavy traffic, stability issues	Crossfall, wet soils, stability issues

### 3.4 Discussions and Recommendations

Summarizing the available case studies of using LCC as a subbase in pavement construction, it is worth saying that LCC can be successfully used in rural and in urban conditions. The ages of the sections reviewed varied from two years up to 18 years, which gives an approximate understanding of pavement performances up-to-date. The oldest of the presented section is Brentwood Light Rail Transit (LRT) Bus-Lane in Calgary (18 years) and is performing well, especially in comparison to the adjacent road sections without LCC installation. The younger cases such as Winston Churchill Boulevard (Ontario), Highway 9 (Ontario) and Dixie Road (Ontario) are also performing well, with no severe cracks. The minor cracks that were observed on Dixie Road by visual survey seven years after construction are, most likely, the result of construction defects of the upper layers (GPR and FWD results confirm this theory). The road sections in the City of Victoria, British Columbia performed well up to 2010 when the last inspection was made. Unfortunately, no further performance data for this section was found.

Three out of five considered road sections are located in Ontario, approximately in one area, with similar weather conditions, one section is in Calgary, and one section is located in British Columbia.

All projects were aiming to solve a settlement problem. It is observed that settlement usually occurs on localized parts of the road and not on the whole length of the road. In four projects, the length of the reconstructions was less than 150 meters and only in one project was a longer section (the City of Victoria) needed. Moreover, this section consisted of two intersecting roads, which formed a bigger area of settlement.

The common time for construction was summer-fall time as the soil is more stable and no freeze-thaw cycles are occurring and the subgrade is thawed. Most of the projects were done in July-November and none in the spring.

In terms of the structure of the sections, they all follow the same pattern: LCC layer at the bottom (usually with the geogrid or geotextile reinforcement), followed by Granular base material and asphalt concrete layer at the top. The thicknesses of the layers are different, depending on the purpose of the road and underlying soil.

FWD and Benkelman Beam tests are the most commonly used methods for evaluating the performance of the LCC sections to date.

Some projects were using “dry” mix process and some “wet”. It is common to use “dry” mix process of producing the material for the projects, where relatively high volumes of LCC were needed. However, in the City of Victoria, the installation process happened in three stages and in different months because of the specific road closures and downtown location of the road. In that project, “wet” mix process was used.

In order to use LCC in a pavement structure as a subbase, certain activities have to be taken into consideration and implemented into the construction process. A number of general observations that are applicable to most LCC projects have been made from studying the road sections across Canada. These observations are presented in the following paragraphs.

## **Soils**

Generally, the main issue that using LCC is intended to address is a process of settlement of road sections. In most of the case studies, settlement is happening because of weak subgrade soils. It can be either organic material (peat) or inorganic soils (soft to firm clayey silt to silty clay or compacted silt and sand). Placing a thick layer of unbound granular material on top of those subgrade types, to solve the settlement issue, may lead to more settlements in the future due to the excessive weight of the whole structure. In addition to that, a lot of excavation is often needed to remove the weak soil before placing the unbound Granular material.

## **Water**

Placement of the LCC during light rain is possible but should be avoided in heavy rain. Water is a significant factor, influencing the construction of pavements using LCC. Groundwater seepage control of the excavations, where LCC will be placed, is required. This needs to be done to prevent floating of the material, as the target density of LCC in the case studies was  $475 \text{ kg/m}^3$ , which is less than water density ( $1000 \text{ kg/m}^3$ ). Ignoring water presence in the excavations may lead to buoyancy forces affecting the pouring and restarting the production and placement from the very beginning may be required.

## **Drainage**

It is very important to prevent moisture from weakening the pavement structure once it is in-service. Usually, pavements require a slope of 2% in order to let the stormwater from the surface of the pavement, and subsurface water to drain by the gravity force. For achieving the 2% slope, LCC must be placed in steps, using formwork.

## **Transitions**

Constructing the quality and proper transition areas between pavement sections with LCC and conventional granular pavement is crucial. Those two different pavement structures have different thermal properties and different densities. Because of that, different performance of the pavement structures can occur in those areas during the freeze-thaw conditions. As frost is unlikely to penetrate through the LCC pavement due to its high porosity, reverse heaving of the transition occurs (Maher and Hagan, 2016). In order to mitigate this effect, granular transition tapers can be made in the transition areas. The commonly used is a 10/1 ratio of horizontal to vertical respectively.

## **Equipment**

All the material brought to site must be transported in pre-cleaned equipment and machinery. The transporting equipment must be cleaned, rinsed and completely emptied of the concrete, aggregates, and any other materials that were previously transported (Maher and Hagan, 2016). This was a general consideration in the case studies that were using “dry” mix process; however, for the View Street and Victoria Street intersection, that used “wet” mix process, it was a significant consideration.

This study provides an overview of the current pavement condition of the five sections that were constructed using lightweight cellular concrete as subbase layer material. Results have shown that all five sections were in good pavement condition. However, in-depth pavement data collection has to be done in order to provide a comprehensive review of the performance of the sections with lightweight cellular concrete as subbase layer. Therefore, further investigation is recommended. This could be achieved by using pavement instrumentation such as asphalt gauges, earth pressure cells, and environmental equipment in the new pavement structures.

## **CHAPTER 4**

### **4 PAVEMENT DESIGN AND ANALYSIS**

This Chapter explains the procedure on how pavement design for LCC can be conducted. The predicted performance of the LCC road sections will be determined by failure criteria analysis. Comparison of LCC section to typical Granular material will also be conducted.

#### **4.1 Introduction into Pavement Design**

Structural design of pavements is a complex process. Several factors have to be considered when designing a road. These factors are traffic (axle or gear loads, repetitions), environment, available materials, desirable performance of the pavement, project cost, sustainability, and construction resources (TAC, 2013).

Traffic volume is usually described by Annual Average Daily Traffic (AADT), which shows the range of vehicles of various sizes, weights, and axle configurations. The 80 kN standard single axle is used for quantifying the traffic in pavement design. It allows transition of the cumulative damage from the range of vehicles into a number of Equivalent Single Axle Loads (ESALs) (ARA, 2015).

Climate is another factor that should be considered in pavement design. According to Applied Research Associates (2015), information about pavement surface temperatures expected for the south and east region of Ontario are summarized in Appendix II.

The above-stated factors and some others, that have significant influence on pavement performance, are implemented in several mechanistic pavement models. One of the commonly used ones is Mechanistic-Empirical Pavement Design Guide (MEPDG), which was developed to predict the deterioration of pavements and their associated expected service lives. The focus of this chapter is studying the pavement structure, although some approximate service life of the pavement without any maintenance was also estimated. The WESLEA software was used in this research - a linear elastic multi-layer program that enables analysis of a pavement structure, including the effects of complex load systems.

#### **4.2 Pavement Design with Lightweight Cellular Concrete (LCC)**

The structure of the typical pavement, with respect to the usage of LCC as a subbase, usually consists of LCC layer placed on the subgrade, followed by unbound Granular base material and the asphalt concrete layer as a top surface. Typical pavement structure with LCC is presented in Figure 4-1. Even though the LCC is different from traditional granular material and should be treated as a cement stabilized material, there are no calibration factors and performance models designed for the lightweight cellular concrete. In the MEPDG manual, it is noted that if

the cement stabilized base layer is beneath an unbound Granular base and hot-mix asphalt layer, the pavement design should treat it as an unbound layer with a constant layer modulus.

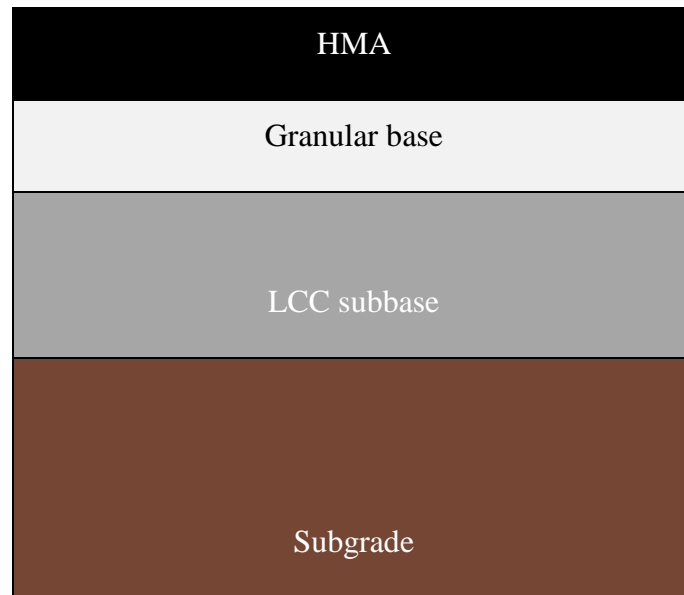


**Figure 4-1: Pavement Structure with LCC**

### **4.3 Analysis Method**

Three roads in Ontario with installed LCC were chosen to be studied: Dixie Road, Highway 9 and Winston Churchill Boulevard. This Chapter aims to predict performance of the installed LCC sections in terms of fatigue cracking and rutting issues as well as to determine the bearing capacity of the road sections. These parameters were discussed as the failure criteria. Furthermore, the comparison between LCC and Granular B subbase materials that were installed on the same road sections was completed and discussed. The predicted service life of the pavements without any maintenance was determined.

The method for the failure criteria analysis consisted of the following approaches:

- Measuring the response of the pavement to different loadings. At this approach, the ability of the pavement to withstand various loads was studied by controlling stress values at the bottom and top of the subbase layer.
- Determining the allowable number of load repetitions on the pavement. The approach obtains the number of maximum load repetitions that can be withstand by the pavement.
- Identifying the maximum ESALs that road section can bear. Damages due to cumulative Equivalent Single Axle Loads were determined and presented in the graphs as potential fatigue cracking and rutting issues.

#### 4.4 Failure Criteria Analysis

In order to understand the expected vertical stress and tensile stress that will occur in the pavement structure the failure criteria analysis was conducted using the WESLEA software. The pavement structure and material properties were taken from the existing projects in Canada. Some unknown values were assumed in this analysis based on engineering experience and recommended values (TAC, 2014). Modulus of elasticity for LCC was taken as 850 MPa as a result of the tests that were conducted by the author's colleagues in CPATT laboratory (for the LCC density of 475 kg/m<sup>3</sup>).

Two types of pavement structure using a different material for subbase layer were analyzed and compared, which are the Lightweight Cellular Concrete and the unbound Granular B subbase material. The pavement structure and material properties are provided in Table 4-1.

ESALs for Dixie Road were taken from the report completed by Griffiths and Popik (2013). The AADT information for Highway 9 was obtained from MTO (provincial highways traffic volumes 2016 report). The ESALs for Dixie Road and for Winston Churchill Boulevard were predicted to be 500,000 and 160,000 respectively (Table 4-2).

**Table 4-1: WESLEA Settings for Dixie Road, Highway 9 and Winston Churchill Boulevard (Material Properties of the Pavement)**

		Surfac	Base	Subbase		Subgrad
		HMA	Granular	Granular B	LC	Soil
<b>Dixie Road</b>	E (MPa)	3445	250	200	850	30
	Poisson's Ratio	0.35	0.4	0.35	0.2	0.45
	Thickness (mm)	140	150	650	650	-
<b>Highway 9</b>	E (MPa)	3445	250	200	850	30
	Poisson's Ratio	0.35	0.4	0.35	0.2	0.45
	Thickness (mm)	200	200	1100	1100	-
<b>Winston Churchill Blvd</b>	E (MPa)	3445	250	200	850	30
	Poisson's Ratio	0.35	0.4	0.35	0.2	0.45
	Thickness (mm)	120	240	550	550	-

**Table 4-2: ESALs for Three Road Sections in Ontario**

	<b>Dixie Road</b>	<b>Highway 9</b>	<b>Winston Churchill Blvd</b>
<b>ESALs</b>	500,000	1,500,000	160,000

LCC is a potential substitution of the granular material for the subbase in some projects. This chapter aimed to compare the predicted performance of the pavements with LCC with the same road but with granular material; thus the same steps for determining the stress values were taken for both pavements – LCC and granular subbase pavements.

#### 4.4.1 First Approach

With the use of WESLEA software, the vertical stress and tensile stress happened on the top of the subbase layer and bottom of the subbase layer respectively at different loads is shown in Figure 4-2. To develop the graphs, the load range was varied from 20 kN to 120 kN of magnitude. The standard axle load number is usually considered to be 80 kN. Figure 4-2 presents the expected vertical stress that will be applied to the subbase layer.

The vertical stress applied to the LCC layer is higher than the one to the Granular B layer for every loading set for all three roads. However, the typical compressive strength of the LCC at low density ranges between 0.5 MPa to 1.0 MPa. Thus, the LCC layer is considered strong enough to support the pavement in the range of 20 kN to 120 kN of axle loads. The output of the WESLEA software is shown in Tables 4-3; 4-4; 4-5.

**Table 4-3: Vertical and Tensile Stresses. Dixie Road**

<b>Dixie Road</b>				
<b>Load, kg</b>	Vertical Stress at the Top of Granular B	Tensile Stress at the Bottom of Granular B	Vertical Stress at the Top of LCC layer	Tensile Stress at the Bottom
<b>2000</b>	55.53	-25.07	83.21	-45.68
<b>4000</b>	105.18	-49.63	156.01	-90.35
<b>6000</b>	150.34	-73.68	220.81	-134.04
<b>8000</b>	191.9	-97.24	279.2	-176.79
<b>10,000</b>	230.47	-120.32	332.28	-218.62
<b>12,000</b>	266.47	-142.93	380.84	-259.57



**Table 4-4: Vertical and Tensile Stresses. Highway 9**

<b>Highway 9</b>				
<b>Load, kg</b>	Vertical Stress at the Top of Granular layer	Tensile Stress at the Bottom of Granular Layer	Vertical Stress at the Top of LCC layer	Tensile Stress at the Bottom of LCC Layer
<b>2000</b>	34.27	-10.14	52.84	-18.68
<b>4000</b>	66.56	-20.19	102.11	-37.19
<b>6000</b>	97.12	-30.14	148.27	-55.51
<b>8000</b>	126.14	-40.01	191.67	-73.66
<b>10,000</b>	153.79	-49.78	232.57	-91.63
<b>12,000</b>	180.19	-59.47	272.2	-109.43

**Table 4-5: Vertical and Tensile Stresses. Winston Churchill Blvd**

<b>Winston Churchill Boulevard</b>				
<b>Load, kg</b>	Vertical Stress at the Top of Granular layer	Tensile Stress at the Bottom of Granular Layer	Vertical Stress at the Top of LCC layer	Tensile Stress at the Bottom of LCC Layer
<b>2000</b>	52.64	-0.92	74.72	-1.85
<b>4000</b>	101.26	-1.76	142.88	-3.56
<b>6000</b>	146.46	-2.51	205.46	-5.11
<b>8000</b>	188.7	-3.17	263.21	-6.53
<b>10,000</b>	228.31	-3.76	316.72	-7.82
<b>12,000</b>	265.58	-4.27	366.43	-8.97

The results of the tensile stress occurring at the bottom of the subbase layer are demonstrated in Figure 4-2. It is clear that the tensile stress happening at the LCC layer is higher than the tensile stress occurring at the Granular B layer. However, according to Narayanan and Ramamurthy (2000), the flexural strength of lightweight cellular concrete ranges from 15% to 35% of its compressive strength, which is between 0.075 to 0.35 MPa for the typical low-density lightweight cellular concrete. Predicted maximum value obtained from the WESLEA

software for tensile stress at the bottom of the LCC subbase layer (at 120 kN load magnitude) throughout all road sections was 0.26 MPa. The right part of Figure 4-2 displays that both of the subbase layers for all three roads are capable of resisting the tensile stress and protect the layer from damage.

Maximum vertical stresses that potentially could happen under 120 kN load magnitude at the top of LCC layer were 0.38 MPa, 0.27 MPa and 0.36 MPa for Dixie Road, Highway 9 and Winston Churchill Boulevard respectively. Those values are lower than typical compressive strength values for the Lightweight Cellular Concrete (0.5 to 1.5 MPa). Thus, LCC layer can potentially hold the vertical stress without being damaged (Figure 4-2).

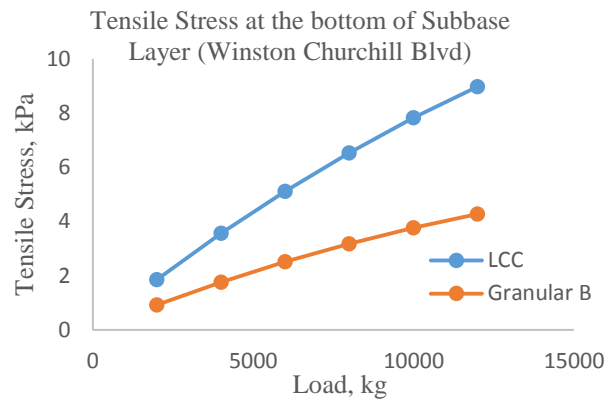
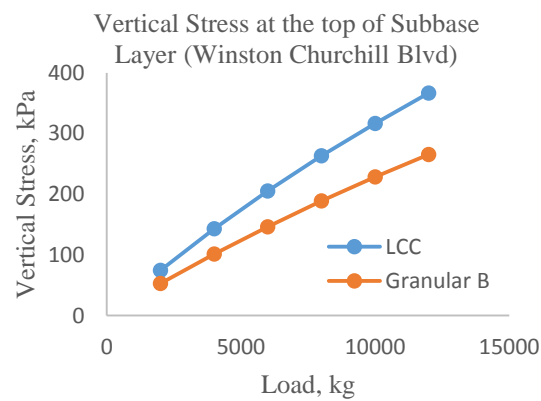
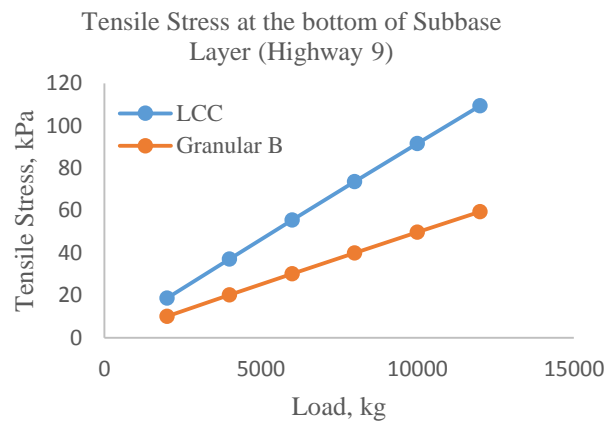
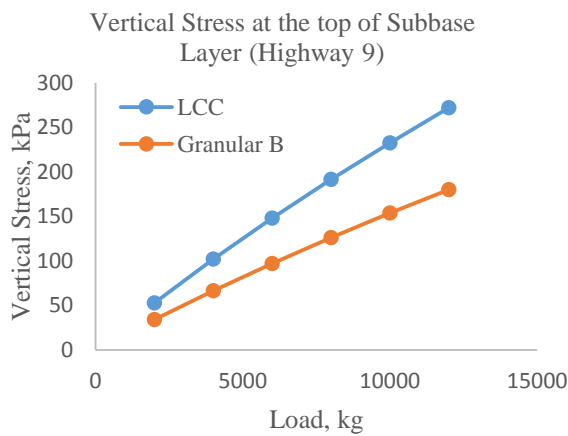
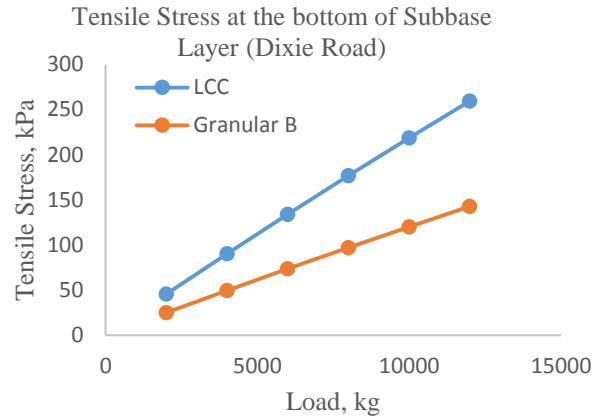
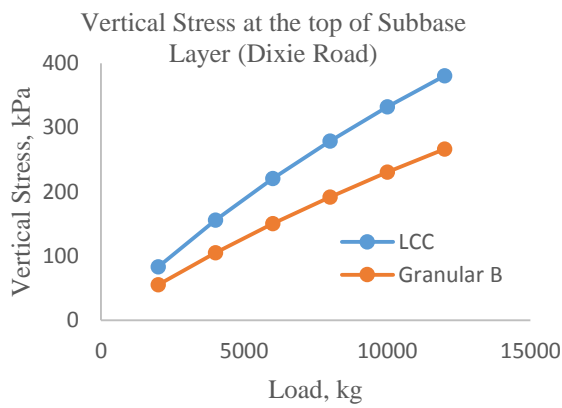


**Figure 4-2: Vertical and Tensile Stresses. Comparison for Dixie Road, Highway 9 and Winston Churchill Blvd (WESLEA software, 2018)**

#### 4.4.2 Second Approach

The vertical stress value at the bottom of AC layer and tensile strength at the bottom of LCC layer were taken as the representatives of the fatigue and rutting measures respectively. By using the WESLEA software, damage analysis for fatigue cracking and permanent deformation was obtained. The equations that were used in the calculation of fatigue cracking and rutting in WESLEA software are presented below:

$$N_{fc} = 2.83 \times 10^{-6} \left( \frac{10^6}{\varepsilon_t} \right)^{3.148} \quad (1)$$

Where:

$N_{fc}$  = Allowable number of load repetition before fatigue cracking

$\varepsilon_t$  = Tensile strain at the bottom of surface layer

$$N_{fr} = 1.0 \times 10^{16} \left( \frac{1}{\varepsilon_v} \right)^{3.87} \quad (2)$$

Where:

$N_{fr}$  = Allowable number of load repetition before rutting

$\varepsilon_v$  = Compressive strain at the top of subgrade layer

The output of the WESLEA software of the predicted damage to the pavements is presented in Tables 4-6; 4-7; 4-8.

**Table 4-6: Allowable Number of Load Repetition. Fatigue Cracking and Rutting for Dixie Road**

<b>Dixie Road</b>				
<b>Load, kg</b>	<b>Fatigue. Pavement with Granular B</b>	<b>Rutting. Pavement with Granular B</b>	<b>Fatigue.Pavement with LCC</b>	<b>Rutting.Pavement with LCC</b>
<b>2000</b>	2,417,552	12,264,561	4,602,352	154,158,424
<b>4000</b>	451,514	870,860	1,005,395	10,962,335
<b>6000</b>	183,018	188,197	443,908	2,372,274
<b>8000</b>	107,632	64,135	287,635	809,479
<b>10,000</b>	76,547	28,049	227,081	354,437
<b>12,000</b>	60,720	14,631	200,912	181,681

It should be noted that the LCC layer could potentially carry more traffic loading than Granular B layer before fatigue cracking happens. This conclusion can be made due to the fact that the Total Allowable Number of Load Repetition (in terms of fatigue cracking) of LCC layer is 1.4 to 3.3 times higher than the Granular B layer depending on the project. Giving the example of the typical axle load of 80 kN for Dixie Road, the Total Allowable Number of Load Repetition with LCC is 287,635 whereas it is 107,632 with Granular B. The ratio comes to 2.67, meaning that pavement with LCC is superior in terms of resistance to fatigue cracking.

**Table 4-7: Allowable Number of Load Repetition. Fatigue Cracking and Rutting for Highway 9**

<b>Highway 9</b>				
<b>Load, kg</b>	<b>Fatigue. Pavement with Granular B</b>	<b>Rutting. Pavement with Granular B</b>	<b>Fatigue. Pavement with LCC</b>	<b>Rutting. Pavement with LCC</b>
<b>2000</b>	8,801,919	348,501,635	15,268,311	5,148,891,932
<b>4000</b>	1,335,740	24,233,438	2,433,609	358,295,756
<b>6000</b>	500,772	5,129,902	962,659	75,899,446
<b>8000</b>	269,727	1,712,909	548,875	25,360,318
<b>10,000</b>	175,802	734,178	379,512	10,876,822
<b>12,000</b>	128,467	368,512	294,602	5,462,865

**Table 4-8: Allowable Number of Load Repetition. Fatigue Cracking and Rutting for Winston Churchill Boulevard**

<b>Winston Churchill Boulevard</b>				
<b>Load, kg</b>	<b>Fatigue. Pavement with Granular B</b>	<b>Rutting. Pavement with Granular B</b>	<b>Fatigue. Pavement with LCC</b>	<b>Rutting. Pavement with LCC</b>
<b>2000</b>	1,605,741	8,847,648	2,279,127	90,925,930
<b>4000</b>	343,393	630,873	538,184	6,482,740
<b>6000</b>	145,964	136,897	241,716	1,406,532
<b>8000</b>	90,887	46,842	160,580	481,185
<b>10,000</b>	68,516	20,567	130,016	211,232
<b>12,000</b>	57,474	10,572	117,682	108,552

The results for predicted rutting performance show even stronger differentiation between values. The performance of the LCC based pavements in terms of rutting is from 10.2 to 14.8 times better than with Granular B. For Highway 9, under the typical axle load of 80 kN, the Total Allowable Number of Load Repetition with LCC and Granular B (in terms of rutting) is 25,360,318 and 1,712,909 respectively. Thus giving the ratio of 14.8. This is due to the fact that LCC material is stiffer itself and because rutting is a result of tensile stress at the bottom of the subbase layer, LCC-based pavements show lower rutting issues.

The results of the Allowable Number of Load Repetition under the various loadings are shown in Figure 4-3. It is clear that the pavement with LCC subbase is more durable than the pavement with Granular B layer at the same thickness since the allowable numbers of load repetitions for fatigue cracking and permanent deformation are higher.

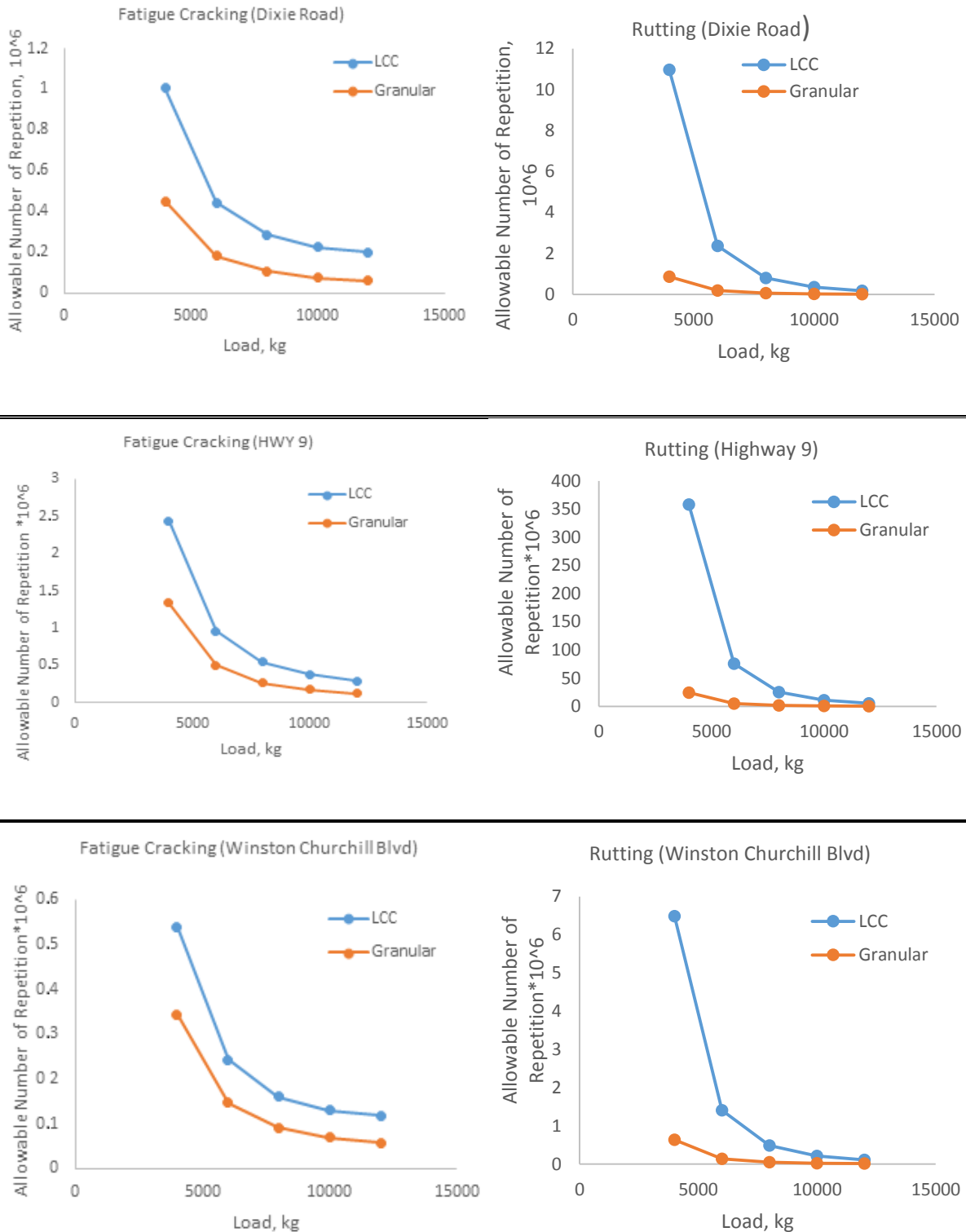


**Figure 4-3: Allowable Number of Load Repetition. Fatigue Cracking and Rutting for Dixie Road, Highway 9 and Winston Churchill Blvd (WESLEA software, 2018)**



#### 4.4.3 Third Approach

In order to understand the approximate service life of the pavement without any maintenance, Allowable Number of Load Repetitions vs ESALs graphs were plotted on Figure 4-4. The maximum Allowable Number of Load Repetitions was calculated by WESLEA software and it was 107,632 for fatigue cracking and 64,135 for rutting (Dixie Road; Granular-based section). In comparison, for LCC-based section for the same road, those values were 287,635 and 809,479 for fatigue cracking and rutting respectively. Values for other sections are presented in Tables 4-11; 4-12; 4-13; 4-14.

The ratio between the range of ESALs and Allowable Number of Load Repetitions was calculated in order to predict the capacity of the particular section. If the damage ratio exceeds one, it indicates that a failure could happen on the pavement as traffic loading surpass the pavement's bearing capacity. Damage ratio under various ESALs for each road section were calculated to determine bearing capacity of the pavements under different traffic loading. Satisfactory result was considered when both rutting and fatigue cracking damage ratio were below one. For Dixie Road, Granular-based pavement, this number was 50,000 ESALs, whereas for the LCC-based it was 250,000 ESALs (Table 4-9; 4-10). The same trend was observed on two other roads – Highway 9 and Winston Churchill Boulevard. For Highway 9 (Tables 4-11; 4-12), both fatigue and rutting damage ratio were lower than one under the 100,000 ESALs (Granular layer) and 500,000 ESALs (LCC layer). For Winston Churchill Boulevard – 40,000 and 160,000 ESALs respectively (Tables 4-13; 4-14).

All three road sections installed with LCC as a subbase could potentially withstand higher ESALs than pavements with Granular material. This can lead to the conclusion that LCC-based pavements could be more durable in terms of fatigue cracking and rutting resistance.

The output from the WESLEA software of the predicted damage of the pavements is presented in Tables 4-9; 4-10; 4-11; 4-12; 4-13; 4-14.

**Table 4-9: Predicted Damage (Fatigue Cracking and Rutting) of Pavement with Granular B Subbase. Dixie Road (WESLEA, 2018)**

<b>Granular B</b>					
		Fatigue cracking. With Granular B		Rutting. With Granular B	
<b>Load,kg</b>	<b>ESALs</b>	<b>Allowable</b>	<b>Damage</b>	<b>Allowable</b>	<b>Damage</b>
<b>80</b>	500,000	107,632	4.65	64,135	7.80
<b>80</b>	450,000	107,632	4.18	64,135	7.02
<b>80</b>	400,000	107,632	3.72	64,135	6.24
<b>80</b>	350,000	107,632	3.25	64,135	5.46
<b>80</b>	300,000	107,632	2.79	64,135	4.68
<b>80</b>	250,000	107,632	2.32	64,135	3.90
<b>80</b>	200,000	107,632	1.86	64,135	3.12
<b>80</b>	150,000	107,632	1.39	64,135	2.34
<b>80</b>	100,000	107,632	0.93	64,135	1.56
<b>80</b>	<b>50,000</b>	<b>107,632</b>	<b>0.46</b>	<b>64,135</b>	<b>0.78</b>

**Table 4-10: Predicted Damage (Fatigue Cracking and Rutting) of Pavement with LCC Subbase. Dixie Road (WESLEA, 2018)**

<b>LCC</b>					
		Fatigue cracking. With LCC		Rutting. With LCC	
<b>Load, kg</b>	<b>ESALs</b>	<b>Allowable</b>	<b>Damage</b>	<b>Allowable</b>	<b>Damage</b>
<b>80</b>	500,000	287,635	1.74	809,479	0.62
<b>80</b>	450,000	287,635	1.56	809,479	0.56
<b>80</b>	400,000	287,635	1.39	809,479	0.49
<b>80</b>	350,000	287,635	1.22	809,479	0.43
<b>80</b>	300,000	287,635	1.04	809,479	0.37
<b>80</b>	<b>250,000</b>	<b>287,635</b>	<b>0.87</b>	<b>809,479</b>	<b>0.31</b>
<b>80</b>	200,000	287,635	0.70	809,479	0.25
<b>80</b>	150,000	287,635	0.52	809,479	0.19
<b>80</b>	100,000	287,635	0.35	809,479	0.12
<b>80</b>	50,000	287,635	0.17	809,479	0.06

**Table 4-11: Predicted Damage (Fatigue Cracking and Rutting) of Pavement with Granular Subbase.  
Highway 9 (WESLEA, 2018)**

<b>Granular B</b>					
		Fatigue cracking. With Granular B		Rutting. With Granular B	
<b>Load, kg</b>	<b>ESALs</b>	<b>Allowable</b>	<b>Damage</b>	<b>Allowable</b>	<b>Damage</b>
<b>80</b>	1,500,000	269,727	5.56	1,712,909	0.88
<b>80</b>	1,300,000	269,727	4.82	1,712,909	0.76
<b>80</b>	1,100,000	269,727	4.08	1,712,909	0.64
<b>80</b>	900,000	269,727	3.34	1,712,909	0.53
<b>80</b>	700,000	269,727	2.60	1,712,909	0.41
<b>80</b>	500,000	269,727	1.85	1,712,909	0.29
<b>80</b>	300,000	269,727	1.11	1,712,909	0.18
<b>80</b>	<b>100,000</b>	<b>269,727</b>	<b>0.37</b>	<b>1,712,909</b>	<b>0.06</b>

**Table 4-12: Predicted Damage (Fatigue Cracking and Rutting) of Pavement with LCC Subbase. Highway  
9 (WESLEA, 2018)**

<b>LCC</b>					
		Fatigue cracking. With LCC		Rutting. With LCC	
<b>Load, kg</b>	<b>ESALs</b>	<b>Allowable</b>	<b>Damage</b>	<b>Allowable</b>	<b>Damage</b>
<b>80</b>	1,500,000	548,875	2.73	25,360,318	0.06
<b>80</b>	1,400,000	548,875	2.55	25,360,318	0.06
<b>80</b>	1,300,000	548,875	2.37	25,360,318	0.05
<b>80</b>	1,200,000	548,875	2.19	25,360,318	0.05
<b>80</b>	1,100,000	548,875	2.00	25,360,318	0.04
<b>80</b>	1,000,000	548,875	1.82	25,360,318	0.04
<b>80</b>	900,000	548,875	1.64	25,360,318	0.04
<b>80</b>	800,000	548,875	1.46	25,360,318	0.03
<b>80</b>	700,000	548,875	1.28	25,360,318	0.03
<b>80</b>	600,000	548,875	1.09	25,360,318	0.02
<b>80</b>	<b>500,000</b>	<b>548,875</b>	<b>0.91</b>	<b>25,360,318</b>	<b>0.02</b>

**Table 4-13: Predicted Damage (Fatigue Cracking and Rutting) of Pavement with Granular Subbase. Winston Churchill Boulevard (WESLEA, 2018)**

<b>Granular B</b>					
<b>Input Parameters</b>		Fatigue cracking. With Granular B		Rutting. With Granular B	
<b>Load, kg</b>	<b>ESALs</b>	<b>Allowable</b>	<b>Damage</b>	<b>Allowable</b>	<b>Damage</b>
<b>80</b>	160,000	90,887	1.76	46,842	3.42
<b>80</b>	145,000	90,887	1.60	46,842	3.10
<b>80</b>	130,000	90,887	1.43	46,842	2.78
<b>80</b>	115,000	90,887	1.27	46,842	2.46
<b>80</b>	100,000	90,887	1.10	46,842	2.13
<b>80</b>	85,000	90,887	0.94	46,842	1.81
<b>80</b>	70,000	90,887	0.77	46,842	1.49
<b>80</b>	55,000	90,887	0.61	46,842	1.17
<b>80</b>	<b>40,000</b>	<b>90,887</b>	<b>0.44</b>	<b>46,842</b>	<b>0.85</b>

**Table 4-14: Predicted Damage (Fatigue Cracking and Rutting) of Pavement with LCC Subbase. Winston Churchill Boulevard (WESLEA, 2018)**

<b>LCC</b>					
<b>Input Parameters</b>		Fatigue cracking. With LCC		Rutting. With LCC	
<b>Load, kg</b>	<b>ESAL</b>	<b>Allowable</b>	<b>Damage</b>	<b>Allowable</b>	<b>Damage</b>
<b>80</b>	220,000	160,580	1.37	481,185	0.6
<b>80</b>	200,000	160,580	1.25	481,185	0.42
<b>80</b>	180,000	160,580	1.12	481,185	0.37
<b>80</b>	<b>160,000</b>	<b>160,580</b>	<b>1.00</b>	<b>481,185</b>	<b>0.33</b>
<b>80</b>	140,000	160,580	0.87	481,185	0.29
<b>80</b>	120,000	160,580	0.75	481,185	0.25
<b>80</b>	100,000	160,580	0.62	481,185	0.21
<b>80</b>	80,000	160,580	0.50	481,185	0.17
<b>80</b>	60,000	160,580	0.37	481,185	0.12
<b>80</b>	40,000	160,580	0.25	481,185	0.08
<b>80</b>	20,000	160,580	0.12	481,185	0.04

Figure 4-4 shows the comparison between LCC and Granular materials in terms of performance. In all three roads, LCC-based pavements showed good performance in terms of fatigue cracking and rutting. In all cases, except for the fatigue cracking resistance on Dixie Road, pavements with LCC layer showed potential ability to resist the load. For Dixie Road, the ESALs of 500,000 was higher than one obtained from the WESLEA software of 250,000 ESALs, meaning that pavement cannot withstand this large number of ESALs without any maintenance. In terms of rutting, there was a significant margin in LCC-based pavements before they reached the allowable limit of load repetitions. By modeling different pavement structures (LCC and Granular B based) there is an opportunity to visually estimate the difference between the two performances. According to WESLEA output, LCC has performed better in all three projects in both fatigue cracking and rutting resistance. It should be noted that the difference in the performance of the sections was more significant in terms of rutting.

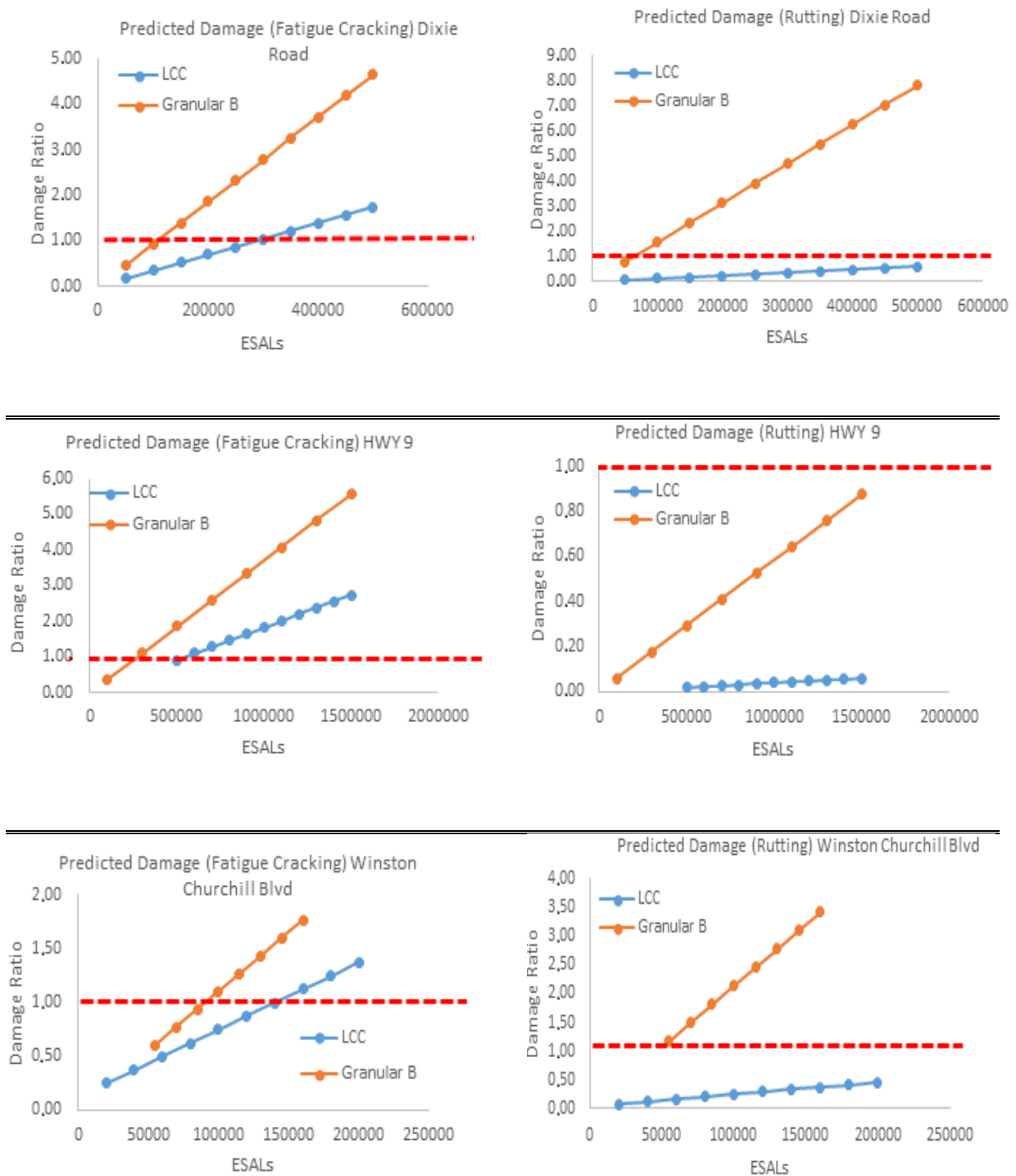


**Figure 4-4: Predicted Damage. Fatigue Cracking and Rutting for Dixie Road, Highway 9 and Winston Churchill Blvd (WESLEA Software, 2018)**

#### **4.5 Summary**

Three roads in Ontario were taken as examples of roads with settlement issues. All three sections were installed with the LCC layer as a subbase and prediction performance of those sections was determined by the criteria analysis.

The result of the failure criteria analysis indicated that the LCC layer is more durable compared to the conventional Granular B materials; thus, pavement thickness using LCC as a subbase material could be thinner than the conventional pavement structure, which may reduce the excavation depth during construction and save time and money. This also shows that using LCC as a subbase layer material could be effective. However, the software does not consider the environmental impact such as temperature and moisture. An in-situ field inspection is needed to evaluate the environmental effect on the pavement using LCC as a subbase layer. The results of the failure criteria analysis indicated that the usage of LCC as a subbase material is more durable than the conventional granular material with similar thickness. The findings demonstrate that LCC could be considered as a potential pavement subbase material in respect to mechanical properties. However, other durability and functional properties have to be assessed.



## **CHAPTER 5**

### **5 TORONTO PROJECT**

Mechanical properties of LCC samples, cast during constructing project will be studied in this Chapter. Results, obtained from the laboratory testing will be compared to the typical values for LCC in the literature.

All of the road sections described and studied in Chapters 3 and 4 were constructed prior to this research being carried out. In order to study the current state and condition of the sections installed with Lightweight Cellular Concrete (LCC) and, to predict the future performance of the pavement, laboratory tests on defining mechanical properties of LCC needed to be done. Some companies, such as CEMATRIX, have been running laboratory tests by using their own laboratories as well as using third-party companies. Typically, preparation of samples in laboratory conditions might not necessarily reflect actual site construction conditions. This could be due to a number of unforeseen circumstances that might occur during the construction process, including but not limited to weather conditions, challenges with equipment and human factor. As a result of this, it is important to assess the characteristics of the actual field-cast material. Therefore, this study obtained LCC samples from the actual site and tested them in the CPATT laboratory. Some of the most important mechanical properties such as Modulus of Elasticity, Poisson's ratio, and UCS were determined and compared to the typical values for the corresponding LCC densities.

#### **5.1 Site Description**

One of the ongoing projects Southern Ontario is a road section of Eglinton Avenue West, East of Black Creek Drive, Toronto, Ontario (Figure 5-1). The purpose of this project is to widen the road. This construction project consists of several measures including but not limited to constructing a retaining wall out of concrete and raising the surface of the road by approximately five meters. The latter was designed to be installed with lightweight material since the reduction in weight of this thick pavement layer was required.



**Figure 5-1: Site Location (Google Maps, 2018)**

## 5.2 Approach

The aim of this Chapter is to determine mechanical properties of the in-situ cast samples and to compare the obtained values to the typical values in literature. In addition, the relationship between the mechanical properties of LCC will be discussed.

Access to the construction site for collecting the fresh samples was provided by the company, which was conducting the Lightweight Cellular Concrete work (CEMATRIX). A total of 2521 m<sup>3</sup> of LCC material was poured over a couple of weeks. As part of this project, cylindrical molds were prepared for casting the LCC samples by University of Waterloo team. Modulus of elasticity, unconfined compressive strength, and Poisson's ratio were determined by testing those samples.

## 5.3 Production and Placement

Lightweight Cellular Concrete with the 475 kg/m<sup>3</sup> plastic density was used in this project. The “dry” mix process was utilized. The composition of the mix was cement (80%), slag (20%), w/c ratio of 0.5 and a foaming agent. The cement and slag were mixed together by a contractor before deliver to the site and after that, this dry mix was sucked into CEMATRIX “dry” mix equipment where it was blended with water. Figure 5-2 represents the construction process.



**Figure 5-2: Construction Process. Toronto, May 2018**

The target plastic density and the slurry temperature were controlled at this stage. Quality Control (QC) is one of the steps for checking the desirable features of the mix. Marsh cone test was conducted to ensure the mix met the desired requirement. According to industrial experience, it is found that 45 to 90 seconds in Marsh cone test could provide a stable and quality cement slurry.

After mixing the slurry, the mix is pumped to the site through a hose. At the same moment, the foaming agent is added to the mix and it is blended while moving inside the hose. In order to blend the LCC mix properly, a special device is installed in the beginning of the hose, which twists the torrent.

Plastic density was checked once per every  $100 \text{ m}^3$  during the pouring to ensure the target plastic density was reached and maintained. No consolidating and vibrating during the placement process was carried out as it may harm the bubble structure of the material.

During the placement of the LCC mix, several buckets were filled with material. Shortly after that, all the prepared molds were cast from the above-mentioned buckets prefilled with LCC (Figure 5-3). The target density for LCC material was  $475 \text{ kg/m}^3$ . According to Maher and Hagan, (2016) plastic density may vary in the range of  $\pm 10\%$  of designed density. Thus, the range for the  $475 \text{ kg/m}^3$  LCC mix is  $427.5$  to  $522.5 \text{ kg/m}^3$ . During the mixing on site, Quality Control showed that the average plastic density of the mix was  $454 \text{ kg/m}^3$ .



**Figure 5-3: Samples, Collected on Site. 75\*150 mm Molds for UCS test. 150\*300 mm Molds for Modulus of Elasticity and Poisson's Ratio Tests**

The following sections discuss the laboratory tests that were performed such as Unconfined Compressive Strength, Modulus of Elasticity and the Poisson's ratio. Samples for UCS test were collected in the amount of four samples per each test date. UCS testing was performed on 7, 14, 21 and 28<sup>th</sup> days. In addition, several samples were collected as spare samples for setting up the testing equipment. Modulus of elasticity and Poisson's Ratio test was conducted on 28<sup>th</sup> day only. Seven samples, including dummy ones, of 150 mm\*300 mm were collected for testing modulus of elasticity and Poisson's ratio. The procedures followed for each test are described below.

#### **5.4 Laboratory Tests**

Laboratory tests were conducted at the University of Waterloo, at the Centre for Pavement Transportation and Technology (CPATT) laboratory from June 1, 2018 to June 22, 2018.



### 5.4.1 Unconfined Compressive Strength

This test was carried out in accordance with ASTM C495 and ASTM C796. Four cylinder specimens with dimensions 75 mm by 150 mm were tested. The samples were cast in-situ and in order to prevent them from being broken and to avoid compaction from vibration, samples were kept on site for three days. The ambient temperature on May 25<sup>th</sup> to May 27<sup>th</sup>, during the field work, is presented in Figure 5-4.

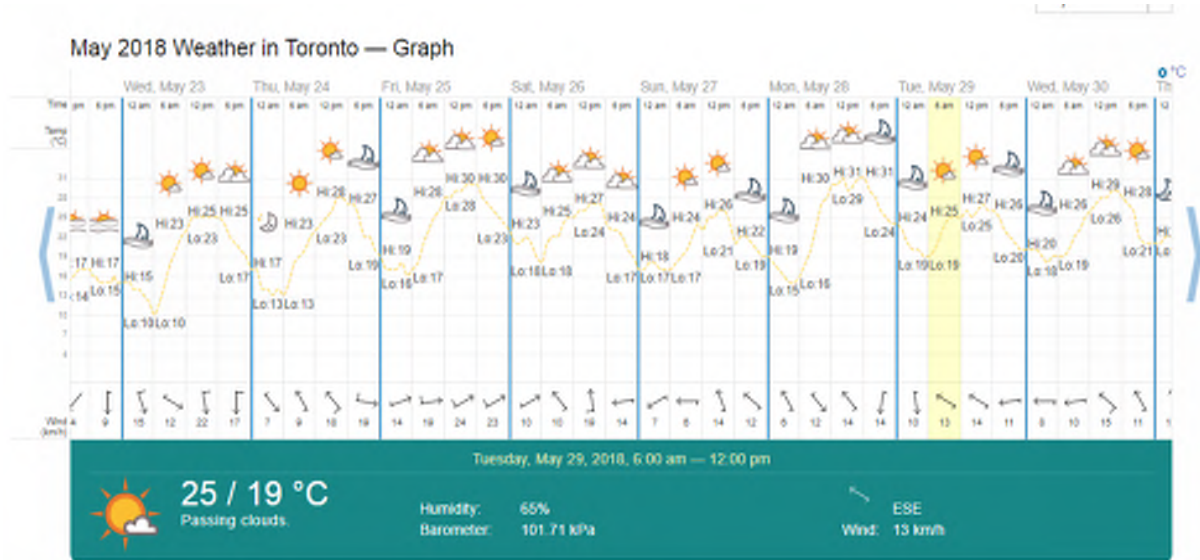


**Figure 5-4: Weather Forecast during Construction and Casting the Samples**  
(<https://www.timeanddate.com/weather/canada/toronto/historic?month=5&year=2018>)

Later, samples were cured at room temperature  $21 \pm 6^{\circ}\text{C}$  from day four to the testing day. Before testing the samples, they were demolded, grinded at the top and the bottom in order to have horizontal flat surfaces. Measurements of the samples were taken such as height, diameter, and weight. The average measured hardened state densities for the different batches of samples were reported as 416, 408, 410, 401  $\text{kg/m}^3$ . The actual density, which is known as a hardened state density, was observed to be lower than plastic density of material that was poured on site. The hardened state density of LCC is typically about 80  $\text{kg/m}^3$  less than its plastic density (Legatski, 1994). Thus, measured densities are within the expected range.

In addition, visual inspection was completed to reveal some possible structural cracks, apart from drying shrinkage, which can affect the test results. During the testing process, the load was applied at a constant rate and the maximum load was reached within considerable time. To calculate the compressive strength for each specimen, the following equation was used:

$$UCS = \frac{P}{A}$$

where:

UCS – Unconfined Compressive Strength, MPa

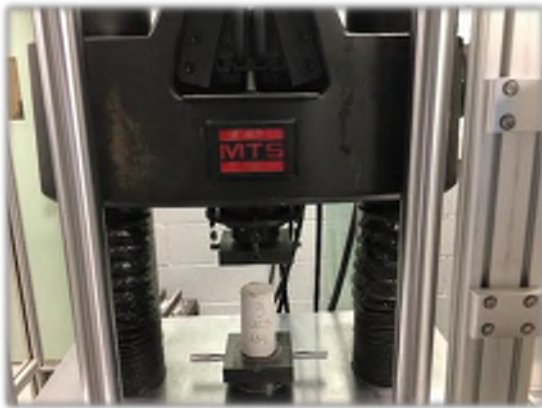
P – maximum load recorded, kN

A – the cross-section area of the specimen, mm<sup>2</sup>

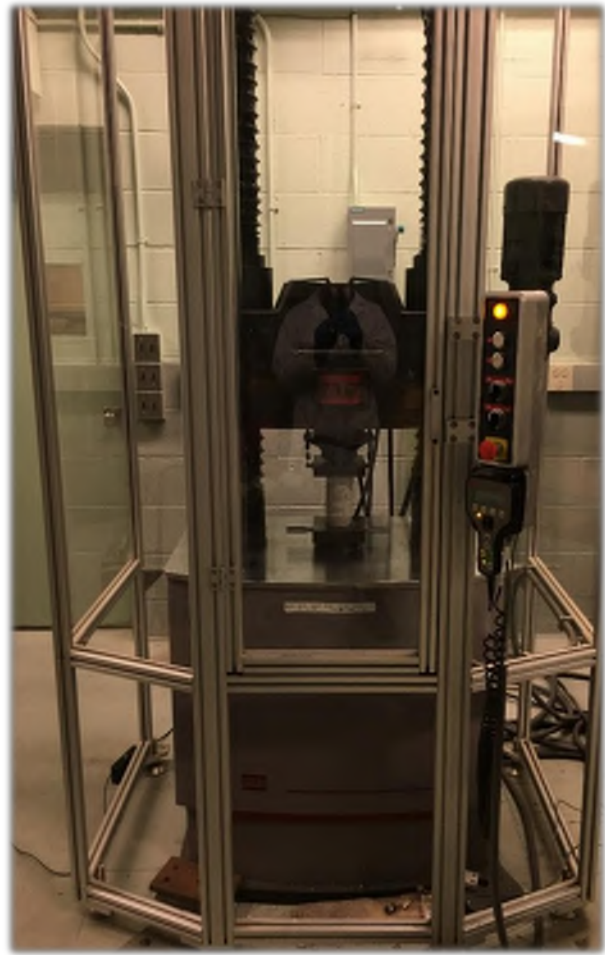
Figure 5-5 demonstrates test setup and frame of the UCS test in the CPATT lab.



(a)



(b)



(c)

**Figure 5-5: Unconfined Compressive Strength. (a) - samples, ready to be tested; (b) and (c) - testing equipment**

The UCS test was performed at 7, 14, 21, and 28 days at the CPATT laboratory. Figures 5-6 and 5-7 show the results from UCS test varies as low as 1.27 MPa to as high as 1.69 MPa. For 7 days and 28 days, the compressive strength was relatively consistent and stayed in the ranges of 1.37 to 1.61 MPa and 1.51 to 1.55 MPa respectively. One of the issues with the testing process was an insufficient number of samples for the 28 days UCS test – only two of them were correctly tested and results were obtained. Following the ASTM C495 procedure, four samples have to be tested in order to obtain reliable results. In addition, a few samples were needed for each testing day in order to calibrate the test frame. Also, a few samples were damaged during the curing period, while on site. Samples were left on site at the ambient temperature during the first three days and were discovered lying on the ground when it was time to pick the samples up from the site. Visually, cracks were observed later on the surface of some samples, but it was hard to say if those cracks were drying shrinkage cracks or some structural cracks. Those damaged samples were not tested to avoid confusion. Some of them were used as “dummy” samples, but overall number was already insufficient to have four good quality samples for 28 days UCS testing. UCS test results for 7, 14, 21 and 28 days are presented in Figure 5-6. The data for the testing are presented in Appendix III.

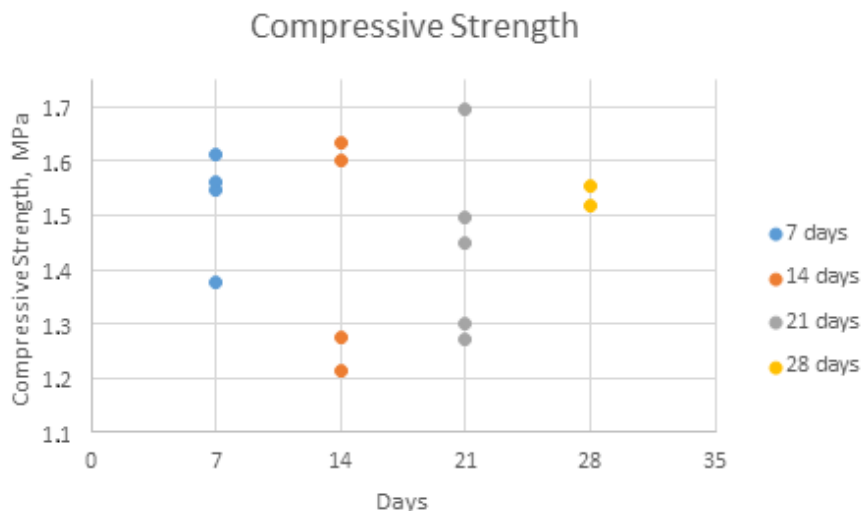


**Figure 5-6: UCS Test Results**

After calculating the average values for each sample age, 7, 14, 21 and 28 days, the compressive strength was determined to be within a small range throughout all the ages of the samples (Figure 5-7). The fluctuation of the results was from 1.44 MPa to 1.53 MPa, meaning no significant difference was observed between 7, 14, 21 and 28 days samples.



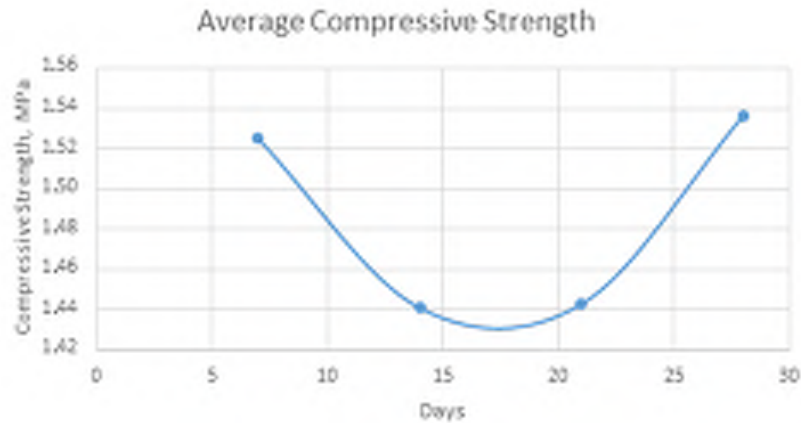


**Figure 5-7: Average UCS Test Results**

Table 5-1 presents typical values for Cellular Concrete. For the densities between 400 and 600 kg/m<sup>3</sup>, compressive strength ranges from 0.5 to 1.5 MPa. Those are the approximate values and the range for compressive strength is relatively large because it may include the cellular concrete with different mix compositions. The target density of the samples, taken from the site in Toronto, was 475 kg/m<sup>3</sup>. This means that the results were more than satisfied and material cast in-situ has gained relatively high compressive strength for its density.

**Table 5-1: Typical Properties of Cellular Concrete Based on British Concrete Association (BCA 1994)**

<b>Dry Density (kg/m<sup>3</sup>)</b>	<b>Compressive Strength (MPa)</b>	<b>Drying Shrinkage (%)</b>	<b>Modulus of Elasticity (MPa)</b>	<b>Thermal Conductivity (W/mK)</b>
<b>400</b>	0.5-1.0	0.30-0.35	800-1,000	0.10
<b>600</b>	1.0-1.5	0.22-0.25	1,000-1,500	0.11
<b>800</b>	1.5-2.0	0.20-0.22	2,000-2,500	0.17-0.23
<b>1000</b>	2.5-3.0	0.15-0.18	2,500-3,000	0.23-0.30
<b>1200</b>	4.5-5.5	0.09-0.11	3,500-4,000	0.38-0.42
<b>1400</b>	6.0-8.0	0.07-0.09	5,000-6,000	0.50-0.55
<b>1600</b>	7.5-10.0	0.06-0.07	10,000-12,000	0.62-0.66

#### 5.4.2 Modulus of Elasticity and Poisson's Ratio

The testing method was completed in accordance with ASTM C469. The dimension of the specimen was 150 mm by 300 mm for the samples with targeted 475 kg/m<sup>3</sup> density. Before testing the samples, they were grinded at the top and the bottom in order to have horizontal flat surfaces. Measurements of the samples were taken such as height, diameter, and weight. In addition, visual inspection was completed to reveal some possible structural cracks, apart from drying shrinkage, which can affect the test results. The same as for the compressive strength, actual density of the samples was calculated by dividing the weight of the sample to its volume. The average hardened state density appeared to be slightly higher than one in the smaller samples (for UCS test) and it was reported as 417 kg/m<sup>3</sup> for this batch of samples.

The configuration of the test apparatus is shown in Figure 5-8. The calculation of the two parameters are described as follows:

- For Modulus of Elasticity:

$$E = \frac{(S_2 - S_1)}{(\varepsilon_2 - 0.000050)}$$

where:

E – modulus of elasticity, MPa

S<sub>2</sub> – stress corresponding to 40% of ultimate load, MPa

S<sub>1</sub> – stress corresponding to a longitudinal strain,  $\varepsilon_2$ , of 50 million, MPa

$\varepsilon_2$  – longitudinal strain produced by stress S<sub>2</sub>

- For Poisson's ratio:

$$\mu = \frac{(\varepsilon_{t2} - \varepsilon_{t1})}{(\varepsilon_2 - 0.000050)}$$

where:

$\mu$  - Poisson's ratio

$\varepsilon_{t2}$  – transverse strain at midheight of the specimen produced by stress S<sub>2</sub>

$\varepsilon_{t1}$  – transverse strain at midheight of the specimen produced by stress S<sub>1</sub>



**Figure 5-8: Modulus of Elasticity and Poisson's Ratio Test Setup**

Prior to the actual test, two specimens were tested to determine the compressive strength. The 40% of the maximum load was determined in this trial test, which then was used as the maximum load for the modulus of elasticity test. The compressometer and extensometer were used to measure the modulus of elasticity and Poisson's ratio as they provide readings for longitudinal strain and transverse strain. In accordance to ASTM C469, the sample should be loaded no less than three times and the first reading is not recorded as valid. During the test at the CPATT lab, each of the three samples was loaded six times, but the first reading was not taken into account since it is considered as a trial loading (according to the ASTM C469). Results are presented in Figure 5-9. Samples were tested at 28 days.

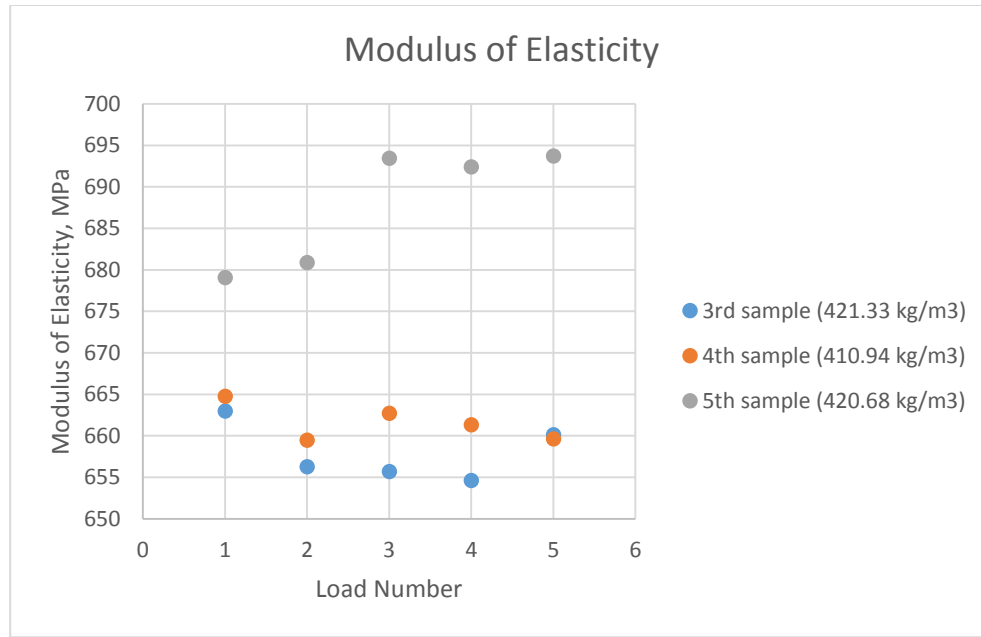


**Figure 5-9: Modulus of Elasticity Test Results for 28 Days Samples**

The average modulus of elasticity was determined as 657, 661 and 687 MPa for the 3<sup>rd</sup>, 4<sup>th</sup>, and 5<sup>th</sup> samples respectively. The result for modulus of elasticity for the 5<sup>th</sup> sample was obtained to be the highest, corresponding to the 420.68 kg/m<sup>3</sup> density, whereas for the 3<sup>rd</sup> sample modulus of elasticity was determined as the lowest with the sample density at 421.33 kg/m<sup>3</sup> (Figure 5-9). During the testing of the 5<sup>th</sup> sample, it was found that the reading increased from 680 to 693 MPa after the second cycle. This may be explained due to the fact that the test frame had some noise during testing and several adjustments were made to the longitudinal extensometer. According to Table 5-1, the lower limit for modulus of elasticity of the 400 kg/m<sup>3</sup> density is approximately 800 MPa, whereas laboratory results observed it to be in the range of 657 to 687 MPa.

The Poisson's ratio was observed in the range of 0.24 to 0.30 (Appendix III), which is consistent to the past literature (BCA, 1994).

#### 5.4.3 Relationship between Properties

Correlation between compressive strength and density is shown in Figure 5-10. The trend for 7 days samples was not typical because the lower density was observed, the higher compressive strength was, though 7 days samples had a good  $R^2$  value of 0.96. For the 14 and 21 days samples with hardened state density of 404 to 414 kg/m<sup>3</sup> the range of the compressive strength was relatively different, laying in the range of 1.2 to 1.69 MPa. For the 28 days samples, despite the expectations, compressive strength was observed to be at approximately same level as for other days samples (1.52 to 1.55MPa).

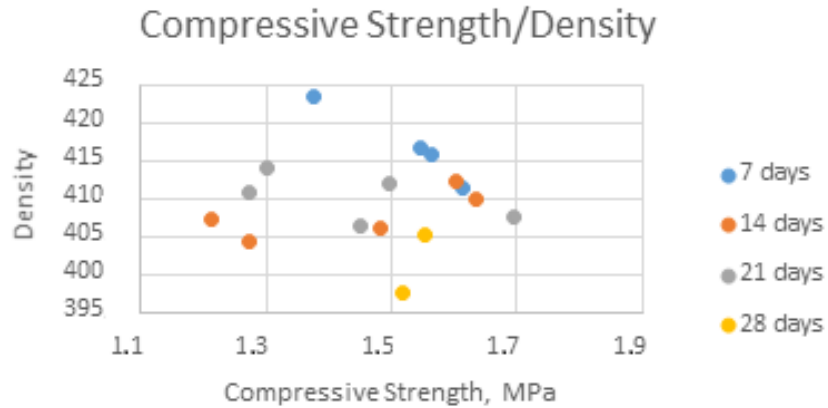


**Figure 5-10: Correlation of Compressive Strength and Density**

## 5.5 Summary

It is worth mentioning that one of the hypothesis of the thesis was that the mechanical properties of the site cast samples would be different from the typical values. As a result of the laboratory testing, some mechanical properties were different from the ones in the literature.

- The field cast samples usually have completely different curing procedure. Because of the high temperatures during the curing period, it is assumed that samples gained high strength in the first few days.
- Obtained results may be the reason of possibly damaged bubbled structure as none of the vibration should be done to the material although in order to test the samples they were transported to the laboratory on the 4<sup>th</sup> day. There is no specific requirement on after what day samples can be transported.
- For field cast samples correlation between compressive strength and modulus of elasticity was not found as strong. This could be studied more thoroughly by collecting more samples, thus having a greater data set.
- High compressive strength values, especially on early stages (before 28 days) may be the result of using good quality material in the field by CEMATRIX.

## CHAPTER 6

### 6 CONCLUSIONS AND FUTURE RECOMMENDATIONS

#### 6.1 Conclusions

Lightweight Cellular Concrete (LCC) is a lightweight product, consisting of Portland Cement, water, and foaming agent which contain air bubbles. LCC is relatively homogeneous compared to conventional concrete, as it does not contain coarse aggregate. It has constructive advantages such as low density with higher pound for pound strength compared with natural concrete and other fill materials. The properties of LCC depend on its microstructure and composition, methods of pore-formation and curing. Apart from being lightweight, LCC is a cost-effective and sustainable material and has superior thermal properties, freeze-thaw resistance, and good flowability. It can be used in a number of applications including but not limited to backfill, soil stabilization, embankment fills and pipe bedding, but this research was focused on studying of this material as an alternative construction material for reducing the weight of the subbase in pavement engineering, thereby mitigating excessive settlements and bearing failures.

In terms of insulation value, LCC also has energy absorbing, thermal insulating, and soundproofing properties. The air voids are homogeneously distributed within LCC and by utilizing the LCC within the roadway structure, pavement damage from frost heave and spring thaw softening are reduced.

This material is potentially cost-effective both in the short and long term. LCC typically replaces granular subbases two-to-three-times greater in thickness; therefore, less underlying soil needs to be excavated.

LCC also has environmental benefits, as it is inert and non-contaminating compared to other potential lightweight materials, and uses relatively easily available materials. It can also include industrial byproducts and waste materials such as fly ash. It is relatively inexpensive, easy to make, and easy to use. It is versatile in that it can be pumped into place and poured into complex forms.

With a greater emphasis on sustainability, materials such as LCC can minimize the generation of waste and deliver better performing pavements that require less maintenance.

**The major conclusions drawn from this research are outlined in the following section:**

- According to the report and visual inspection that were done at the Dixie Road, no significant transverse and longitudinal cracks were observed. Both, Winston Churchill Boulevard and Highway 9 sections are in good condition with no visual distresses. The

bus-lane in Calgary (the oldest section) is performing well. No recent data from the road section in British Columbia was collected.

- The inspections were done after the construction on the studied sections at different times. The results of the visual inspection, Falling Weight Deflectometer (FWD) as well as Benkelman Beam Test (for some cases) showed that the road sections are performing well and have some minor distresses on the surface (Dixie Road). FWD and Benkelman Beam Test are the most common tests for evaluating performance.
- However, in-depth pavement data collection must be complete to provide a comprehensive review of the performance of the sections with LCC as a subbase layer. Therefore, further investigation is recommended. This could be achieved by using pavement instrumentation such as asphalt gauges, earth pressure cells, and environmental equipment.
- In order to use LCC in a pavement structure as a subbase, certain activities have to be taken into consideration and implemented into the construction process. A number of general observations that are applicable to most LCC projects have been made from studying the road sections across Canada. These recommended construction activities include controlling the water table, constructing the proper drainage, transition areas between the sections and using quality equipment and professional personnel.
- It is clear from the failure criteria analysis that the pavement with LCC subbase is more durable than the pavement with Granular B layer at the same thicknesses.
- The result of the failure criteria analysis indicated that the pavement thickness using LCC as a subbase material could be thinner than the conventional pavement, which reduces the excavation depth during the construction and saves time and cost.
- The WESLEA software does not consider the environmental impact of temperature and moisture. In-situ field inspection is needed to evaluate the environmental effect on the pavement using LCC as a subbase layer.
- The mechanical properties of the site cast samples were found to be different from the typical values in the literature.
- For field cast samples correlation between the compressive strength and modulus of elasticity were not highly correlated. This could be studied more thoroughly by collecting more samples to obtain more data.
- The use of LCC as a pavement subbase layer could be practical and feasible in particular scenarios.

## **6.2 Future Recommendations**

In terms of disadvantages of LCC, its high flowability means LCC must typically be placed into forms and cannot have a surface slope of more than 1 degree. Due to its low density, upward buoyancy forces must be taken into account if the concrete is expected to be submerged



in water. Its initial cost may be higher, depending on the density and composition. This area may also need clarification and analysis in the future

**Based on this research, the following are recommended areas for future work:**

- New road sections must be built to provide data collection opportunities for researchers regarding LCC performance.
- Those new pavements may be equipped with instrumentation such as earth pressure cell, horizontal strain gauge, and vertical strain gauge. This will help to quantitatively estimate pavement performance and will serve as a solid base for its evaluation.
- More in-depth study of the LCC properties is required.
- Correlation between laboratory and field cast samples could be determined in order to understand the effect of curing conditions and the quality of the material in general.
- LCC has many potential benefits in terms of sustainability in construction such as low ease of application, reduction in use of virgin materials, using by-products as a substitute to cement, for example. In order to evaluate and calculate those benefits, Life Cycle Cost Assessment and Life Cycle Cost Analysis must be performed, which was not accomplished in the past studies.

## REFERENCES

- Aldridge, D. (2005). Introduction to foamed concrete: what, why, how? In Use of Foamed Concrete in Construction: Proceedings of the International Conference held at the University of Dundee, Scotland, UK on 5 July 2005 (pp. 1-14). *Thomas Telford Publishing*.
- American Society for Testing and Materials (ASTM) C796/C796M. (2012). Standard Test Method for Foaming Agents for Use in Producing Cellular Concrete Using Preformed Foam.
- American Society for Testing and Materials (ASTM) D4694-09 (2015). Standard Test Method for Deflections with a Falling-Weight-Type Impulse Load Device.
- American Society for Testing and Materials (ASTM) D4695-03 (2015). *Standard Guide for General Pavement Deflection Measurements*.
- American Society for Testing and Materials (ASTM) D6433 – 18 (2012). Standard Practice for Roads and Parking Lots Pavement Condition Index Surveys.
- Amran, Y. M., Farzadnia, N., and Ali, A. A. (2015). Properties and applications of foamed concrete; a review. *Construction and Building Materials*, 101, 990-1005.
- Applied Research Associates ARA (2015) Methodology for the Development of Equivalent Pavement Structural Design Matrix for Municipal Roadways.
- Arulrajah, A., Disfani, M. M., Maghoolpilehrood, F., Horpibulsuk, S., Udonchai, A., Imteaz, M., and Du, Y. J. (2015). Engineering and environmental properties of foamed recycled glass as a lightweight engineering material. *Journal of Cleaner Production*, 94, 369-375.
- Awang, H., Aljoumaily, Z. S., Noordin, N., & Al-Mulali, M. Z. (2014). The Mechanical Properties of Foamed Concrete containing Un-processed Blast Furnace Slag. *In MATEC Web of Conferences (Vol. 15, p. 01034). EDP Sciences*.
- British Cement Association (BCA) (1994). “*Foamed concrete - Composition and properties*”. *First published in 1991*, British Cement Association.
- Brady, K. C., Jones, M. R., & Watts, G. R. (2001). Specification for foamed concrete. TRL Limited.

- Byun, K. J., Song, H. W., Park, S. S., & Song, Y. C. (1998). Development of structural lightweight foamed concrete using polymer foam agent. *ICPIC-98*, 9.
- Darshan, M. (2016). Comparison on Auto Aerated Concrete to Normal Concrete. *GRD Journals, Global Research and Development Journal for Engineering*, 5.
- Dolton, B., Witchard, M., Luzzi, D., & Smith, T. J. (2016). Application of Lightweight Cellular Concrete to Reconstruction of Settlement Prone Roadways in Victoria. *GEOVancouver*.
- Dransfield, J. M. (2000, March). Foamed concrete: Introduction to the product and its properties. In One-day awareness seminar on Foamed Concrete: Properties, Applications and Potential, University of Dundee, Scotland (pp. 1-11).
- Friesen, J., Adedapo, D., Kenyon, R., & Eden, R. J. (2012). Bridge Embankment Stabilization in Deep Soft Lacustrine Clays Under High Artesian Pressures. *GEOManitoba*.
- Golder Associates (2008). Technical Memorandum. View Street and Vancouver Street, Victoria. Benkelman Beam Testing and Falling Weight Deflectometer Testing.
- Griffiths F. and Popik, M. (2013). Pavement Evaluation - CEMATRIX Site Dixie Road, Caledon, Ontario. Thurber Engineering Ltd. 2010 Winston Park Drive, Oakville, ON.
- Hoff Inge, Watn A, Oiseth E, EMDAL A., Amundsgard, K O., (2002). Light Weight Aggregate (LWA) Used In Road Pavements. Proceedings of the 6th international conference on the bearing capacity of roads and airfields, Lisbon, Portugal, 2, pp. 1013-22.
- Horpibulsuk, S., Suddeepong, A., Suksiripattanapong, C., Chinkulkijniwat, A., Arulrajah, A., & Disfani, M. M. (2014). Water-void to cement ratio identity of lightweight cellular-cemented material. *Journal of Materials in Civil Engineering*, 26(10), 06014021.
- Jones M.R., (2001). Foamed concrete for structural use. Proceedings of one-day seminar on foamed concrete: properties, applications, and latest technological developments. Loughborough University, pp. 27–60.
- Jones, M.R., & McCarthy, A. (2005). Utilising unprocessed low-lime coal fly ash in foamed concrete. *Fuel*, 84(11), 1398-1409.
- Jones, M.R., & McCarthy, A. (2005). Preliminary views on the potential of foamed concrete as a structural material. *Magazine of concrete research*, 57(1), 21-31.
- Jones, M.R., & McCarthy, A. (2006). Heat of hydration in foamed concrete: Effect of mix constituents and plastic density. *Cement and concrete research*, 36(6), 1032-1041.

- Jones, M.R., Zheng, L., Yerramala, A., Rao, K.S. (2012). Use of recycled and secondary aggregates in foamed concrete. *Magazine of Concrete Research*, 64(6), pp. 513-525.
- Jones, M.R., Ozlutas, K., & Zheng, L. (2016). Stability and instability of foamed concrete. *Magazine of Concrete Research*, 68(11), 542-549.
- Jones, M. R., Ozlutas, K., & Zheng, L. (2017). High-volume, ultra-low-density fly ash foamed concrete. *Magazine of Concrete Research*, 1-11.
- Kadela, M., Kozłowski, M., & Kukielka, A. (2017). Application of foamed concrete in road pavement–weak soil system. *Procedia Engineering*, 193, 439-446.
- Kearsley, E.P. (1996) The Use of Foamed Concrete for Affordable Development in Third World Countries. In *Appropriate Concrete Technology*; Dhir, R.K., McCarthy, M.J., Eds.; E & FN Spon: London, UK, pp. 233–243
- Kearsley E.P., Wainwright P.J. (2001). The effect of high fly ash content on the compressive strength of foamed concrete. *Cement Concrete Research*, 31, pp. 105–12.
- Kearsley E.P, Wainwright PJ (2002). Ash content for optimum strength of foamed concrete. *Cement Concrete Research*, 32, pp. 241–6
- Khayat, K. H., & Assaad, J. (2002). Air-void stability in self-consolidating concrete. *ACI Materials Journal*, 99(4), 408-416.
- Koudriashoff IT (1949). Manufacture of reinforced foam concrete roof slabs. *J Am Concr Inst*, 21(1), pp. 37–48.
- Lee, Y. L., Goh, K. S., Koh, H. B., & Bakar, I. (2009). Foamed aggregate pervious concrete—an option for road on peat.
- Legatski, L. A. (1994). Cellular concrete. In *Significance of Tests and Properties of Concrete and Concrete-Making Materials*. ASTM International. Loewen, E. B., Baril, M., & Eric, R. (2012). Rapid Design and Construction of an Integral Abutment Bridge with MSE Walls and Cellular Concrete Backfill. *Conference of the Transportation Association of Canada*.
- Maher, M. L., & Hagan, J. B. (2016). Constructability Benefits of Using Lightweight Foamed Concrete Fill in Pavement Applications. *CSCE Annual Conference, London*.

- McGovern, G. (2000, March). Manufacture and supply of ready-mix foamed concrete. In One Day Awareness Seminar on Foamed Concrete: Properties, Applications and Potential, University of Dundee, Scotland (pp. 12-25).
- Mohammad, M. (2011). Development of foamed concrete: enabling and supporting design (*Doctoral dissertation, School of Engineering, Physics and Mathematics*).
- Nambiar, E.K.K., Ramamurthy, K. (2006). 'Influence of filler type on the properties of foam concrete'. *Cement and concrete composites*, Vol.28, pp. 475-480.
- Narayanan, N., & Ramamurthy, K. (2000). Structure and properties of aerated concrete: a review. *Cement and Concrete Composites*, 22(5), 321-329.
- Neville, A. M. (2011). Properties of concrete. *5th edition, Pearson Education Ltd*.
- Oginni, F. A. (2015). Continental application of foamed concrete technology: Lessons for infrastructural development in Africa. *British Journal of Applied Science & Technology*, 5(4), 417.
- Ozlutas, K. (2015). Behavior of ultra-low density foamed concrete (*Doctoral dissertation, University of Dundee*).
- Ramamurthy, K., Nambiar, E. K., & Ranjani, G. I. S. (2009). A classification of studies on properties of foam concrete. *Cement and Concrete Composites*, 31(6), 388-396.
- Raphael, J. M. (1984, March). Tensile strength of concrete. In Journal Proceedings (Vol. 81, No. 2, pp. 158-165).
- Sabir, B. B., Wild, S., & O'farrell, M. (1998). A water sorptivity test for mortar and concrete. *Materials and Structures*, 31(8), 568.
- Sari, K. A. M., & Sani, A. R. M. (2017). Applications of Foamed Lightweight Concrete. In *MATEC Web of Conferences* (Vol. 97, p. 01097). *EDP Sciences*.
- Taylor, R., Eric, R., Wiebe, D., & Loewen, S. (2016). Waverly West Arterial Roads Project Kenaston Overpass. *Conference of the Transportation Association of Canada*.
- Tiwari, B. *et al.* (2017) 'Mechanical Properties of Lightweight Cellular Concrete for Geotechnical Applications', *Journal of Materials in Civil Engineering*, 29(7), p. 6017007. doi: 10.1061/(ASCE)MT.1943-5533.0001885.
- Transportation Association of Canada –TAC (2013). Transport Asset Design and Management Guide.

- Transportation Association of Canada TAC (2014) Default Parameters for AASHTOWare Pavement ME Design Canadian Guide.
- Valore, R. C. (1954b). Cellular concretes part 2 physical properties. *In Journal Proceedings* (Vol. 50, No. 6, pp. 817-836).
- Valore, R. C. (1954a). Cellular concretes Part 1 composition and methods of preparation. *In Journal Proceedings* (Vol. 50, No. 5, pp. 773-796).
- Van Deijk, S. (1919). Foam concrete. *Concrete*, 25(5).
- Wei, S., Yigiang, C., Yunsheng, Z., Jones, M.R. (2013). “Characterization and simulation of microstructure and thermal properties of foamed concrete”. *Construction and Building Materials*, 47, pp. 1278-1291.
- WCED, (1987).Our Common Future. *World Commission on Environment and Development*. Oxford University Press, Oxford.
- Yakovlev, G., Kerienė, J., Gailius, A., & Girnienė, I. (2006). Cement based foam concrete reinforced by carbon nanotubes. *Materials Science [Medžiagotyra]*, 12(2), 147-151.

# **APPENDIX I**

## **FWD Dixie Road Data**



Station (km)	Layer Thickness (mm)			ND (microns)	$E_s$ (MPa)	$M_R$ (MPa)	$E_p$ (MPa)	$SH_{LR}$ (mm)	LCC Structural Coefficient
	Asphalt	Base	Subbase						
Dole Road Northbound Lane									
10+280	137	150	400	201	200	66	690	154	
10+285	137	150	400	229	179	59	749	148	
10+290	137	150	400	248	197	65	650	141	
10+292	137	150	400	269	186	61	596	137	
10+294	137	150	400	303	203	67	495	129	
10+296	137	148	650	239	194	64	639	150	0.185
10+298	135	129	650	260	197	65	575	180	0.173
10+300	133	122	650	248	220	73	595	180	0.176
10+310	157	119	650	231	139	46	736	190	0.19
10+320	142	128	650	444	69	23	399	159	0.138
10+330	145	95	650	446	53	17	434	159	0.143
10+340	151	106	650	316	68	22	636	184	0.176
10+350	149	97	650	273	77	25	747	192	0.19
10+360	151	71	650	271	98	32	700	183	0.18
10+370	146	109	650	197	102	34	1055	218	0.229
10+380	159	97	650	205	98	32	1017	215	0.22
10+390	135	122	650	267	76	25	770	196	0.201
10+400	130	115	650	274	159	52	570	175	0.173
10+410	152	91	650	189	218	72	844	199	0.201
10+415	155	97	650	206	234	77	741	193	0.188
10+417	155	152	650	164	237	78	970	224	0.226
10+419	155	184	650	188	241	80	810	218	0.211
10+421	155	184	650	197	224	74	775	215	0.206
10+423	155	202	650	263	197	65	557	196	0.173
10+425	155	150	400	267	178	59	552	137	
10+430	155	150	400	277	227	75	536	135	
10+435	155	150	400	306	267	88	454	128	
NB Approach			Average	250	193	64	670	142	
			Std Dev.	39	10	3	140	10	
NB Cemetery Site			Average	257	152	50	714	193	
			Std Dev.	77	69	23	180	19	
NB Lease			Average	290	224	74	514	133	
			Std Dev.	15	45	15	52	5	

Station (km)	Layer Thickness (mm)			ND (microns)	E <sub>s</sub> (MPa)	M <sub>s</sub> (MPa)	E <sub>p</sub> (MPa)	SH <sub>MR</sub> (mm)	LCC Structural Coefficient
	Asphalt	Base	Subbase						
Dixie Road - Southbound Lane									
10+280	150	150	400	271	225	74	554	136	
10+285	150	150	400	290	205	68	521	133	
10+290	150	150	400	284	261	86	501	132	
10+292	150	150	400	313	249	82	451	127	
10+294	152	150	400	307	220	73	476	130	
10+296	157	111	650	229	225	74	649	166	0.177
10+298	157	117	650	201	219	72	771	200	0.195
10+300	155	111	650	194	225	74	805	201	0.199
10+310	149	111	650	205	199	66	774	198	0.195
10+320	141	132	650	276	108	36	632	167	0.181
10+330	138	128	650	385	56	19	514	174	0.163
10+340	144	131	650	226	88	29	907	212	0.217
10+350	143	103	650	248	115	38	725	190	0.19
10+360	149	99	650	206	128	42	887	204	0.208
10+370	150	69	650	196	115	36	994	210	0.218
10+380	140	100	650	206	115	36	942	206	0.217
10+390	130	143	650	227	112	37	818	204	0.211
10+400	164	109	650	235	99	33	817	204	0.198
10+410	132	197	650	208	171	56	779	213	0.214
10+415	131	195	650	236	185	61	650	200	0.195
10+417	138	203	650	214	214	71	705	208	0.203
10+419	145	220	650	220	192	63	696	213	0.201
10+421	160	212	650	195	202	67	796	224	0.212
10+423	168	224	650	236	188	62	633	212	0.196
10+425	175	150	400	253	183	60	639	148	
10+430	160	150	400	253	189	62	636	144	
10+435	150	150	400	316	179	59	495	130	
SB Approach			Average	251	188	62	638	171	
			Std Dev.	43	9	3	110	43	
SB Cemetery Site			Average	239	166	63	737	193	
			Std Dev.	49	58	19	151	25	
SB Leave			Average	282	230	76	526	134	
			Std Dev.	90	20	9	27	2	

**APPENDIX II**

**TYPICAL PAVEMENT SURFACE  
TEMPERATURE IN SOUTHERN AND  
EASTERN ONTARIO**

<b>Month</b>	<b>1st Quintile (°C)</b>	<b>2nd Quintile (°C)</b>	<b>3rd Quintile (°C)</b>	<b>4th Quintile (°C)</b>	<b>5th Quintile (°C)</b>	<b>Mean Temp. (°C)</b>	<b>Std. Dev. (°C)</b>
January	-13.0	-8.4	-5.5	-2.9	0.3	-5.9	4.8
February	-13.2	-8.7	-5.5	-2.7	1.4	-5.7	5.2
March	-7.9	-3.4	-0.6	2.3	7.3	-0.4	5.4
April	-1.1	3.3	6.7	10.7	17.4	7.4	6.7
May	5.2	10.4	14.1	18.4	26.0	14.8	7.4
June	11.9	16.9	20.7	25.2	32.4	21.4	7.3
July	14.6	19.6	23.4	27.8	34.4	23.9	7.1
August	13.3	17.9	21.3	25.6	32.1	22.1	6.7
September	8.3	13.1	16.6	20.3	26.7	17.0	6.6
October	2.8	6.8	9.9	13.3	19.2	10.4	5.9
November	-2.2	1.1	3.1	5.3	9.1	3.2	4.1
December	-9.3	-5.4	-3.1	-0.7	2.8	-3.1	4.3

**APPENDIX III**  
**DATA FOR**  
**LABORATORY TESTING**

7 days

Date cast	Date Tested	Code	Casted Density (kg/m <sup>3</sup> )	Average Diameter (mm)	Average Height (mm)	volume (mm <sup>3</sup> )	Weight of Specimen (g)	Applied Load (KN)	Surface Area (mm <sup>2</sup> )	Comp. Strength (MPa)	Actual density (kg/m <sup>3</sup> )
25-May-18	1-Jun-18	3	475	75,910	146,590	663425,574	276	7,072427	4525,722	1,563	416,023
		4		76,250	146,300	668057,592	283	6,286667	4566,354	1,377	423,616
		5		76,305	142,420	651278,672	268	7,375137	4572,944	1,613	411,498
		6		76,190	143,680	655061,609	273	7,052352	4559,170	1,547	416,755

14 days

25-May-18	8-Jun-18	1	475	76,325	144,595	661571,492	272,8	7,326274	4575,341	1,601	412,352
		2		76,435	150,085	688670,866	282,3	7,492442	4588,539	1,633	409,920
		3		76,520	146,995	675993,261	275,4	5,576168	4598,750	1,213	407,401
		4		76,320	145,860	667271,866	269,8	5,829073	4574,742	1,274	404,333
		5		76,425	144,245	661700,624	269,2		4587,338	0,000	406,831
		6		76,465	147,985	679568,068	276	6,810149	4592,142	1,483	406,140

21 days

25-May-18	15-Jun-18	1	475	77,14	76,840	151,020	151,280	701529,777	285,2	6,721827	4637,294	1,450	406,540
				76,54		151,540							
		2		77,05	76,645	150,490	150,575	694720,973	285,4	5,870159	4613,787	1,272	410,812
				76,24		150,660							
		3		76,96	76,615	149,610	149,615	689751,463	285,6	5,994846	4610,176	1,300	414,062
				76,27		149,620							
		4		77,44	76,825	147,850	147,605	684220,510	285,3	6,750173	4635,483	1,456	416,971
				76,21		147,360							
		5		76,25	76,170	151,290	151,280	689349,252	281	7,730247	4556,777	1,696	407,631
				76,09		151,270							
		6		76,72	76,220	151,340	151,000	688976,989	283,9	6,824816	4562,762	1,496	412,060
				75,720		150,660							

28 days

25-May-18	22-Jun-18	1	475	76,12	76,140	146,950	146,920	668954,448	271,2	7,073447	4553,188	1,554	405,409
				76,16		146,890							
		2		76,16	76,220	149,760	149,820	683592,931	271,9	6,932021	4562,762	1,519	397,751
				76,28		149,880							



	Height	average	Diameter	average	Weight	ultimate load	Cycle	E	P	S1	S2	$\varepsilon_2$	$\varepsilon_{t2}$	$\varepsilon_{t1}$		E	average of 3 samples	P	average of 3 samples			Density
3	300,36	300,24	150,97	151,51	2,280,7	9,00	1	642,519396	-0,2729921	0,049773	0,477093	0,00071507	-0,000179	2,614E-06		657,9486	669,1461	-0,28118	-0,26964	0,005413	2,281	421,33
	300,12		152,05				2	662,972431	-0,2711261	0,055746	0,47716	0,00068564	-0,000181	-8,325E-06						421,33		
							3	656,295094	-0,2962172	0,057138	0,478145	0,00069149	-0,000193	-3,44E-06						421,33		
							4	655,710551	-0,275486	0,056313	0,478632	0,00069406	-0,000191	-1,342E-05						421,33		
							5	654,634951	-0,2767729	0,055863	0,478132	0,00069505	-0,000169	9,632E-06						421,33		
							6	660,130068	-0,2862974	0,052951	0,479353	0,00069594	-0,0002	-1,493E-05						421,33		
4	301,08	301,43	153,28	153,37	2,288,4	9,00	1	615,43521	-0,241753	0,054	0,462443	0,00071367	-0,000159	0,000001		661,5838	669,1461	-0,24469	-0,26964	0,005569	2,288	410,94
	301,78		153,46				2	664,758994	-0,2373706	0,072788	0,466588	0,00064239	-0,000142	-1,359E-06						410,9365		
							3	659,488162	-0,2365564	0,061116	0,465074	0,00066253	-0,000151	-6,049E-06						410,9365		
							4	662,701418	-0,2536113	0,066985	0,455737	0,00063662	-0,000139	9,379E-06						410,9365		
							5	661,320369	-0,2409747	0,063958	0,455644	0,00064228	-0,000141	1,903E-06						410,9365		
							6	659,650138	-0,2578742	0,066265	0,45761	0,00064326	-0,000156	-2,719E-06						410,9365		
5	301,02	300,73	151,88	151,94	2,293,8	9,00	1	667,210312	-0,3033913	0,043022	0,459577	0,00067432	-0,000191	-1,989E-06		687,9059	669,1461	-0,28306	-0,26964	0,005453	2,294	420,68
	300,43		152,00				2	679,073003	-0,2991068	0,064895	0,475148	0,00065414	-0,000185	-4,322E-06						420,68		
							3	680,879413	-0,2735181	0,057177	0,472678	0,00066024	-0,000177	-9,604E-06						420,68		
							4	693,436836	-0,2587153	0,051636	0,476211	0,0006623	-0,0002	-3,77E-06						420,68		
							5	692,415536	-0,2766003	0,050982	0,474138	0,00066113	-0,000165	4,116E-06						420,68		
							6	693,724756	-0,2870394	0,058131	0,475953	0,00065229	-0,000177	-4,116E-06						420,68		

**EXHIBIT F**  
**Proposed Excavation and Backfill**  
**Procedures for Lightweight Cellular**  
**Concrete in Mission Rock Streets**

(Exhibit by Mission Rock Partners)

**PROPOSED EXCAVATION AND BACKFILL PROCEDURE FOR  
LIGHTWEIGHT CELLULAR CONCRETE**

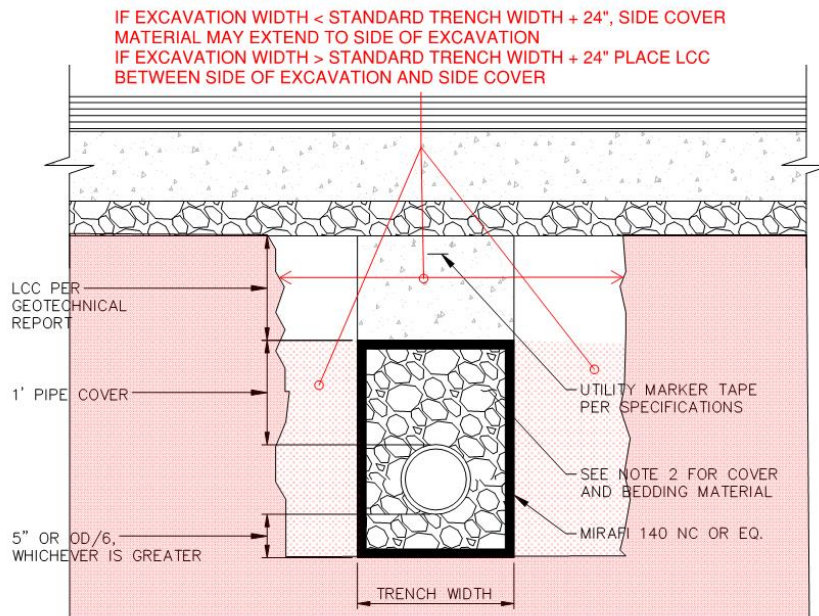
Revision 01

10 February 2020

1. **Purpose:** The purpose of this proposed procedure is describe utility excavation and backfill procedures in streets with Lightweight Cellular Concrete (LCC).
2. **Codes, Regulations:** Unless otherwise noted, DPW Order 187005 Section 10 Trench Backfill Requirements and all codes, regulations and standards referenced therein shall apply to excavation, trenching and backfill in LCC.
3. **Safety:** All trenching and excavation safety requirements required under Cal/OSHA CCR 1540 Article 6, Excavation shall be followed including, but not limited to
  - 3.1. Obtain DOSH Excavation Permit for all trenches deeper than 5'
  - 3.2. Trench shoring shall be installed and removed under the supervision of a Competent Person as defined by Cal/OSHA
4. **Control:** In order to ensure that excavation and trenching in Mission Rock streets, the following controls shall be implemented:
  - 4.1. Signs shall be posted prominently on street sign and/or street light poles with the following wording: "SUBGRADE IN MISSION ROCK STREETS IS LIGHTWEIGHT CELLULAR CONCRETE. EXCAVATION, TRENCHING AND BACKFILL ARE SUBJECT TO SPECIAL REQUIREMENTS. FOR MORE INFORMATION CONTACT SFPW AT (415) 554-5810 OR THE MISSION ROCK MASTER ASSOCIATION AT (415) NNN-NNN"
  - 4.2. All excavation and trenching in streets shall be performed under Excavation Permit. The Permit Section of SFPW shall be provided with a map showing the extend of LCC in Mission Rock Streets which shall be kept on file or recorded in the City Geographic Information System (GIS) and any other maps or other databases.
  - 4.3. When issuing Excavation Permits for street in in Mission Rock with LCC, SFPW shall require that this procedure be followed as a condition of the permit.
5. **Excavation:** LCC can be easily excavated using the same techniques and equipment as normal soil
  - 5.1. Remove pavement per standard practice
  - 5.2. Trenching can be done with standard back hoes, mini excavators and larger excavators with standard buckets as required for the particular trench width, depth and length. LCC can also be excavated by hand, or with the aid of small electric chipping hammers in tight places.
  - 5.3. LCC can also be excavated using a Vactor truck with a 2500-3000 psi water wand where it is necessary to excavate fill without damaging adjacent pipes.
  - 5.4. Standard Cal/OSHA shoring practices shall be followed. LCC in Mission Rock streets generally meets the criteria for Type A Soil having a compressive strength of > 1.5 tons/SF (typically the minimum compressive strength is >40 psi or 2.8 tons/SF).

## 6. Backfill:

- 6.1. In general the bedding, shading and backfill should be restored to its original condition after pipe repair. Trench widths, bedding and shading material and dimensions for new laterals or mains should follow standards for original utilities in Mission Rock—these are generally the same as standards for other City utilities with the following exceptions:
- 6.1.1. Filter fabric such as Mirafi 140 NC or equal should be placed between bedding/shading and LCC to prevent fines from migrating into the LCC
- 6.1.2. Low Pressure Water (LPW) with standard depth of 44" for 12' mains shall be backfilled with beach sand up to the bottom of pavement basecourse.
- 6.2. Place bedding and shading around the pipe per applicable standards. In general, side cover should be the same as the original installation. If the excavation is up to 1' wider than the original width, sand or pea gravel shading may be placed up to 24" wider than the original trench for up to 20' where the added width is necessary for installing repair sleeves, valves or other appurtenances. However if excavation is > 24' wider than original standard trench or longer than 20', then space between side of excavation and side cover or shading shall be filled with LCC. (see figure below) The reason for this is to maintain the weight of the lightweight fill within the 10% safety margin of the design.



- 6.3. Backfill to top of subgrade (bottom of pavement basecourse) shall be LCC per the specification in Appendix A of this Procedure. LCC > 2-3' below top of subgrade shall have cast density of 26 PCF (+/- 2 PCF). LCC < 2-3' below top of subgrade shall have cast density of 30 PCF (+/- 2 PCF).
- 6.4. LCC shall be placed in 3' lifts. If multiple lifts are required, trench shall be covered with road plates or protected with barricades between lifts.
- 6.5. Quality Control of LCC backfill shall be as described in the LCC Specifications

- 6.6. Restore warning tape in backfill per applicable City standards.
- 6.7. A list of approved LCC contractors can be found in Appendix B.
- 7. **Emergency backfill with other material:** In an emergency unplanned repair where the street must be restored immediately, it is permissible to temporarily use normal standard soil backfill, Class II AB or similar materials which have a higher density than LCC, as long as the temporary backfill is removed and replaced with LCC within three months or less, it is not expected to not cause differential settlement because a small amount of localized extra weight should not be enough to induce rapid settlement.
- 8. **Pavement Restoration:** Shall be per SFPW Standards. 4" of aggregate basecourse shall be placed on top of LCC below PCC pavement or concrete sidewalk.

**Appendix A:** LCC specification (see Exhibit H of TAP Comment and Response Exhibit. (Note: Final procedure will have same spec attached. It is omitted here to avoid redundancy.

**Appendix B:** List of approved LCC Contractors

**Cell-Crete Corporation**

995 Zephyr Ave,  
Hayward, CA 94544  
(800) 696-0433  
<https://cell-crete.com/>

**Throop Lightweight Fill**

701 Hazelwood Drive  
Walnut Creek, CA 94596  
415-419-6876  
<http://www.cellularconcrete.com>

**Confoam (A Conco Company)**

5141 Commercial Circle  
Concord, CA 94520  
925-685-6799  
<https://www.conconow.com/commercial-concrete-contractors/confoam/>

**EXHIBIT G**  
**Results of Long Term Test of LCC Cured**  
**in Fresh Water and Salty/Brackish Water**  
**Compared to Normal Dry Curing**  
**Conditions**

(Exhibit by Mission Rock Partners)

Summary of Effects of Fresh Water and Salty/Brackish Water Curing on LCC

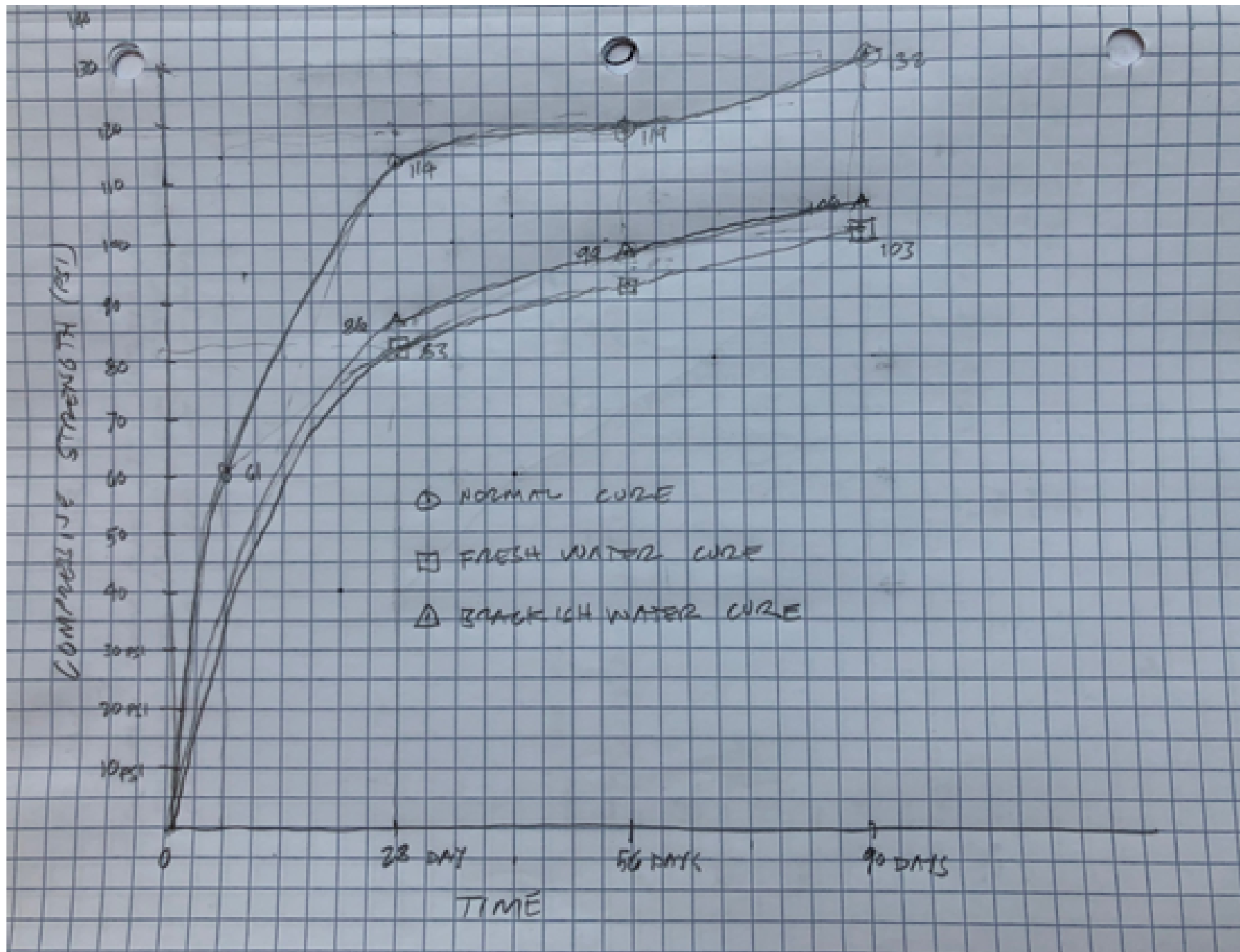
Samples Cast 18 Oct 2019

			Sample ID: 19-562 A (Normal Curing Conditions)			Sample ID: 19-562 B (Cylinders Continue Curing in Fresh Water)			% of Normal	Sample ID: 19-562 C (Cylinders Continue Curing in Brackish Water)			% of Normal	% of FW
Date	No.	Age	Density	load	Strength	Density	load	Strength		Density	load	Strength		
25 Oct 2019	1	7 Days	23.3 pcf	412 lbs	58 psi									
	2	7 Days	23.3 pcf	434 lbs	61 psi									
				(Avg @ 28 days	= 60 psi)									
15 Nov 2019	3	28 Days	20.3 pcf	817 lbs	116 psi	40.3 pcf **	582 lbs	82 psi	71%	39.1 pcf **	601 lbs	85 psi	73%	104%
	4	28 Days	21.0 pcf	799 lbs	113 psi	40.7 pcf **	602 lbs	85 psi	75%	39.0 pcf **	613 lbs	87 psi	77%	102%
				(Avg @ 28 days	= 114 psi)		(Avg @ 28 days	= 83.5 psi)	73%		(Avg @ 28 days	= 86 psi)	75%	103%
13 Dec 2019	5	56 Days	21.5 pcf	843 lbs	119 psi	42.9 pcf	632 lbs	89 psi	75%	39.9 pcf	706 lbs	100 psi	84%	112%
	6	56 Days	21.6 pcf	802 lbs	114 psi	42.0 pcf	681 lbs	96 psi	84%	39.2 pcf	685 lbs	97 psi	85%	101%
				(Avg @ 28 days	= 117 psi)		(Avg @ 56 days	= 93 psi)	79%		(Avg @ 56 days	= 99 psi)	79%	106%
16 Jan 2020	7	90 Days	20.7 pcf	925 lbs	131 psi	42.6 pcf	711lbs	101psi	77%	39.7	706lbs	106psi	81%	105%
	8	90 Days	20.7 pcf	925 lps	133 psi	42.1 pcf	732lbs	104 psi	78%	41.1	745lbs	106psi	80%	102%
				(Avg @ 90 days	=132psi		(Avg @ 90 days	=103 psi	78%		(Avg @ 90 days	106psi	80%	103%
15 Apr 2020	9	180 Days												
	10	180 Days												
14 Jul 2020	11	270 Days												
	12	270 Days												
16 Oct 2020	13	364 Days												
	14	364 Days												

Mix Design 19-562 A

\*\* These cylinders were allowed to drain absorbed water for 1-hour





SUMMARY OF AVERAGE COMPRESSIVE STRENGTH OVER TIME



## Mix Design Laboratory Form

Date: 18 Oct 2019

Sample ID: 19-562 A (Normal Curing Conditions)

Client: Tishman Speyer

Application: Study Effects of Salt/Brackish Water on PLDCC for Mission Rock Project

Target Density: 27 pcf (Actual = 27.2 pcf)

Target Strength: To Be Determined

Date	No.	Age	Density	load	Strength
25 Oct 2019	1	7 Days	23.3 pcf	412 lbs	58 psi
	2	7 Days	23.3 pcf	434 lbs	61 psi
				(Avg @ 7 days	= 60 psi)
15 Nov 2019	3	28 Days	20.3 pcf	817 lbs	116 psi
	4	28 Days	21.0 pcf	799 lbs	113 psi
				(Avg @ 28 days	= 114 psi)
13 Dec 2019	5	56 Days	21.5 pcf	843 lbs	119 psi
	6	56 Days	21.6 pcf	802 lbs	114 psi
				(Avg @ 56 days	= 117 psi)
16 Jan 2020	7	90 Days	20.7 pcf	925 lbs	131 psi
	8	90 Days	20.7 pcf	943 lbs	133 psi
				(Avg @ 90 days	= 132 psi)
15 Apr 2020	9	180 Days			
	10	180 Days			
14 Jul 2020	11	270 Days			
	12	270 Days			
16 Oct 2020	13	364 Days			
	14	364 Days			

	Log No.	Lab Batch Weight	Unit
Cement	Quikrete Type I/II	40.0	lbs
Fly ash	N/A	N/A	g.
Sand	N/A	N/A	g.
Water	0.55 W/C Ratio	22.0	lbs
Chemical	Aquaerix	20	ml/L
Additive			
Base Density		111.5	pcf

This testing was conducted in accordance with ASTM C495 under laboratory conditions. Field testing is recommended to provide a comparison with the laboratory data, as field conditions do vary per project.

Foam Density = 2.2 pcf



## Mix Design Laboratory Form

Date: 18 Oct 2019

Sample ID: 19-562 B (Cylinders Continue Curing in Fresh Water)

Client: Tishman Speyer

Application: Study Effects of Salt/Brackish Water on PLDCC for Mission Rock Project

Target Density: 27 pcf (Actual = 27.2 pcf)

Target Strength: To Be Determined

Date	No.	Age	Density	load	Strength
25 Oct 2019		7 Days **			
15 Nov 2019	1	28 Days	40.3 pcf **	582 lbs	82 psi
	2	28 Days	40.7 pcf **	602 lbs	85 psi
				(Avg @ 28 days	= 83.5 psi)
13 Dec 2019	3	56 Days	42.9 pcf	632 lbs	89 psi
	4	56 Days	42.0 pcf	681 lbs	96 psi
				(Avg @ 56 days	= 93 psi)
16 Jan 2020	5	90 Days	42.6 pcf	711 lbs	101 psi
	6	90 Days	42.1 pcf	732 lbs	104 psi
				(Avg @ 90 days	= 103 psi)
15 Apr 2020	7	180 Days			
	8	180 Days			
14 Jul 2020	9	270 Days			
	10	270 Days			
16 Oct 2020	11	364 Days			
	12	364 Days			

	Log No.	Lab Batch Weight	Unit
Cement	Quikrete Type I/II	40.0	lbs
Fly ash	N/A	N/A	g.
Sand	N/A	N/A	g.
Water	0.55 W/C Ratio	22.0	lbs
Chemical	Aquaerix	20	ml/L
Additive			
Base Density		111.5	pcf

This testing was conducted in accordance with ASTM C495 under laboratory conditions. Field testing is recommended to provide a comparison with the laboratory data, as field conditions do vary per project.

Foam Density = 2.2 pcf

\*\* A total of twelve cylinders were demolded and placed in sealed 4" x 8" cylinder molds filled with fresh, potable water.

\*\* These cylinders were allowed to drain absorbed water for 1 hour.



## Mix Design Laboratory Form

Date: 18 Oct 2019

Sample ID: 19-562 C (Cylinders Continue Curing in Salty/Brackish Water)

Client: Tishman Speyer

Application: Study Effects of Salt/Brackish Water on PLDCC for Mission Rock Project

Target Density: 27 pcf (Actual = 27.2 pcf)

Target Strength: To Be Determined

Date	No.	Age	Density	load	Strength
25 Oct 2019		7 Days **			
15 Nov 2019	1	28 Days	39.1 pcf **	601 lbs	85 psi
	2	28 Days	39.0 pcf **	613 lbs	87 psi
				(Avg @ 28 days	= 86 psi)
13 Dec 2019	3	56 Days	39.9 pcf	706 lbs	100 psi
	4	56 Days	39.2 pcf	685 lbs	97 psi
				(Avg @ 56 days	= 99 psi)
16 Jan 2020	5	90 Days	39.7 pcf	746 lbs	106 psi
	6	90 Days	41.1 pcf	745 lbs	106 psi
				(Avg @ 90 days	= 106 psi)
15 Apr 2020	7	180 Days			
	8	180 Days			
14 Jul 2020	9	270 Days			
	10	270 Days			
16 Oct 2020	11	364 Days			
	12	364 Days			

	Log No.	Lab Batch Weight	Unit
Cement	Quikrete Type I/II	40.0	lbs
Fly ash	N/A	N/A	g.
Sand	N/A	N/A	g.
Water	0.55 W/C Ratio	22.0	lbs
Chemical	Aquaerix	20	ml/L
Additive			
Base Density		111.5	pcf

This testing was conducted in accordance with ASTM C495 under laboratory conditions. Field testing is recommended to provide a comparison with the laboratory data, as field conditions do vary per project.

Foam Density = 2.2 pcf

\*\* A total of twelve cylinders were demolded and placed in sealed 4" x 8" cylinder molds filled with salty, brackish water.

\*\* These cylinders were allowed to drain absorbed water for 1-hour.



EXHIBIT H  
Draft Final LCC Specification including  
QC/QA Testing and Inspection Schedule

# Permeable/Open Cell Lightweight Cellular Concrete (P-LCC)

## 1. GENERAL

### 1.1. DESCRIPTION

- 1.1.1. Work Included: This work shall consist of batching, mixing, placing and testing P-LCC of the appropriate density as indicated by the specifications. A trained P-LCC installer shall furnish labor, material, equipment, and supervision for the installation of the P-LCC in accordance with the drawings and specifications.

### 1.2. QUALITY ASSURANCE

- 1.2.1. Use skilled labor that is thoroughly trained, experienced, and familiar with the specified requirements and the methods for proper performance of this work.
- 1.2.2. The P-LCC installer shall be approved in writing by Owner.

### 1.3. SUBMITTALS

- 1.3.1. The prime contractor shall list the product and qualified installer of the P-LCC and shall not employ any product or producer without the prior approval of the geotechnical engineer of record (GEOR).
- 1.3.2. Product data: within 30 calendar days after award of the contract, the prime contractor shall submit a mix design for approval by the GEOR and civil engineer of record (CEOR)
- 1.3.2.1. Manufacturer's specifications, catalog cut sheet, and other engineering data needed to demonstrate to the issuing authority compliance with the specified requirements.
- 1.3.3. Mix Design: Submit a mix design that will produce a cast density that complies with those listed in Section 2.2.1 of this specification at point of placement and a compressive strength within the range listed in Section 2.2.1. Include laboratory data using the mix design verifying un-foamed density, final foamed density, permeability (cm/sec) and compressive strengths. Mix design shall include water/cementitious ratio and foam solution dilution ratio, in accordance with manufacturer's recommendations. The mix design should also include Field Permeability Check Testing, by testing the percolation rate in modified 6" x 12" cylinder molds, filled half-way.
- 1.3.4. Work Plan: Submit a work plan before placement of P-LCC material. The plan shall include:
- 1.3.4.1. Proposed construction sequence and schedule
- 1.3.4.2. Type of equipment and tools to be used.
- 1.3.4.3. Material list of items and manufacturer's specifications
- 1.3.4.4. P-LCC lift thickness
- 1.3.4.5. P-LCC cure time and minimum strength prior to placing the next lift
- 1.3.4.6. QA/QC and testing items and protocols frequency.

January 24, 2020

**SUBMITTAL No.: 31 20 00 – Permeable/Open Cell Lightweight Cellular Concrete (P-LCC)**

This submittal has been reviewed for the Geotechnical aspects of the design only. Contractor is responsible for all corrections indicated hereon, for dimensions quantities, fabrications, construction techniques, and coordination with other contractors, subcontractors and suppliers. This review does not authorize changes to the contract requirements unless stated in a separate letter or change order.

☒ NO EXCEPTIONS TAKEN ☐ AMEND & RESUBMIT  
☐ EXCEPTIONS NOTED ☐ REJECTED-SEE COMMENTS

Checked By: P. Brady Date: 11 February 2020

**LANGAN**  
 135 Main Street  
 Suite 1500, S.F. CA 94105

31 20 00 -1

## 2. PRODUCTS

### 2.1. MATERIALS

2.1.1. Foaming Agent: A foaming agent shall be used and shall comply with the standard specifications of ASTM C 869 when tested in accordance with ASTM C 796. Admixtures shall be tested by the foam concentrate manufacturer for compatibility with the foaming agent.

2.1.2. Cement: the Portland cement shall comply with ASTM C 150. Other supplemental cementitious material such as fly ash may be used when approved by the project engineer. Supplementary cementitious materials shall be tested prior to the start of the project for compatibility with the foaming agent.

2.1.3. Admixtures: admixtures for accelerating, water reducing, and other specific properties may be used when specifically approved by the GEOR. Admixtures shall be tested in mix design prior to the start of the project for compatibility with the foaming agent.

2.1.4. Water: use water that is potable and free from deleterious amounts of alkali, acid, and organic materials, which would adversely affect the setting or strength of the P-LCC.

2.1.5. Filter Fabric: Shall have permeability equal to or greater than that of the P-LCC. Filter fabric shall also have a maximum apparent opening size (AOS, ASTM D4751) of 0.212 mm (U.S. sieve size 70).

### 2.2. PROPERTIES

2.2.1. The P-LCC shall meet the following properties:

	Target	Maximum	Minimum
General Cast Density, pcf (ASTM C 796)	26	28	24
Cast Density for Upper Two Feet of LCC, pcf (ASTM C 796)	30	32	28
Compressive Strength, psi (ASTM C 495)	50	200	50
Coefficient of Permeability, cm/sec (ASTM D 2434 – modified)	0.005 (5e-3)	NA	0.005 (5e-3)
Natural Saturated Density, pcf (per method described in TQC/QA procedures at the end of this Spec)	50	68	45

### 3. EXECUTION

- 3.1. Subgrade: Subgrade to receive P-LCC material shall be free of all loose and extraneous material. Subgrade shall be uniformly moist, and any excess water standing on the surface shall be removed. The subgrade shall be approved by the GEOR before placing P-LCC material.
- 3.2. Curing: A minimum 12-hour curing period between lifts is required. Backfill or other usual loadings, including additional lifts of P-LCC, on the P-LCC shall not be permitted until the P-LCC has attained a compressive strength of at least 5 psi.
- 3.3. Weather Conditions: If ambient temperatures are anticipated to be below 40 degrees F within 24 hours after placement, the mixing water shall be heated when approved by the manufacturer of the foaming agent or placement shall be prohibited. Placement shall not be allowed on frozen ground.
- 3.4. Batching and Mixing: Cellular concrete shall be job site batched, mixed with the foaming agent and placed with specialized equipment certified by the manufacturer of the cellular concrete lightweight material. Cement and water may be premixed and delivered to the job site and the foaming agent added on site. Dilution ratio shall be adjusted as needed per manufacture's recommendation to achieve required end product.
- 3.5. Placement:
  - 3.5.1. Place P-LCC in lifts not to exceed 36 inches in thickness, unless otherwise recommended by the P-LCC manufacturer and approved by the GEOR.
  - 3.5.2. After curing for minimum of 12 hours, any crumbling area on the surface shall be removed before the next layer is placed. Surface stepping to achieve grade and super elevation shall not be less than 6 inches in thickness. Grades of up to 5 percent may be made by adding a thickening agent to the mix in conformance with the manufacturer's recommendation.
  - 3.5.3. Subgrade and P-LCC should be protected from water inundation until the P-LCC is sufficiently cured and has sufficient overlying weight so it does not become buoyant.
  - 3.5.4. Freshly placed P-LCC should be protected from rain until it has been sufficiently cured to prevent damage.
  - 3.5.5. Freshly placed P-LCC should be cured at least 3 hours before exposed to vibrations higher than a peak particle velocity 0.05 inches per second – such as those that may be generated during ground improvement activities.
- 3.6. Handling: Avoid excess handling of P-LCC according to industry standards.
- 3.7. Filter Fabric: Use filter fabric between P-LCC and adjacent soil and between P-LCC and shoring, where shoring will be removed after P-LCC placement.

### 4. QUALITY CONTROL TESTING BY CONTRACTOR AND OWNER

- 4.1. GENERAL: See Quality Control/Quality Assurance Testing and Inspection Schedule at the end of this specification.
- 4.2. DENSITY CONTROL
  - 4.2.1. During placement of the initial batches, check the un-foamed and foamed densities and adjust the mix as required to obtain the specified cast density at the point of placement per ASTM.
  - 4.2.2. Field saturated density test per attached procedures prepared by Castle Rock Consulting.
- 4.3. COMPRESSIVE STRENGTH: The compressive strength shall be tested under ASTM C 495 except as follows:
  - 4.3.1. Four (4) specimens (one 7-day and three 28-days) shall be taken for each 100 cubic yards of P-LCC or as recommended per the GEOR. Unless otherwise approved, the

- specimens shall be 3 x 6 inch cylinders. During molding, place the LCC in 2 equal layers and raise and drop the cylinders 1 inch, 3 times on a hard surface or lightly tap the side or bottom of the cylinder to close any accidental entrained air. No rodding is allowed.
- 4.3.2. Specimens must be covered and protected immediately after casting to prevent damage and loss of moisture. Specimens shall be moist cured in the molds for 7 days and air dry a minimum of 24 hours and minimum of 72 hours before the 7-day and 28-day compressive strength testing, respectively. Specimens shall not be oven dried.
- 4.3.3. Contractor should maintain process control "run" charts of un-foamed and foam density, field percolation result, and compressive strength data, updated daily for review by Owner's representative, and distributed weekly to applicable project team members.
- 4.4. PERMEABILITY:
- 4.4.1. Proof of permeability (per ASTM D 2434 – Modified) of the proposed P-LCC mix design shall be provided in the mix design submittal. If there is any change to the mix design during production, additional permeability testing will be required.
- 4.4.2. Field falling head permeability per attached procedures prepared by Castle Rock Consulting performed on two samples per day.
- 4.5. MOCK UP TEST SECTION: One mock up test section shall be installed prior to construction to prove out the contractor's construction methods.
- 4.6. Side-by-side sampling and testing by QC and QA staff should occur once daily during the LCC placement on the Pilot Project to identify any issues. At least one set of permeability samples should also be taken for saturation and drain down density and a permeability verification.
- 4.7. UNFOAMED SLURRY TESTING: Test unfoamed slurry density periodically during foaming to verify actual density (PCF) is +/- 1.5% of target. Target to be established in mix submittal.
- 4.8. QUALITY ASSURANCE INSPECTIONS & ACCEPTANCE TESTING BY OWNER'S AGENCY
- 4.8.1. Owner shall employ a qualified Special Inspector to observe LCC placement and test LCC as described below.
- 4.8.2. Daily Inspections should include review of previous day's density testing of un-foamed and foamed test data, field percolation test results, and any 7-day & 28-day compressive strength data. Initially use mix design for 7-day to 28-day strength correlation, switching to project data when three sets are available to predict 28-day strengths.
- 4.8.3. Perform one side-by-side comparison test with Contractor every 1000 cubic yards, and verify saturation & drain-down densities and permeability values every 5000 cubic yards placed, or whenever the field percolation rates are more than 20% lower than the mix design values.

ATTACHMENT: Quality Control/Quality Assurance Testing and Inspection Schedule

## **TQC & QA TESTING & INSPECTION SCHEDULE**

### **Mission Rock Permeable LCC**

#### **Pilot Project Only**

- First & Second Lifts of 26pcf, two full sets of the following:  
Compressive strengths – 2@3, 2@7, 3@28  
Un-foamed slurry and foamed cast densities  
Record approximate location of sample  
Permeability – laboratory D2434 & Natural Saturated Density  
Field Falling Head Permeability tests  
Field Natural Saturation
- Third and fourth lifts of 26pcf, one full set described above
- Fifth set of 30pcf, two full sets as described above.

#### **Final Construction LCC Placements**

##### **Contractor QC Testing**

- Once per every 100CY, four compressive strength specimens (1@7, 3@28)
- Also measure un-foamed slurry and foamed cast Density every 100CY

##### **Daily QA Testing by Special Inspector**

- Record location of every 100CY QC sample location
- Cast one Saturation Sample for each 100CY
- Cast two Field Falling-Head Permeability samples per day, one with the 1000CY
- Once per day (1000CY sample, early in day), cast 7 compressive samples, 3x6
- On this 1000CY sample, cast one of the Field Permeability 6x12s
- After three days, test previous samples for saturated density and Field Permeability

##### **Weekly QA Testing by Special Inspector**

- Once per week, preferably on Monday, cast 2 D2434 molds with the 1000CY samples
- Ship to Denver on Tuesday for testing

##### **QA Documentation by Special Inspector**

- Maintain a QA worksheet, and distribute weekly
- One sheet for strength, (including comparison to Contractor's QC result)
- One sheet for Saturated Densities
- One sheet for Field Falling-Head Permeability, include D2434 comparison permeability

## **Procedure for Field Estimation of Saturated Density of PLCC**

1. PLCC samples for this test should be cast in 4 x 8 cylinder molds.
2. One 4 x 8 cylinder should be cast for each test.
3. Carefully strip the PLCC sample from the cylinder mold. Suggested methods for stripping the samples from the molds are:
  - a. Carefully cutting the cylinder walls vertically on opposite sides with a boxcutter, taking care not to cut into the sample too deeply. Invert the cylinder and gently pull the two halves apart to free the cylinder.
  - b. Pre-drilling a small hole in the bottom of the mold before filling, placing tape over the hole. Before stripping, place the mold in a soil oven at 140°F for 5 – 10 minutes to soften and expand the plastic. Remove the tape covering the hole on the bottom of the mold and use compressed air (at about 20-40 psi) to extrude the cylinder.
4. Use a large rasp file, such as a farrier's file to remove about ¼" of material from the top and bottom ends of the cylinder to roughen the surface and expose the cellular structure. Remove material in a uniform fashion, maintaining as best as possible the squareness of the ends to the longitudinal axis. If larger amounts of material must be removed, a hand saw can be used, but be sure to square the ends as best as possible with the file.
5. Measure the height of the PLCC cylinder. Measure to the nearest 1/8". Take the average of 3 to 4 heights around the circumference of the cylinder. Record this value (A).
6. Fully submerge the PLCC cylinder in a full 5 gallon bucket of water, upright and weighting the cylinder down to prevent floatation. Keep the cylinder fully submerged for at least 30 minutes. Multiple cylinders can be submerged simultaneously, provided they remain identified.
7. Weight a standard concrete air pot assembly, pot and cap, and record the tare weight (B).
8. Fill the air pot completely with water, with the cap on, fill and remove excess air through the petcocks as though for a concrete air test, close the petcocks when full.
9. Dry the air pot assembly off as best as possible, weight the water filled assembly and record this value (C).
10. Remove the cap from the air pot and place it beside the bucket containing the submerged PLCC cylinder. The air pot should be full of water.
11. In one quick motion, quickly transfer the PLCC cylinder from the bucket to the air pot, submerging the cylinder completely.
12. Holding the PLCC cylinder under water with one hand, place the air pot cap on with the other and clamp it down.

13. Fill the air pot assembly completely with water through the petcocks as before, closing the petcocks when full.
14. Again dry the entire assembly off as best as possible, weigh and record this value (D).
15. Measurements can be recorded and the approximate saturated unit weights can be calculated using the following worksheet:

Cylinder height, A: \_\_\_\_\_ in  
Air pot assembly tare weight (pot + Cap), B: \_\_\_\_\_ lb  
Air pot assembly tare weight filled with water, C: \_\_\_\_\_ lb  
Air pot assembly with water + cylinder, D: \_\_\_\_\_ lb  
  
Cylinder Volume,  $E = (12.57 \times A)/1728$ : \_\_\_\_\_ cf  
Displacement water weight,  $F = 62.4 \times E$ : \_\_\_\_\_ lb  
Full pot water weight,  $G = C - B$ : \_\_\_\_\_ lb  
Balance Water weight,  $H = G - F$ : \_\_\_\_\_ lb

**Approximate Saturated Unit Weight =  $(D-H-B)/E$ : \_\_\_\_\_ pcf**

Example:

Cylinder height, A: 7.375 in  
Air pot assembly tare weight (pot + Cap), B: 17.600 lb  
Air pot assembly tare weight filled with water, C: 33.340 lb  
Air pot assembly with water + cylinder, D: 32.855 lb  
  
Cylinder Volume,  $E = (12.57 \times A)/1728$ : 0.054 cf  
Displacement water weight,  $F = 62.4 \times E$ : 3.348 lb  
Full pot water weight,  $G = C - B$ : 15.740 lb  
Balance Water weight,  $H = G - F$ : 12.392 lb

**Approximate Saturated Unit Weight =  $(D-H-B)/E$ : 53.4 pcf**



## Falling Head Field Permeability Test Procedure

### Overview:

Samples for the falling head field test should be cast in modified 6x12 cylinder molds. The molds, when modified are essentially ordinary 6x12 cylinders with the bottoms cut off, and the lids taped on (Figure 1).

When the material is cast in the molds, they are placed top side down, with the open bottoms up. The mold is then filled to a depth of 6".

These samples are then used to run a field permeability test by the falling head method.

A few notes on the fabrication and preparation of the molds that may be helpful:

- A. When removing the bottoms of the molds, do so as closely as possible to the base. This will leave a suitable volume above the 6" depth sample in the mold to fill with enough water for the test.
- B. It is helpful to scribe a line around the inside of the cylinder at a distance of 6" as measured from the un-cut top end, to aid in filling to a depth of 6". A simple scribing tool can be made from a narrow piece of wood, a nail, and a screw. (Figures 2-4)
- C. The cellular material will not stick to smooth surfaces very well, so it is also helpful to roughen the inside walls of the cylinder mold below the scribe line to help the material bond to the walls and prevent side leakage. 100 grit sand paper works well. The roughened area also helps visually, in conjunction with the scribe line when filling the mold (Figure 5).
- D. Roughen the inside surface of the lid as well. When removed, it should take some material off and help in scarifying the bottom surface prior to testing.
- E. The lids of the molds are taped onto the un-cut tops of the cylinder molds, making the bottom of the mold when filled. The green painters tape works best as it limits liquid migration. Tape completely around the lid when it meets the cylinder mold. The idea is to prevent material from leaking out (Figure 6).

### Sampling Procedure:

1. Prepare and label the modified 6x12 mold.
2. Place the modified 6x12 mold open side up, on a flat and as level as possible surface.
3. Gather material to be sampled in a bucket or other suitable container. The use of a 4 cup measuring cup, 3x6 cylinder mold, or 4x8 cylinder mold is useful for transferring material from the bucket and gives good control when filling the 6x12 molds.

4. Fill the mold to the scribed line, which will be a depth of approximately 6 inches, tapping the sides to release large bubbles and level the surface. Avoid if possible getting excess material on the inside walls of the mold above the fill line.
5. After the molds are filled, handle them carefully when moving them, or transferring them to a suitable location where they will not be disturbed for at least 24 hours.
6. Cover the open tops of the molds with a damp cloth, or other suitable material such as plastic and a rubber band to prevent excessive moisture loss while curing.

### **Testing Procedure:**

1. After the samples have cured for 3 days, they may be tested.
2. Although cured, handle the samples carefully when prepping and testing, to avoid breaking the bond of the material to the sidewalls.
3. Place the mold open side down and carefully remove the tape and lid.
4. Some material should stick to the lid and come off with the lid. If not, use a putty knife to gently scarify the surface to expose the cellular structure.
5. Turn the mold upright and again use a putty knife to scarify the top surface and expose the cellular structure.
6. Remove as little material as possible when scarifying the surfaces, just enough to break through the surface skin and expose the cellular structure (Figures 7 - 8).
7. Remove any dust or debris from the surfaces that accumulated when scarifying. This is best accomplished by blowing the surfaces off with compressed air. The surfaces can also be rinsed off with a hose, or dunked in a bucket prior to testing. Take care not to wash any dust into the pores of the cellular structure. Orient the cylinder such that wash water runs off of the surface, carrying the material with it.
8. With the cylinder mold with the open end up, press a ruler into the surface of the material to a depth of 1 inch, at the edge of the surface with the ruler oriented vertically. This is the depth scale for the falling head test. With one inch inserted, the next increment should be the 2" mark, corresponding to 1" of water above the surface, 3" will correspond to 2" of water, and so on (Figure 9).
9. Fill a 5 gallon bucket completely with clean water.
10. Place a heavy wire screen or 12" bass sieve on top of another, empty 5 gallon bucket. When the sample is removed from the water bucket, it will be transferred to the screen to allow it to drain freely (Figure 10).
11. Immerse the mold, bottom surface first into the bucket of water, holding the top edges of the cylinder and pushing the sample down vertically, allowing water to infiltrate from the bottom and move upward through the cellular material (Figure 11).
12. Once water has infiltrated and covered the top surface of the material, fully submerge the entire mold in the bucket, allowing the entire top half of the mold to fill with water (Figures 12 - 13).

13. Holding the top edges of the mold, lift the entire mold vertically from the water and quickly transfer it to the screen over the empty bucket (Figures 14 - 15).
14. The water should begin draining freely from the sample. Allow all of the water to pass through the sample until the surface of the material is exposed. This washes water through the sample as a primer to the test, this is only done once and does not need to be repeated for the remaining trials.
15. Get a stopwatch handy and ready to use.
16. Re-submerge the sample in the bucket of water as in steps 11 and 12, fully filling the mold with water. You will need to refill your bucket with water as you go.
17. Again, as in step 13, holding the top edges of the mold, lift the entire mold vertically from the water and quickly transfer it to the screen over the empty bucket.
18. With the stopwatch ready, start timing when the water level reaches the 5" mark (4" above the material surface).
19. Continue timing until the water level reaches the 2" mark (1" above the surface), stop timing.
20. Record the time.
21. Repeat steps 11 – 16 two more times, recording the time for the water level to drop from the 5" mark to the 2" mark, for a total of three trials.
22. The approximate permeability coefficient can now be calculated from the average of the three recorded times by the falling head formula as follows:

$$K = \frac{L}{T} \ln \frac{h_1}{h_2}$$

Where:

K = Coefficient of Permeability in  
cm/sec

L = sample length in cm, in this case  
15.24 cm (6")

$h_1$  = Initial elevation of the water  
surface, in this case 4"

$h_2$  = Final elevation of the water  
surface, in this case 1"

T = Average time in seconds from  $h_1$   
to  $h_2$ .

**Figures:**



*Figure 1: Modified 6x12 cylinder mold for falling head field permeability test.*



*Figure 2: Scribing tool. The screw protrudes slightly through the wood and acts as the scribe. The nail acts as a stop on the cylinder rim. The distance between the center of the nail and the center of the screw is 6".*



*Figure 3: The nail is the stop that rides on the rim of the cylinder molds un-cut edge, the screw point scribes the line. Shown here on the outside of the cylinder for demonstration. Scribe the line on the inside.*





*Figure 4: Scribe the line on the inside. Hold the tool against the cylinder wall, with the stop on the edge of the mold and rotate while pushing the screw against the wall.*

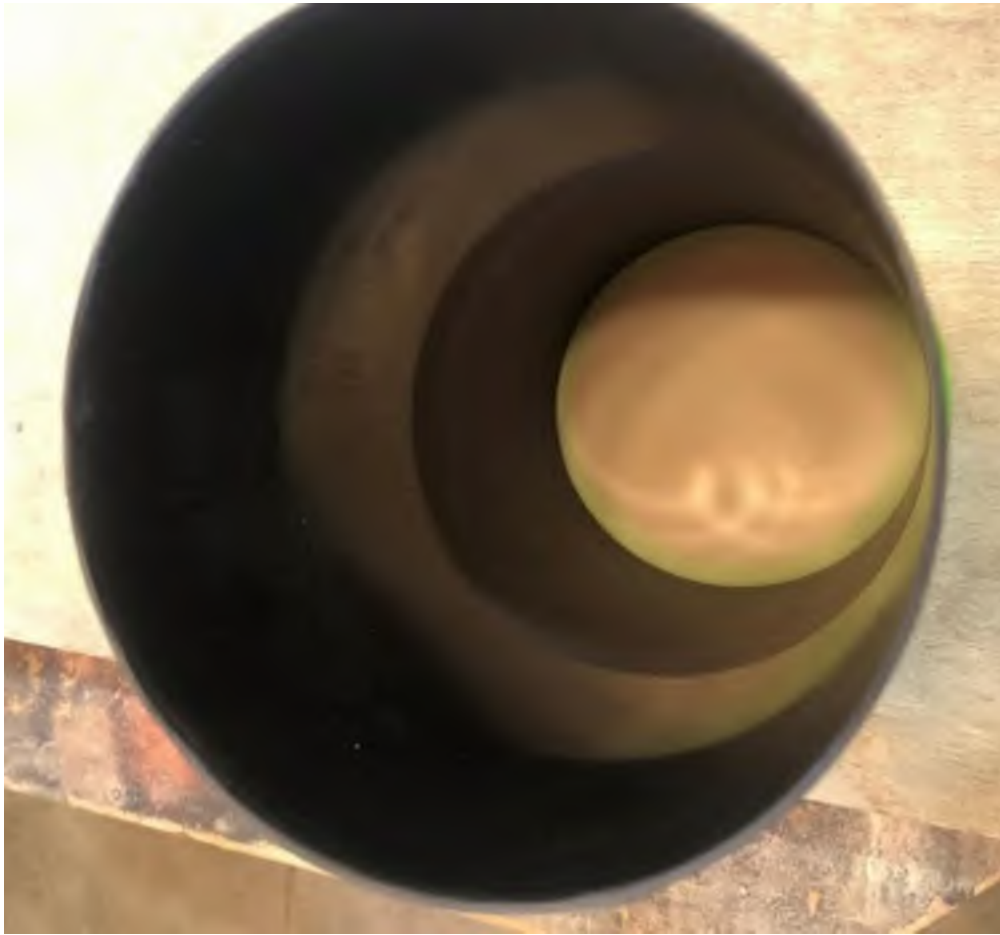


*Figure 5: An assembled mold, with a scribed line and roughened sidewall.*





*Figure 6: Mold lid taped and sealed.*



*Figure 7: Lid removed, scarified bottom surface.*



*Figure 8: Scarified and cleaned top surface. Sample ready for testing.*



*Figure 9: Ruler inserted into sample surface to a depth of one inch. The scale for the test.*



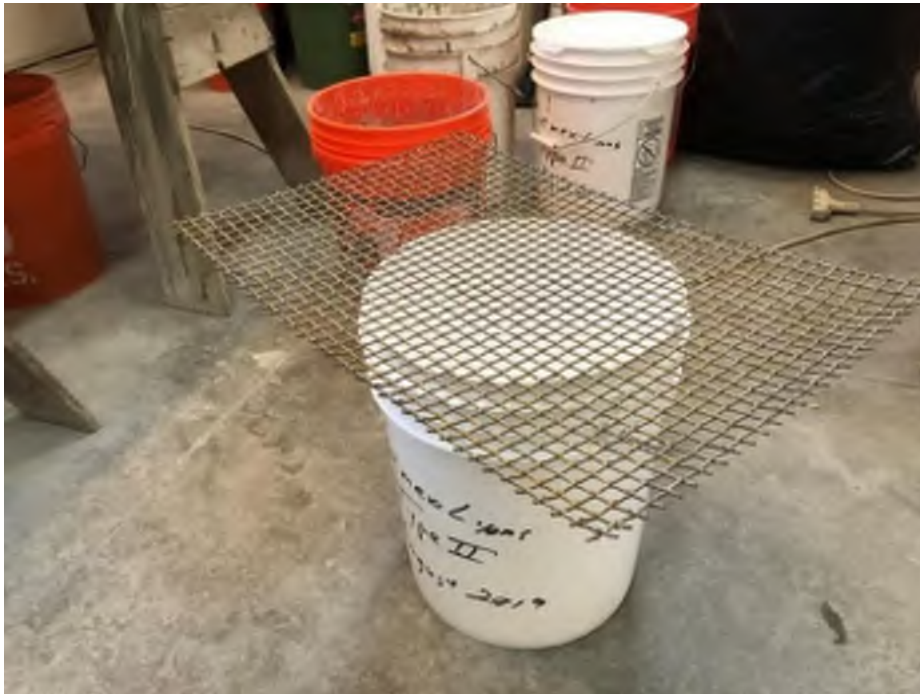


*Figure 10: Empty bucket with heavy screen for draining sample, or 12" Brass Sieve Alternate*

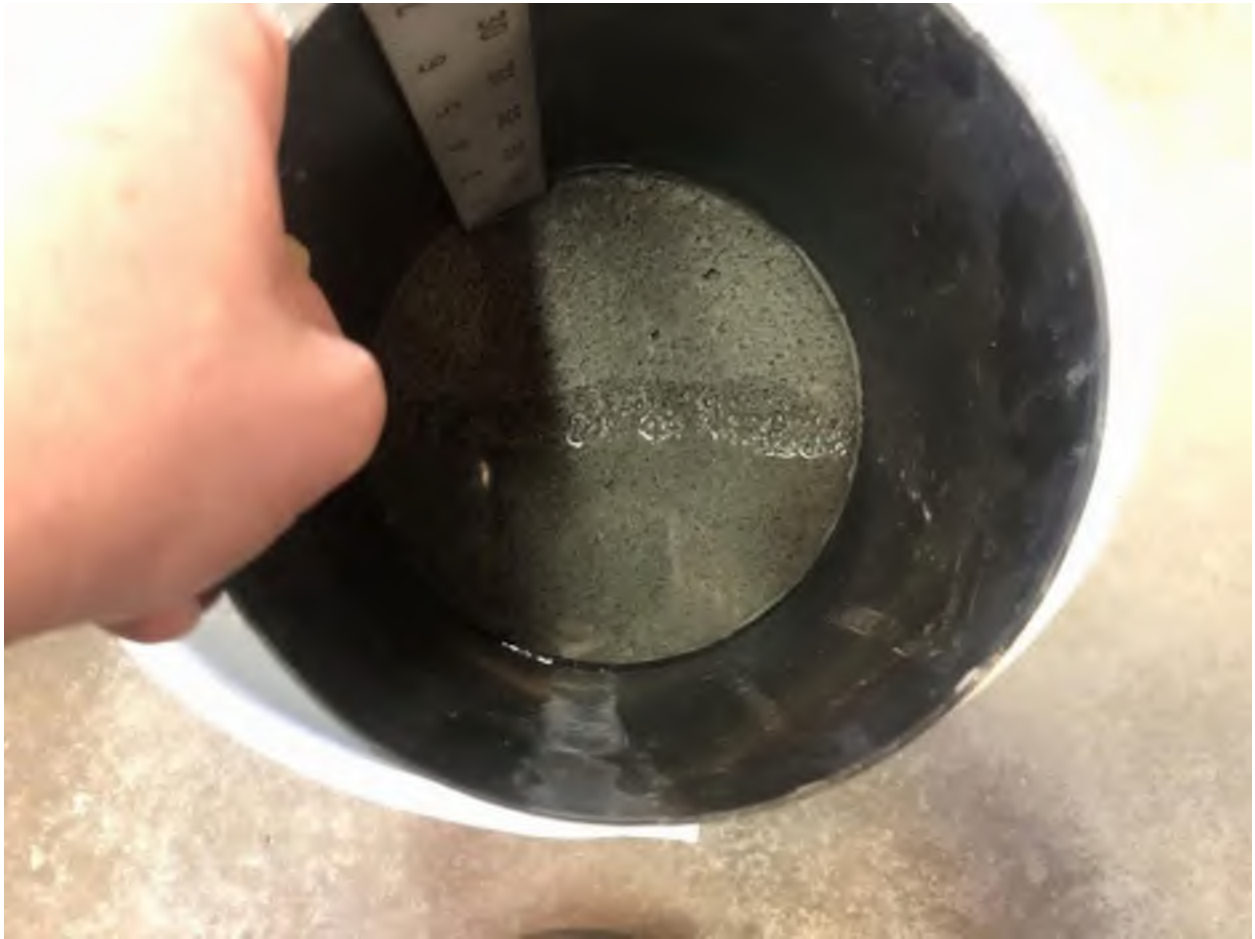


*Figure 11: Initial immersion of the sample in the water bucket, water is infiltrating from the bottom to the top surface.*



*Figure 12: Water is covering the surface, now ready for total submersion.*



*Figure13: Submerging the entire mold to full fill with water.*





*Figure14: Submerged sample, ready to be lifted out for draining and or testing.*



*Figure15: Free draining sample. The time is recorded for the water surface to drop from the 5" mark to the 2" mark.*



*Figure 2: Scribing tool. The screw protrudes slightly through the wood and acts as the scribe. The nail acts as a stop on the cylinder rim. The distance between the center of the nail and the center of the screw is 6".*

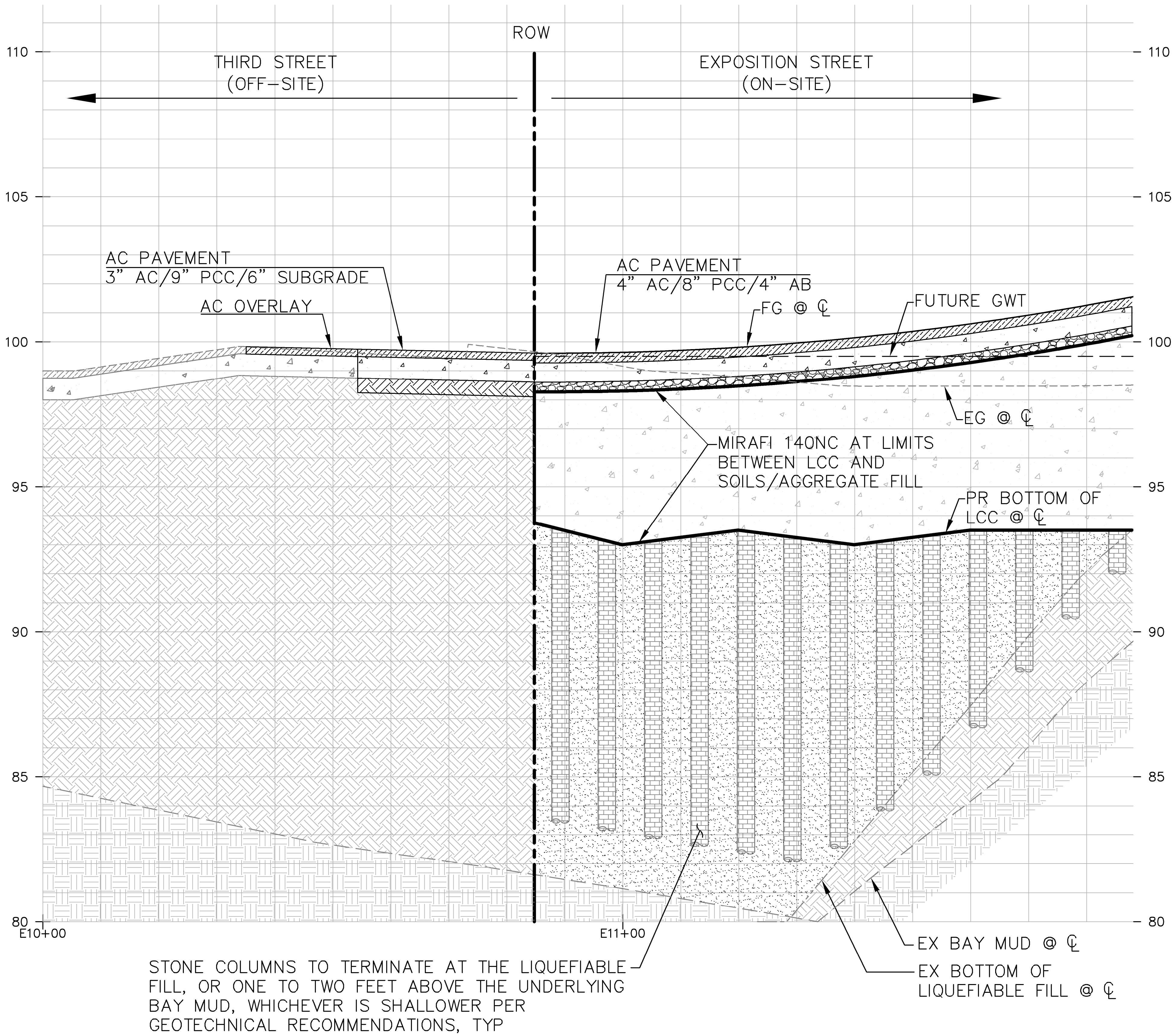
## EXHIBIT I

### Typical Sections at LCC Interfaces

- Typical Interface with Existing Street
- Typical Interface with Vertical Parcel



DRAWING NAME: \\BKF-st\vol\4\2008\080006 Mission Rock\ENG\Exhibits\20\_0206 Expo Third Cross Section.dwg  
PLOT DATE: 02-07-20 PLOTTED BY: mey



**LEGEND:**

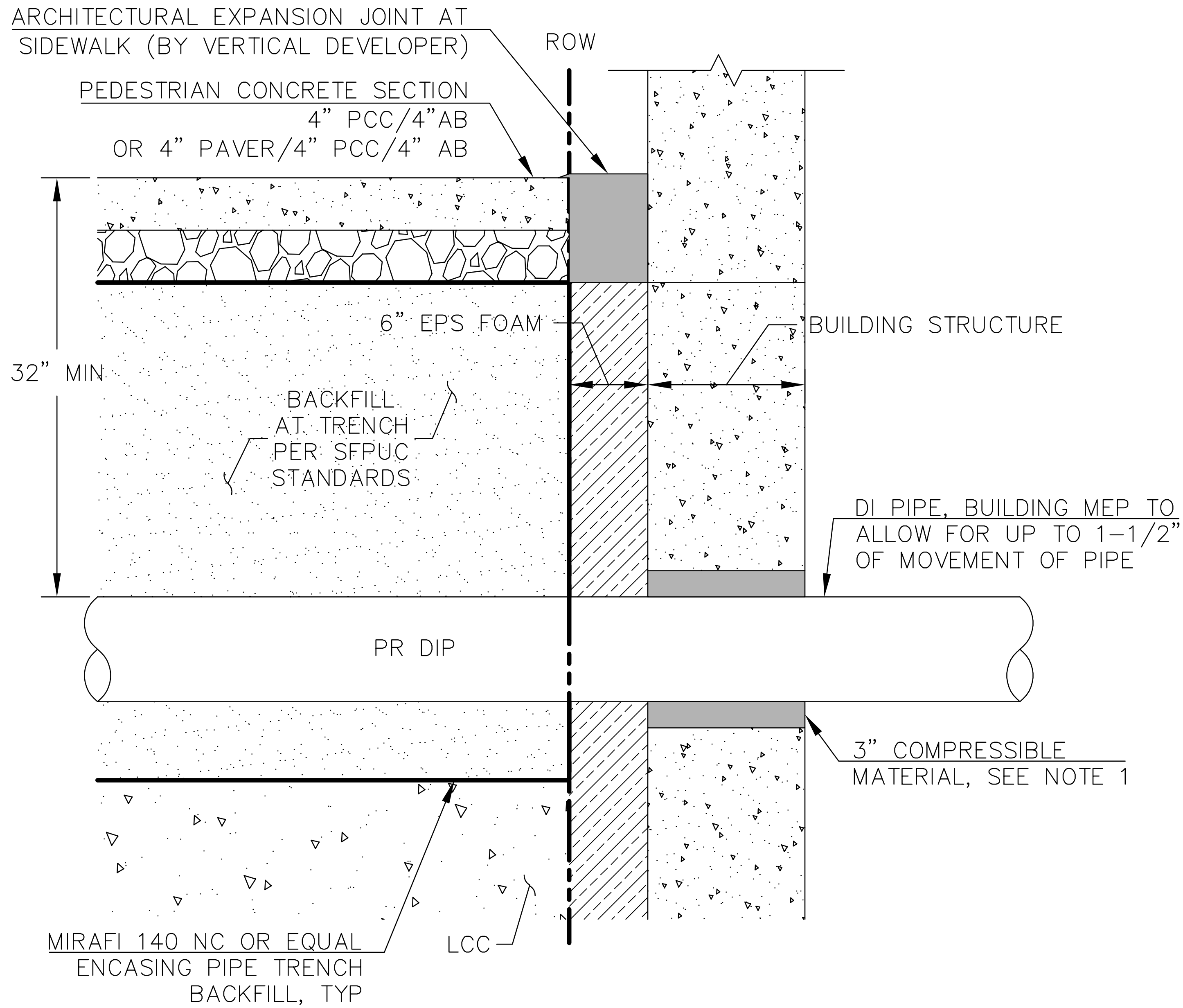
	AC
	PCC
	AB
	SUBGRADE
	LCC
	STONE COLUMNS
	DENSIFIED SOIL
	EX SOIL
	EX BAY MUD

**ABBREVIATIONS:**

AB	AGGREGATE BASE
AC	ASPHALT CONCRETE
CL	CENTERLINE
EG	EXISTING GRADE
EX	EXISTING
FG	FINISHED GRADE
LCC	LIGHTWEIGHT CELLULAR CONCRETE
PCC	PORTLAND CONCRETE CEMENT
PR	PROPOSED
ROW	RIGHT OF WAY
TYP	TYPICAL

**THIRD STREET/EXPOSITION STREET CROSS-SECTION**

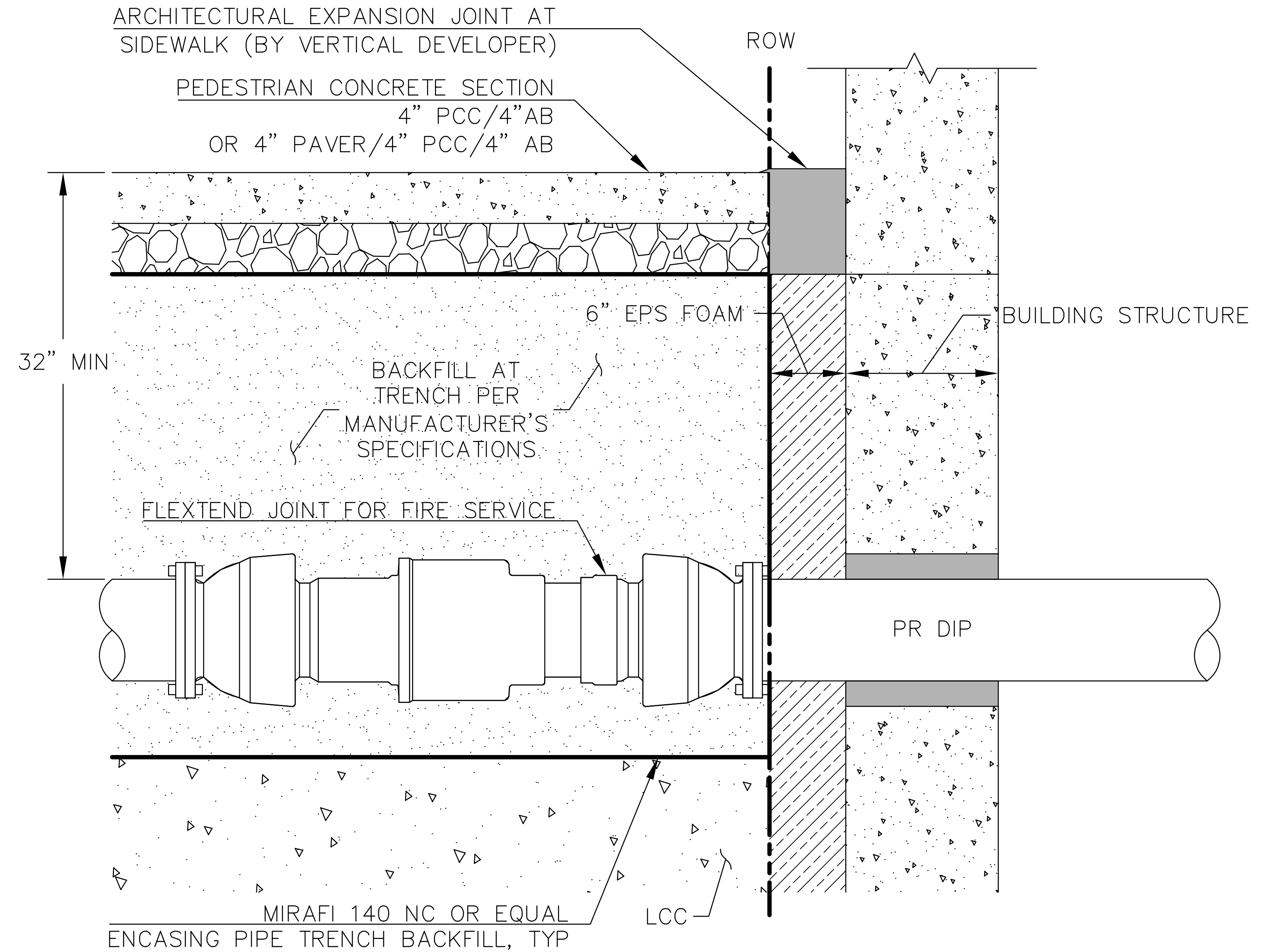
SCALE: 1"=10'



NOTES:

1. WATERPROOFER/MEP/STRUCTURAL ENGINEER TO COORDINATE AND SPECIFY WALL PENETRATION MATERIAL, WATERPROOFING DETAIL, ETC. COMPRESSIBLE MATERIAL TO ALLOW UP TO 1-1/2" OF MOVEMENT.
2. HDPE CONNECTIONS TO UTILIZE LINK-SEAL AND WATER STOPS IN LIEU OF COMPRESSIBLE MATERIAL.

**DIP LPW/NPW WALL PENETRATION DETAIL**  
NTS



NOTES:

1. WATERPROOFER/MEP/STRUCTURAL ENGINEER TO COORDINATE AND SPECIFY WALL PENETRATION MATERIAL, WATERPROOFING DETAIL, ETC.

**DIP FS WALL PENETRATION DETAIL**  
NTS

Revisions		No.	
Date 02/12/2020	Scale AS SHOWN		
	Design		
	Drawn		
	Approved		
	Job No 20080006		